2012

Quantifying Watershed Loads to a Low Relief, Coastal Plain Estuary, the New River Estuary, N.C

Brittani J. Koroknay
College of William and Mary - Virginia Institute of Marine Science

Quantifying Watershed Loads to a Low Relief, Coastal Plain Estuary: the New River Estuary, NC

A Thesis
Presented to

The Faculty of the School of Marine Science

The College of William and Mary in Virginia

In Partial Fulfillment
of the Requirements for the Degree of
Master of Science

by

Brittani J. Koroknay

2012

APPROVAL SHEET

This thesis is submitted in partial fulfillment of

the requirements for the degree of

Master of Science

Brittani J. Koroknay

Approved, by the Committee, November 2012

Mark J. Brush, Ph.D.
Committee Chairman/Advisor

Iris C. Anderson, Ph.D.

John M. Brubaker, Ph.D.

Carlton H. Hershner, Jr., Ph.D.

Michael F. Piehler, Ph.D.
University of North Carolina
Morehead City, North Carolina

TABLE OF CONTENTS

ACKNOWLEDGEMENTS

After a significant amount of effort and dedication, I am proud to present this master's thesis. I first want to thank my advisor, Dr. Mark Brush for his open door policy and providing me with numerous hours of help and guidance that led to the success of my project. I never would have imagined that I could have learned so much in such a short amount of time, thank-you. I am also extremely grateful to my committee members, Dr. Iris Anderson, Dr. John Brubaker, Dr. Carlton Hershner, and Dr. Michael Piehler for their guidance and expertise to my project. Dr. Jian Shen and Dr. Hongzhou Xu were also essential to my project success, they were gracious enough to provide hours of help and guidance with my project. Their time and insight were essential to my success. I also want to thank the Coast Guard for providing me with the time and funding to obtain a life goal of a higher education degree. I want to especially thank CDR Eric Miller, you have been a mentor and supporter from the beginning of my Coast Guard career until now, and your guidance through academia and the Coast Guard are greatly appreciated.

I also want to thank Sam Lake, for not only being a great friend, mentor, and lab mate, but also listening to my struggles and providing insightful advice. Thank you also to Britt Dean for the hours of laughter and homework that we did together, your friendship and support made me look forward to driving to VIMS every day. It was truly a joy sharing an office with you. Thank you, also, to my friends for providing much needed distractions and laughter.

To my family I am forever grateful for your continued support. Mom and dad, I would not be where I am today without your guidance and encouragement through all of challenges I have taken on over the years. My brother Ryan, thank you for all of the "school talk" and the "sailing talk" distractions, they were very much needed and appreciated. Thank you to Tom, Debbie and Rachel, I am so grateful to call you family; thank you for the support and the kitchen table space to work over the holidays and visits. To my daughter, Emma, I hope you enjoy science and learning as much as I do and never stop setting goals and dreaming of making yourself a better person. Finally, I want to thank my husband Ryan, you are my best friend and biggest supporter and I am truly grateful to have you by my side through all of life's challenges and successes.

List of Tables

List of Figures

ABSTRACT

Watershed modeling is an important tool for quantifying the inputs of fresh water, sediments, and nutrients into receiving estuaries and potential changes in those loads under scenarios including changes in land use and climate. There are a variety of existing watershed loading models available, from simple to complex, but a spectrum of these models have yet to be applied and compared in a low relief, coastal plain setting. This project has been conducted as part of the Defense Coastal/Estuarine Research Program (DCERP), which has focused on the impact of Marine Corp Base Camp Lejeune (MCBCL) and activities in the surrounding watersheds on the New River Estuary (NRE), located in southeastern North Carolina. As part of DCERP, nine sub-watersheds on MCBCL with contrasting land use were monitored to allow computation of freshwater, sediment, and nutrient loads to the NRE. In the current project, these loads were used to assess the performance of two existing watershed models using the Environmental Protection Agency's (EPA) Better Assessment Science Integrating point and Nonpoint Sources (BASINS) 4.0 modeling suite: the relatively complex, temporally-resolved Hydrologic Simulation Program-Fortran (HSPF), and the relatively simple, annually-resolved Pollutant Loading (PLOAD) model. For both models, the 2001 National Land Cover Data were used for analysis; this dataset was compared to the recently released 2006 NLCD dataset and changes were found to be small. Monthly HSPF model output generally followed precipitation trends, and tended to over-predict freshwater stream flow and under-predict sediment and nutrient loads. PLOAD reproduced annual loads of total nitrogen within measured ranges, under-predicted annual loads of total suspended solids, and was less successful at predicting PO_4^{3-} loads. Results from HSPF and PLOAD were combined with those from six other modeling approaches applied during DCERP to complete a spectrum of models from simple to complex. Model output from HSPF and PLOAD was scaled up to estimate loads entering the NRE from that portion of its watershed lying on MCBCL. Model estimates suggest that approximately 5-6% of the total nitrogen entering the NRE from external sources originates from the MCBCL watershed, a value on the lower end but within the range of estimates from other models applied to the system. Scenarios were run within HSPF to investigate how the conversion of forested land to impervious surfaces on MCBCL may alter existing loads; the model was relatively insensitive to changes in impervious surfaces. Neither PLOAD nor HSPF predicted nitrogen, phosphorus, and sediment loads better than the other watershed models applied during DCERP. The results of this study combined with development of other models suggest that simpler models, such as PLOAD, are able to estimate loads to the NRE as well as more highly technical models, such as HSPF, and that regardless of model choice a focus on loads at the annual scale is most justifiable.

Quantifying Watershed Loads to a Low Relief, Coastal Plain Estuary: the New River Estuary, NC

INTRODUCTION

Importance of Watershed Loading to Estuaries

Estuaries are among the most productive ecosystems in the world, with the presence of seagrasses, phytoplankton, benthic macroalgae and benthic microalgae contributing to the high rates of production (Boynton and Kemp, 1982; Boynton et al., 1996; Valiela et al., 1997; McGlathery et al., 2007). Estuaries are also economically important and provide essential habitat for the life cycles of recreationally and commercially important fish species such as striped bass, oysters, salmon, and crabs (Houde and Rutherford, 1993; Nixon and Buckley, 2002; Breitburg et al., 2009). The United States has taken steps to protect these vital habitats from pollution, development, and overuse (Clean Estuaries Act of 2010). Eutrophication is widely recognized as the most serious threat to estuarine ecosystems and is typically related to human activity (Nixon, 1995; NRC, 2000; Pinckney et al., 2001; Duarte et al., 2009; Paerl, 2009). Eutrophication is defined as an increase in the rate of supply of organic matter to an ecosystem (Nixon, 1995, 2009), and most often results from increased nutrient loading. Despite the efforts that the United States and other countries have taken to protect estuaries, eutrophication has become a significant problem worldwide and studies of eutrophic systems have been on the rise over the last half-century (Nixon, 1995, 2009; Boynton and Kemp, 2000; NRC, 2000; Borah et al., 2006). Shifts in the amount of organic material supplied to a system can vary as a function of changes in climate, coastal population sizes, and land use. As a result of increased combustion of fossil fuels, land clearing and development, increased coastal population size, increased use of fertilizers, and large scale farming operations, the amount of nutrients delivered to coastal waters has significantly increased and disrupted the fragile balance between ecosystem production and respiration (Nixon, 1995; Cloern, 2001).

For decades it was thought that this increase in productivity due to nutrient enrichment would flow up the food web to promote fish stock growth. However, continuously high inputs of nutrients allow for primary productivity to remain high, and significant and often detrimental changes to estuarine ecosystems can result (Nixon, 1995, 2009; Kemp et al., 2005). Nixon et al. (1996) reviewed data from a variety of phytoplankton-based marine systems and demonstrated a direct relationship between loading of dissolved inorganic nitrogen (DIN) and primary production. Depending on the characteristics of a particular system, this increase in production could be detrimental to essential ecosystem functions (Cloern, 2001; Pinckney et al., 2001; Kemp et al., 2005). For example, impacts due to nutrient loading depend on how quickly nutrient inputs and phytoplankton biomass are flushed out of a system (Valiela et al., 1997; Monbet, 1992; Pinckney et al., 2001; Lucas et al., 2009). If increased loading is persistent, especially in systems with residence times on the order of months to years, community composition can be permanently modified, and lower trophic levels will be favored (Pinckney et al., 2001). Long-term trophic shifts can result in zones of anoxic and hypoxic waters caused by intense deposition and degradation of nutrient-fueled organic material (Paerl, 1998; Hagy et al., 2004; Kemp et al., 2005). Seagrass growth and coverage in estuarine systems can also be indicators of eutrophic conditions, where increased phytoplankton and macroalgal biomass can decrease light availability and reduce seagrass abundance and distribution (Valiela et al., 1997; Kemp et al., 2005; Greening and Janicki, 2006). Additionally, increased water temperatures related to climate change can induce stronger water column stratification, and increase the rate of organic matter respiration. Increased temperatures and stratification combined with increased nutrient loading promote ideal conditions for harmful algal blooms (Paerl and Scott, 2004; Paerl and Huisman, 2008).

A great deal of effort has been put forth to reduce nitrogen and phosphorus inputs to estuarine and coastal marine systems that are not well flushed in an attempt to reverse the negative effects of greater nutrient influx (e.g., EPA, 1999). Updated sewage systems, enhanced control over fertilizer production and regulated agricultural use have significantly reduced nutrient inputs and reversed negative effects in some estuarine systems (Mallin et al., 2005; Greening and Janicki, 2006; Nixon, 2009). However, reduced watershed loads to a system do not necessarily result in improved water quality as there may be significant lag times before improvements can be detected due to possible shifts in ecological diversity within the system or hysteresis effects as the system works towards a new equilibrium (Duarte et al., 2009).

Watershed nutrient loads are typically accompanied by inputs of river-borne sediments. Sediment loading to estuaries is a natural process and contributes to functions such as nutrient supply, marsh accretion and therefore buffering against coastal erosion, and burial of contaminated sediments (Valette-Silver, 1993; Boynton et al., 1995, 2008; Mudd et al., 2009). However, increased development and agricultural land use have the potential to significantly elevate sediment inputs above background levels (Howarth et al., 1991; Brush, 2001). Elevated sediment concentrations can increase water turbidity, restrict light penetration, and inhibit seagrass growth resulting in drastic shifts in ecosystem structure and function (Thrush et al., 2004; Kemp et al., 2005). Reduced light penetration also limits production by microphytobenthos, thus limiting their ability to sequester nutrients and mediate against the effects of increased allochthonous nutrient inputs (Anderson et al., 2003; Kemp et al., 2005; McGlathery et al., 2007). Elevated land-based sediment loads can also transport particle-bound nutrients that further stimulate primary production of organic matter (Boynton et al., 1995, 2008) which further contributes to hypoxia (Paerl et al., 1998).

Nutrients and sediments are carried through watersheds to estuaries in freshwater discharge. Watershed inputs of fresh water affect various estuarine processes, including primary production, secondary benthic production, increased stratification, increased nutrient inputs and fish recruitment (Boynton and Kemp, 2000; Kemp et al., 2005; Kim and Montagna, 2009; Gillson, 2011). Salinity distributions can be used to track freshwater influxes, which can also introduce chromophoric dissolved organic matter (CDOM) to an estuary in addition to nutrients and sediments (Anderson et al., 2012). The combined effects of nutrient-stimulated algal blooms, suspended sediments and CDOM can increase light attenuation, decrease the amount of light that reaches the bottom and negatively impact benthic primary production (Anderson et al., 2012). Fresh water inflow also determines the flushing rate of estuaries, and prolonged flushing rates combined with low benthic primary production can make estuaries more susceptible to anthropogenic nutrient loading and eutrophication (Bricker et al., 1999; Cloern, 2001; Hagy and Murrell, 2007). Finally, freshwater inputs increase stratification through strengthening of vertical density gradients, which can exacerbate bottom water hypoxia (Boynton and Kemp, 2000; Hagy et al., 2004; Kemp et al., 2005).

Importance of Watershed Modeling

Given the importance of watershed loads to estuarine ecosystems, monitoring and modeling of those loads is critically important. Watershed monitoring involves the measurement and observation of environmental parameters over time. It can effectively be used to analyze the efficacy of point and non-point source pollution reduction practices or to enforce environmental protection law infringements. Watershed modeling requires monitoring data for model development, calibration, and validation (NRC, 2000). The modeling approach is comprised of several steps including data collection, model input preparation, parameter evaluation, calibration and validation/verification, and scenario analysis. When completed, a user is able to gain insight into changes in watershed nutrient, sediment, and freshwater loads through the analysis of alternative scenarios including changes in land use, climate change and increased frequency of storm events. Watershed monitoring and modeling tools can be used for the management and regulatory decision making process and to assist in developing national marine environmental protection policy (NRC, 2000).

As the application of watershed models continues to rise, it is increasingly important to address the assumptions and inaccuracies in models and to compare a range of modeling approaches from simple to complex. Alexander et al. (2002) compared a range of models for predicting nitrogen export from 16 large, regional watersheds of the northeastern U.S. The models tested differed in the method of calibration, degree of spatial resolution, and complexity of rate processes. While most models estimated loads within 50% of measured values, model bias differed widely among the models, with the more complex models generally having lower bias and higher precision, where bias was defined as the median of the prediction errors and precision as the reciprocal of the interquartile range. Alexander et al. (2002) also determined that a key facet of inaccurate watershed model predictions could be attributed to the inability of some models to account for the full range of sources, sinks, and processing of total nitrogen within the watersheds.

A similar comparison of multiple watershed models has yet to be conducted for the relatively small watersheds throughout the low relief coastal plain of the U.S. Mid-Atlantic coast. Im et al. (2007) compared annual and monthly loads of fresh water and sediments predicted by two watershed models, the Soil and Water Assessment Tool (SWAT) and Hydrologic Simulation Program-Fortran (HSPF) in Polecat Creek, VA, which lies on the border of the Piedmont and Coastal Plain provinces of Virginia. Both models adequately simulated hydrologic and sediment loads, with HSPF more accurately predicting monthly loads of fresh water and SWAT more accurately predicting loads of sediment While this comparison is a start, there exists a need for a more thorough comparison of a wider range of models in terms of their ability to simulate fresh water, sediment, and nutrient loads on a variety of time scales in a coastal plain setting.

New River Estuary, NC

The New River Estuary (NRE), NC is an example of a coastal system subjected to elevated nutrient and sediment loading. The NRE is a dynamic system with numerous confined animal feeding operations (CAFOs) and harvest crops within its watershed. There is also a concentrated population within the city of Jacksonville, NC at the head of the estuary, and living

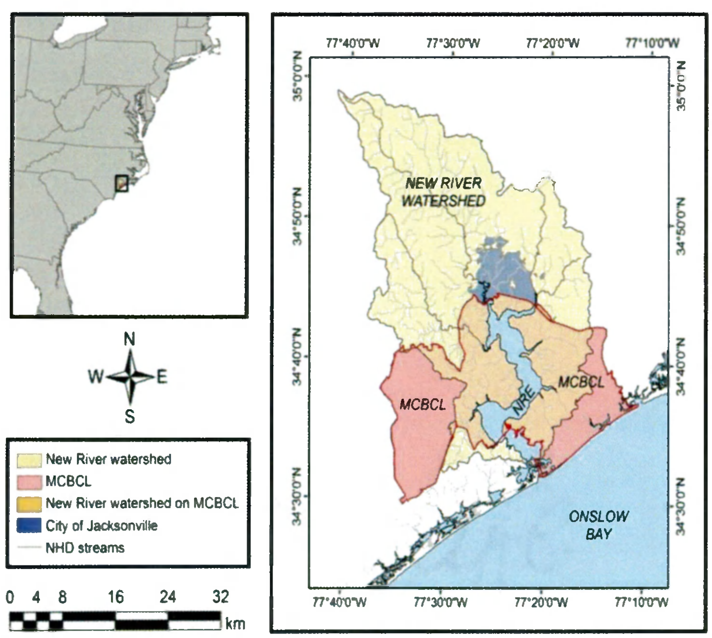

Figure 1. New River Estuary and watershed from Brush (2012). Streamlines are from the USGS National Hydrography Dataset (NHD).

on Marine Corp Base Camp Lejeune (MCBCL) which surrounds almost the entire lower portion of the system (Fig. 1). The estuary is shallow (mean depth ~ 2 m), has a median flushing time of 64 days, and phytoplankton primary productivity in the system is nitrogen limited (Ensign et al., 2004; Mallin et al., 2005; Brush, 2012.; Paerl and Reckhow, 2012). The presence of barrier islands at the mouth of the estuary creates a system with small restrictive channels requiring frequent dredging. Therefore, the estuary is primarily comprised of low flow creeks and broad polyhaline and mesohaline lagoons (Mallin et al., 2005).

During the 1980s and 1990s the combined effects of outdated sewage treatment plants and numerous CAFOs made the NRE one of the most eutrophied estuaries in the southeastern United States, with widespread anoxia and hypoxia (i.e., low dissolved oxygen or DO) and massive phytoplankton blooms (Bricker et al., 1999; Mallin et al., 2005). In 1998, the city of Jacksonville and MCBCL updated their respective sewage treatment plants resulting in increases in bottom water DO and light penetration, and decreases in key nutrients for phytoplankton growth such as orthophosphate and ammonium (Mallin et al., 2005). While average bottom water concentrations of DO increased, there were still periods of severe hypoxia, indicating a greater need for efforts to improve water quality. As the population in and around the city of Jacksonville continues to grow and MCBCL continues to expand its population and training efforts, there will be increasing anthropogenic stress placed on the NRE. For that reason, it will become even more vital to track, predict, and model these changes to ensure the long-term sustainability of the NRE.

The need to sustain the NRE for the military training efforts at MCBCL combined with the degree of anthropogenic impacts on the system led the Department of Defense to institute the Defense Coastal / Estuarine Research Program (DCERP) as a research and management effort in

July 2007. DCERP is focused on the need for greater understanding of NRE physical, geological, chemical, and biological processes in order to sustain military training efforts without further negative impacts on the NRE. Fundamental to the objectives of DCERP is the quantification of watershed loads of fresh water, nutrients, and sediments to the estuary, which are being measured by DCERP researchers. Currently, the DCERP project monitors loads from 10 small sub-watersheds with contrasting land use located on MCBCL, while the United States Geological Survey (USGS) maintains two gauging stations on the New River, the major source of fresh water to the estuary from the upland watershed.

Given the importance of fresh water, nutrient, and sediment loads to receiving estuaries, quantification of current loads to the NRE and potential changes in those loads is an essential part of DCERP. A spectrum of watershed models from simple to complex are being developed, tested, and applied to determine their accuracy and ease of use for management personnel at MCBCL. The Environmental Protection Agency (EPA) has developed the Better Assessment Science Integrating point and Nonpoint Sources (BASINS) software package that incorporates a variety of watershed models and calibration tools that operate within a Windows-based GIS interface. The purpose of the current project is to apply two of these models, HSPF and PLOAD (Pollutant Loading), within BASINS to compute loads and likely changes in those loads due to changes in land use, as marked by increases in impervious surfaces on MCBCL, and climate, as manifested by changing water temperature and precipitation patterns. These two models will complete the spectrum of DCERP watershed models under development and facilitate selection of an optimal model for use by management personnel.

MATERIALS AND METHODS

Study Sites and Loading Data

Twelve sub-watersheds have been monitored within the NRE watershed during DCERP, referred to as Airport, Camp Johnson, Cogdels, Courthouse, Freeman, French, Gillets, Gum Branch, Southwest, Tarawa, Traps, and Jacksonville (Fig. 2). Camp Johnson and Jacksonville were excluded from model calibration due to insufficient data collection for computing reliable loading rates. Gauge stations were either maintained by the USGS (Gum Branch, Jacksonville) or Dr. Michael Piehler (University of North Carolina) as part of the DCERP program. Stations on MCBCL (Piehler) were located at the furthest accessible point downstream within each sub-watershed, while remaining above the influence of tides. The USGS gauge at Jacksonville was located in tidal waters, while the gauge at Gum Branch was rarely tidal.

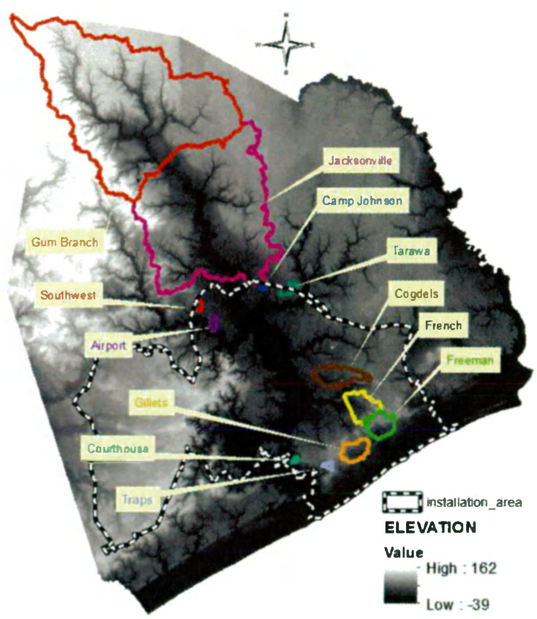

Figure 2. NRE watershed and gauged sub-watersheds. Elevation values are in feet and were obtained from the MCBCL 20-foot resolution digital elevation model for Onslow

Rates of freshwater flow at the MCBCL sites were recorded every 30 minutes beginning at various times during 2008 and running through June 30, 2010. Concentrations of *in situ* dissolved inorganic nutrients (NH_4^+, NO_x^-, and PO_4^{3-}), total dissolved nitrogen (TDN), total nitrogen (TN), and total suspended solids (TSS) were measured monthly. Two methods were used to calculate stream flow; some streams were equipped with automated samplers while others were equipped with water level gauges. Sites equipped with automated samplers (ISCO models 6700 or 6712) were also equipped with ISCO model 750 Area Velocity Modules. The automated flow sensors used ultrasonic Doppler technology to measure velocity and a pressure transducer to measure water level at each station at 30-minute intervals, except during storm events when continuous measurements were recorded. At sites that were equipped with water level gauges, handheld continuous flow meters were used to calibrate the mathematical conversion of stream depth to flow rate. Gauges were placed in culvert pipes with known dimensions, thus reducing calculation errors due to variable cross-sectional stream morphology. Flow velocity was translated into stream discharge using the Manning Equation ($Q_{discharge} = V_{velocity} A_{area}$). When mechanical errors resulted in missing discharge data, interpolations were performed through the resulting gaps.

Water samples were collected before, during and after storm events, filtered (0.7 µm nominal pore size), and analyzed using a Lachat Quick-Chem 8000 automated ion analyzer to determine concentrations of nitrite and nitrate (NO_x^-), total dissolved nitrogen (TDN), ammonium (NH_4^+), and phosphate (PO_4^{3-}). When concentrations were below the analytical detection limit, values were set at the limit (NO_x^-: 0.043μM, NH_4^+: 0.182 μM, PO_4^{3-}: 0.059 μM and TDN: 2.529 μM) (Schwartz, 2010). Additional water samples were filtered (0.7 µm nominal pore size), dried, and weighed to determine the concentration of total suspended solids (TSS) using standard protocols ("Standard Methods for the Examination of Water and Wastewater" 20^{th} Edition, 1998 Method 2540 D, 2-57) (Schwartz, 2010).

At the USGS Gum Branch station, freshwater flow was recorded approximately every 15 minutes over the same period as for the MCBCL sites. Nutrient loads were computed by Brush (2012) using a combination of mean concentrations and flow-concentration regressions using nutrient data collected approximately monthly from 1987 to 2001 (NH_4^+, NO_x^-, TKN = total Kjeldahl nitrogen, PO_4^{3-}, and TP = total phosphorus). All available data for the two year period at the MCBCL sites and Gum Branch were used for model calibration and to scale the HSPF model to the entire watershed.

Model Input Data

Data were loaded into BASINS 4.0 (www.epa.gov/waterscience/basins/) and manipulated for use in the HSPF and PLOAD watershed models. Sub-watershed boundaries were previously delineated in ArcGIS by Juliette Giordano and Mark Brush using a 6.1 m (20 foot) resolution, LIDAR-based digital elevation model (DEM) provided by MCBCL (Brush, 2012). These boundaries were used directly in PLOAD but had to be modified for use in HSPF (see below). Land use distributions were obtained from the 2001 National Land Cover Data (NLCD) downloaded from the BASINS 4.0 website which included 26 different land use classes. The 2001 NLCD were reclassified into a simpler set of 13 land use classes: open water, developed (open space), developed (low intensity), developed (medium intensity), developed (high intensity), barren land, deciduous forest, evergreen forest, mixed forest, shrub/scrub, herbaceous, woody wetlands, and emergent herbaceous wetlands. The simplified land use classification scheme was used for both MCBCL (Fig. 3) and each sub-basin (Fig. 4). During the course of this project, the 2006 NLCD were released so land use distributions were compared to those in the 2001 dataset. The percent of impervious surfaces on MCBCL increased minimally from 4.02% to 4.28%, and the area of land within the 13 land use categories was highly correlated between the two datasets (r^2=0.91). When the land use categories for the 2001 and the 2006 datasets were refined and grouped into four major categories (water, barren, developed, and natural vegetation) the two datasets were again highly correlated (r^2=0.99). Therefore, the decision was made to continue using the 2001 NLCD for the entire project. High resolution USGS National Hydrography Dataset (NHD) flowlines were used in the manual and automatic watershed delineation tools to burn-in streams and define the stream network (see below). The USGS Map Accuracy standards define high resolution NHD data as having 90% of the NHD flowlines lying within 40 feet of their true geographic position on a 1:24,000 to a 1:5,000 scale.

Solar radiation data were downloaded from the nearest available station, NOAA station 312517 in Durham, NC, approximately 200 km northwest of the NRE, and the remainder of the required meteorological data were downloaded through BASINS for NOAA station 723096 (New River MCAS) at the head of the NRE (Table 1). Except for daily minimum and maximum air temperature, hourly meteorological data were used instead of daily values to avoid use of the WDMutil disaggregation tool in BASINS. Cloud cover data were not available in the initial meteorological dataset so the data were downloaded from the NOAA National Climatic Data Center (NCDC) for the New River MCAS station. The initial cloud cover dataset was coded as clr (clear), sct (scattered), brk (broken), ovc (overcast), or obs (obscured). BASINS 4.0 requires data on a tenths scale; therefore all data labeled 'clr' were assigned a value of 0, all data labeled 'sct' were assigned a value of 0.3, all data labeled 'brk' were assigned a value of 0.7, and all data labeled 'ovc' or 'obs' were assigned a value of 1. Meteorological data were uploaded into WDMUtil, a data pre-processor tool within BASINS, and formatted into a .wdm file for use in

HSPF. Point source loads were obtained from the EPA Water Discharge Permits website (EPA-PCS, 2009).

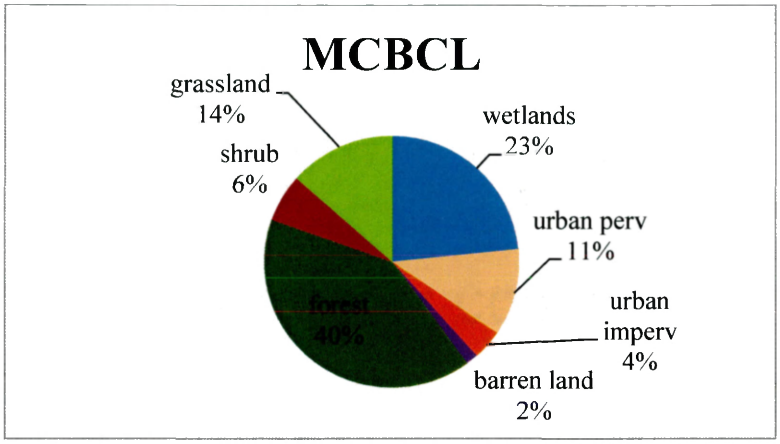

Figure 3. Land distribution on MCBCL determined from the 2001 National Land Cover Dataset. Total area of MCBCL is approximately 26,836 hectares.

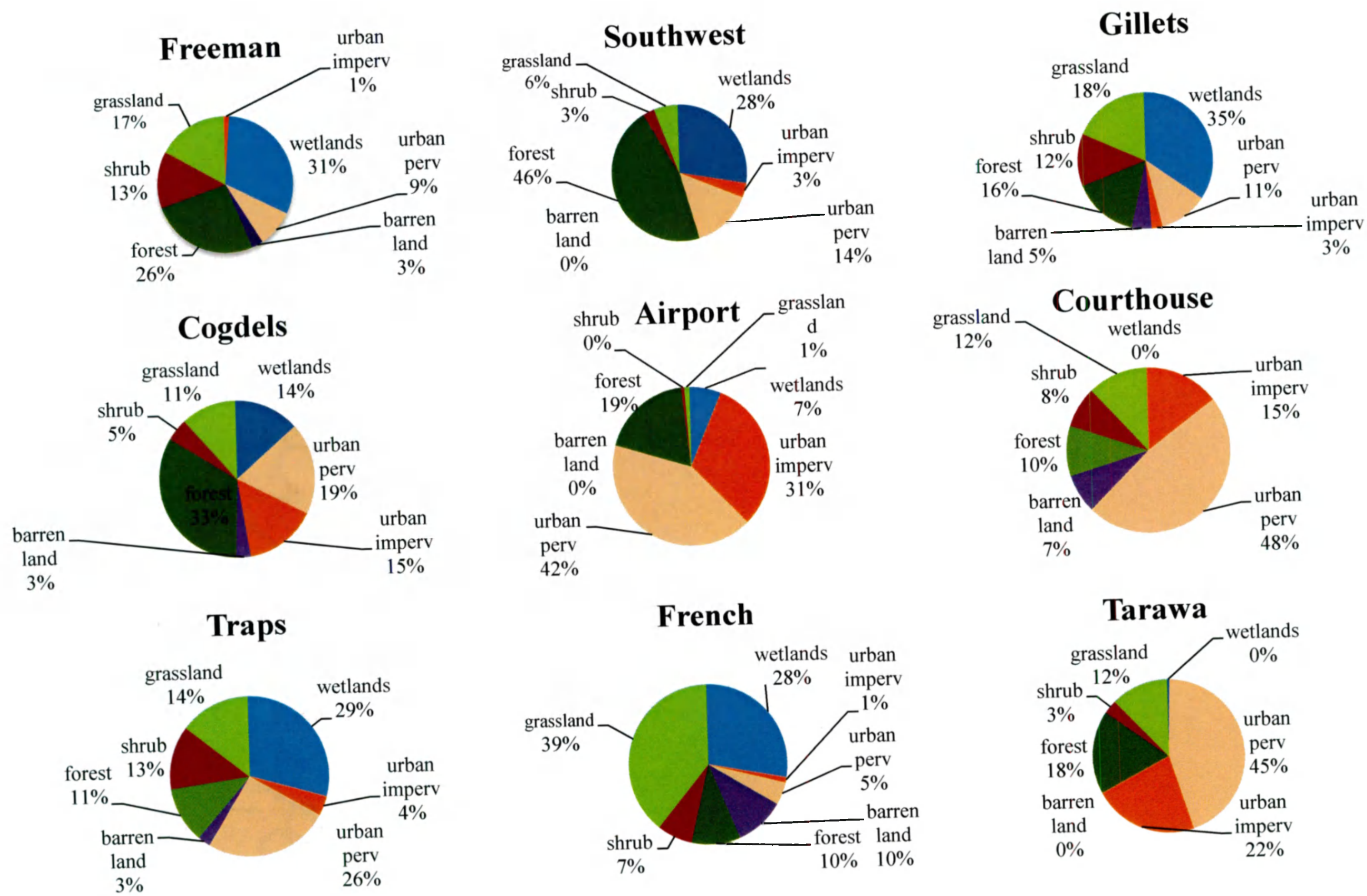

Figure 4. Distribution of land use within each sub-basin on MCBCL, determined from the 2001 National Land Cover Dataset.

Table 1. Meteorological data used for the BASINS HSPF watershed model.

Variable	Time Step	Abbreviation	Units	Station
Dew point	hourly	DEWP	F	New River MCAS
Mean wind speed	hourly	WIND	mph	New River MCAS
Solar radiation[1]	hourly	SOLR	Langleys	Durham, NC
Precipitation	hourly	PREC	mm	New River MCAS
Minimum temperature	daily	TMIN	F	New River MCAS
Maximum temperature	daily	TMAX	F	New River MCAS
Cloud cover[2]	hourly	CLOU	tenths	New River MCAS

[1]Units converted for use
[2] Calculated

Once all required data were loaded into BASINS 4.0, the location of each gauge (based on GPS coordinates) was checked to ensure that it was located as far downstream as possible within the delineated sub-watershed and overlapped the NHD flowlines. The HSPF model requires use of the automatic watershed delineation tool to specify the desired outlet (i.e., the gauge station for each sub-watershed), and to burn in the NHD flowlines. The NHD flowlines were then extended to include the drainage ditches using the automated delineation tool based on the MCBCL DEM. However, the automated delineation tool did not permit use of our previously delineated sub-watersheds, but instead created its own delineation. (Conversely, the manual watershed delineation tool can use previously delineated sub-watersheds, but does not permit specification of outlet points or input of NHD flowlines.) Given our desire to use watershed boundaries consistent with our previously delineated boundaries used in other DCERP watershed models, a combination of the output from both delineation methods was used. The previously delineated sub-watershed boundaries were input into the manual watershed delineation tool, and were combined with stream networks and outlet points created with the automated watershed delineation tool.

HSPF Model

The Stanford Watershed Model (SWM) was developed by Dr. Norman H. Crawford and Dr. Ray K. Linsley in 1966 to help civil engineers understand the value of a continuous digital simulation of hydrological processes. The SWM model has evolved into the HSPF model and is a process-based, lumped-parameter model. Over the years, the EPA and USGS have worked to maintain and enhance the model by incorporating it into the BASINS 4.0 program, but the same basic principles that were designed for the SWM still apply to HSPF. One important enhancement in HSPF has been to account for multiple land use types and simulation of natural and man-made changes to land use over time, and the resulting effects on aquatic systems (Donigian and Imhoff, 2006).

HSPF uses meteorological, watershed land use, hydrographic, and water quality data to model watershed processes. The HSPF model is also capable of simulating various dynamic conditions within a watershed, including transport of sediments, nutrients, and fresh water overland and within stream channels (USEPA, 2009). The watershed environment is simulated using nodes and zones, where nodes are points in space and zones are finite areas of the watershed that contain homogenous storage characteristics (i.e., similar land use). Nodes and zones can be linked to represent channel reaches and land characteristics in order to model the hydrologic cycle. Once the composition of the land and reaches are established for the watershed, sub-basins are created to directly determine the area of land that drains into each reach segment and to compute material transports from each segment. The model simulates major watershed processes in three modules: pervious land, impervious land, and channel reaches.

Specific watershed processes govern how HSPF computes pollutant transport over and through the land within the pervious and impervious land modules (Bicknell et al., 2005). Modeling of the hydrologic cycle over pervious areas of land is conducted using a linked set of theoretical and empirical mathematical functions to represent overland flow along with representation of soil processes. The pervious land module computes storages and fluxes of ground water, interflow and overland flow. Variations in erosion and sediment transport over the pervious land module are simulated by the wash-off of sediment in storage and the scour of the soil matrix (Bicknell, 2005; Gutiérrez-Magness, 2005; Im et al., 2007). The impervious module uses the land use input data and simulates the urban/impervious areas where infiltration to the surface detention storage zone is negligible. Simulation of processes on impervious surfaces is conducted similar to that of the pervious module; however the ability to regulate the rate of evaporation has been modified due to the changes in rates of impervious retention storage. River reach processes are modeled using the reaches module, which simulates the unidirectional flow of water through areas as small as a stream segment or as large as the entire watershed. Within a reach, the HSPF model can simulate sediment accumulation, nutrient input, water temperature, hydrology, and solids that are directly input into the stream. It is assumed that once the constituents flow into the reach they are uniformly distributed and move at the same horizontal velocity as the surrounding water. Mass balance theory controls the inflow and outflow of nutrients and sediments, and processes such as precipitation and evaporation affect outflow from the stream reaches (Bicknell, 2005; Gutiérrez-Magness, 2005).

HSPF Parameterization, Calibration, Scale-up, and Scenario Analysis

Calibration of the HSPF model was based on recommendations in the BASINS Technical Notes available through the supporting website (http://water.epa.gov/scitech/datait/models/basins/bsnsdocs.cfm#tech), which suggest that calibration of HSPF is done first for hydrology, followed by sediments, and lastly for nutrients. Because the New River is on the coastal plain, the model was set up with no losses to deep ground water (DEEPFR). The parameters that the hydrology portion of the model is most sensitive to include the index to infiltration capacity (INFILT), base ground water recession (AGWRC), and the amount of evapotranspiration (which is controlled through the meteorological data) (BASINS Technical Note #6, 2000).

Modeled sediment loads are controlled by transport-limited and sediment-limited conditions. Transport-limited conditions occur when the transport parameters are the driving force for sediment transport, such as near the beginning of major storms, periods following tillage or land disturbance, and during storms after an extended dry period on impervious surfaces. Sediment-limiting conditions occur when accumulation parameters are the primary factors influencing sediment transport, such as during small weather events, near the middle/end of major storms, during the latter part of the growing season and in general on impervious surfaces. The coefficient in the sediment washoff equations for pervious surfaces (KSER) and impervious surfaces (KEIM) are the primary controlling sediment parameters (BASINS Technical Note #8, 2006).

Nutrients from non-point source pollution are modeled using wash-off processes of constituents and are based on simple relationships that constituents have with solids and/or water. Nutrient wash-off from the land is greatly impacted by soil temperature. For impervious surfaces, the build-up and wash-off process assumes that constituent accumulation occurs at a constant rate and there is no association with the sediment. For the constituents associated with sediment, it is assumed that there is an unlimited supply of sediment within the system and build-up is not calculated for sediment associated particles. Constituent modeling on pervious surfaces that are not associated with sediment particles are associated with overland flow processes and are independent of storm/weather events. Constituents that are associated with sediment particles on pervious surfaces are impacted by wash-off and sediment scour processes (Lumb et al., 1994). For pervious surfaces, the primary controlling parameters include the amount of nutrient storage on the surface (SQO), the accumulation of the nutrient at the start of each calendar month (ACQOP), and the rate of surface runoff which will remove 90% of the stored nutrient per hour (WSQOP). For impervious surfaces, SQO, ACQOP, and WSQOP are also primary controlling parameters, but for these surfaces the maximum storage for each nutrient (SQOLIM) is also important (Bicknell et al., 2005).

HSPF allows for monthly variation of some parameters; however, given a lack of information on variation in these parameters and to make the most accurate comparison to other models applied to the NRE which use constant parameters, all model parameters were held constant throughout all model runs. Stream length was determined not to have a significant effect on the model and was therefore approximated using the ArcGIS measuring tool on NHD flowlines within delineated sub-watersheds. A mean stream length of 2.4 km was used for all MCBCL sub-watersheds and a stream length of 11.3 km was used for MCBCL as a whole.

When HSPF was initially opened after the data input process within BASINS 4.0, parameter values were automatically populated for each sub-watershed. The automated parameter values were often not within reasonable ranges and often resulted in warning/error messages that would cause the model to crash. Therefore, parameter values used by Dr. Jian Shen (pers. comm.) in an ongoing application of the HSPF model on the Delmarva Peninsula, another low relief, coastal plain system with similar land uses, were often used as a starting point for model calibration. For each calibration step (i.e., hydrology, sediments, nutrients), one MCBCL sub-watershed was selected at random, and the parameters were manipulated, focusing on the parameters listed above, to obtain the best possible fit to monthly mean observations, assessed both visually and through regression of observed and modeled values. In general, parameter values were adjusted according to grouped land use types, where parameters for pervious surfaces, impervious surfaces, and water/wetlands were adjusted independently. The resulting .uci file containing model parameters was then copied and used as a template for the other MCBCL sub-watersheds, changing only the date range for the model run (to match that of the available data from each gauge) and the land use distribution within each sub-watershed. Monthly means of daily modeled and observed loads were compared by visual fit and regression analysis for each sub-watershed, and annual means of daily loads were compared by regression across all MCBCL watersheds for all monitoring data when available.

Once calibration was complete for each sub-watershed, the .uci file was adapted to reflect that of the entire NRE watershed located on MCBCL. Stream length was increased to 11.3 km based on the NHD flowlines and the change in elevation from the most upland portion of the watershed on the base to the estuary was increased from 3 m to 9.1 m based on the DEM, and the area of each land use type was modified to reflect that of MCBCL. HSPF was used to compute monthly loads of fresh water, sediments, and nutrients to the NRE from that portion of its watershed on MCBCL for January 1, 2008 through June 30, 2010. Modeled loads of TN were compared to the other main external sources of TN to the NRE (the upland watershed off-base, the MCBCL wastewater treatment facility, atmospheric deposition, and advection from Onslow Bay) determined as part of DCERP by Brush (2012) and Anderson et al. (2012), to assess the importance of MCBCL watershed processes to estuarine nutrient loading.

Finally, the calibrated HSPF model was used to assess potential changes in watershed loads from MCBCL to the NRE due to ongoing development on the base.. The effect of ongoing and future development on MCBCL was assessed by running HSPF with 5%, 10%, 15%, 20%, 25% and 30% conversion of forested land to impervious surface relative to current land use distributions. Approximately 13% of MCBCL is currently covered by impervious surfaces based on the 2001 NLCD.

PLOAD Model

In contrast to the complex HSPF model, the Pollutant Loading Model (PLOAD) is a simple, generic export coefficient model for computing annual loads that has been adapted for use within the BASINS GIS interface. The model was designed to provide initial estimates of annual non-point source pollution within a watershed. The model can be run using two separate methods, the export coefficient method or the simple method. Within the export coefficient method, each of the pollutant loads from each watershed is calculated using export coefficient tables provided by the model. The simple method was the method chosen for use in this study, because it allows for the specification of annual precipitation and storm ratio values. The simple method calculates pollutant loads through derivation of the runoff coefficient for each land use specified within the watershed and the estimated percent imperviousness of each land use type (PLOAD User's Manual, 2001).

The model requires, at a minimum, GIS-based National Land Cover Data (NLCD 2001), precipitation data and shapefiles of the watershed boundaries. There is an option to input various tabular data including pollutant loading rates, an impervious factor for each land cover type, and the efficiency of best management practices within the desired area. The model uses land use specific event mean concentrations of each pollutant to compute loads; standard tabular data values provided with PLOAD were used for all model runs given the lack of land use specific values. To facilitate a comparison of the ability of the simple PLOAD and complex HSPF models to compute annual loads, PLOAD was used to estimate the annual loads of total nitrogen (TN), PO_4^{3-}, and total suspended solids (TSS) in each MCBCL sub-watershed using the July 2008-June 2009 and July 2009-June 2010 annual rainfall totals recorded during DCERP (116.8 and 124.5 cm y^{-1}, respectively).

RESULTS

HSPF Model

Stream Flow

All HSPF results presented here focus on monthly and annual averages of daily predicted values. Time series of daily predictions and observations are provided in the Appendix. HSPF-predicted stream flows closely followed the observed patterns of precipitation (Fig. 5). In general, HSPF over-predicted stream flow in most sub-watersheds, except in Southwest and Airport where the model under-predicted flow (Fig. 5, Table 2). Across all nine sub-watersheds, the coefficient of determination (R^2) between measured and modeled monthly flows ranged between 0.035 in Tarawa and 0.5429 in Airport (Table 2). HSPF requires 12 months of gauge data to compute an annual average, which does not necessarily correspond to a calendar year. For 2008, Cogdels, Giletts, Traps, French and Tarawa had enough data to calculate an annual average, while all nine sub-watersheds had sufficient data in 2009 (Fig. 6, Appendix Table 1). Annual average loads confirm the tendency for HSPF to over-estimate flows in 2008, with little relationship to measured flows in 2009 once the much higher values from Southwest were removed.

Figure 5. Modeled (HSPF) and observed stream flows for each MCBCL sub-watershed. Upper panel gives regression results for mean monthly flows across all months where data were available. Annual mean flows are plotted for comparison but are not included in the regression. Lower panel gives the output as a monthly time series with observed precipitation (mean daily values each month). The time span of each plot is dependent on the time frame of gauge data available for each sub-watershed.

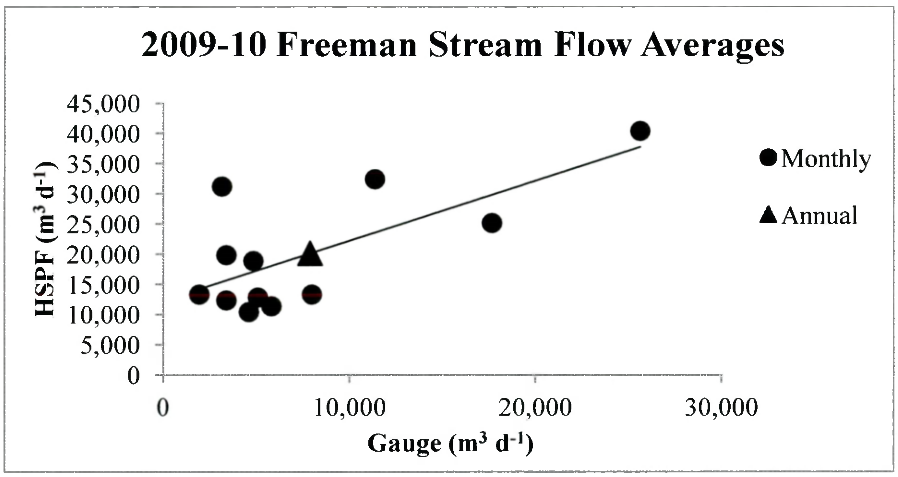

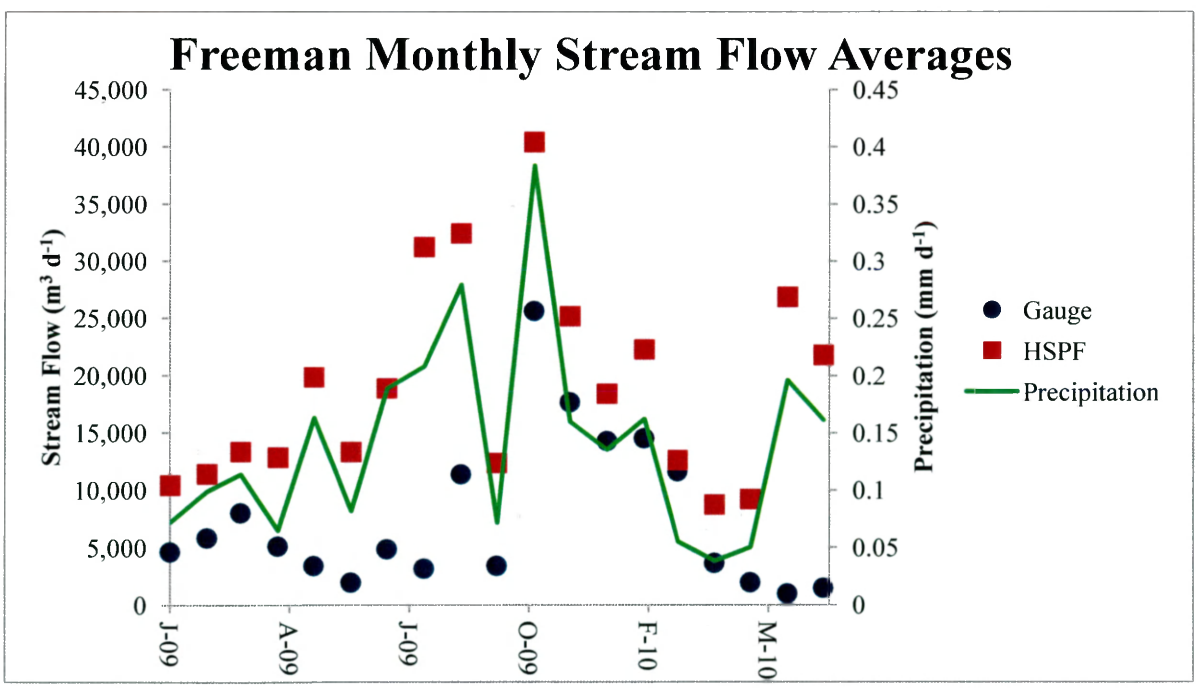

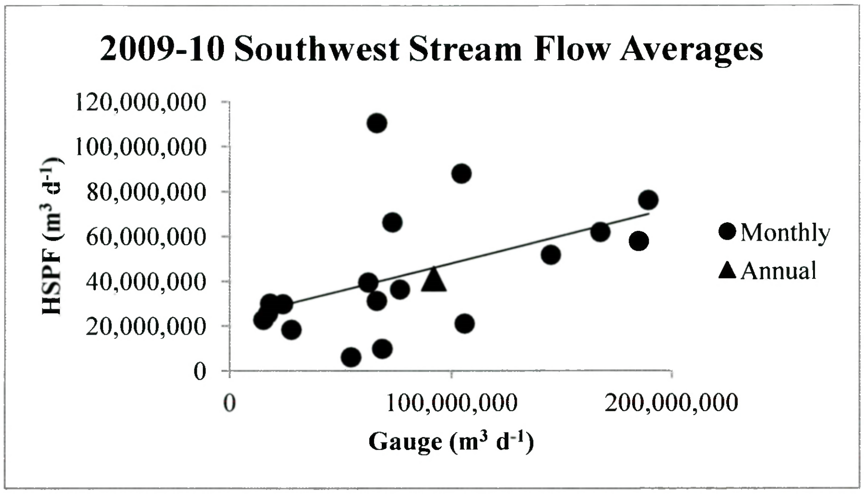

2009-10 Southwest Stream Flow Averages
120,000,000
100,000,000
80,000,000
60,000,000
40,000,000
20,000,000
0
HSPF (m³ d⁻¹)
0
100,000,000
200,000,000
Gauge (m³ d⁻¹)
Monthly
Annual

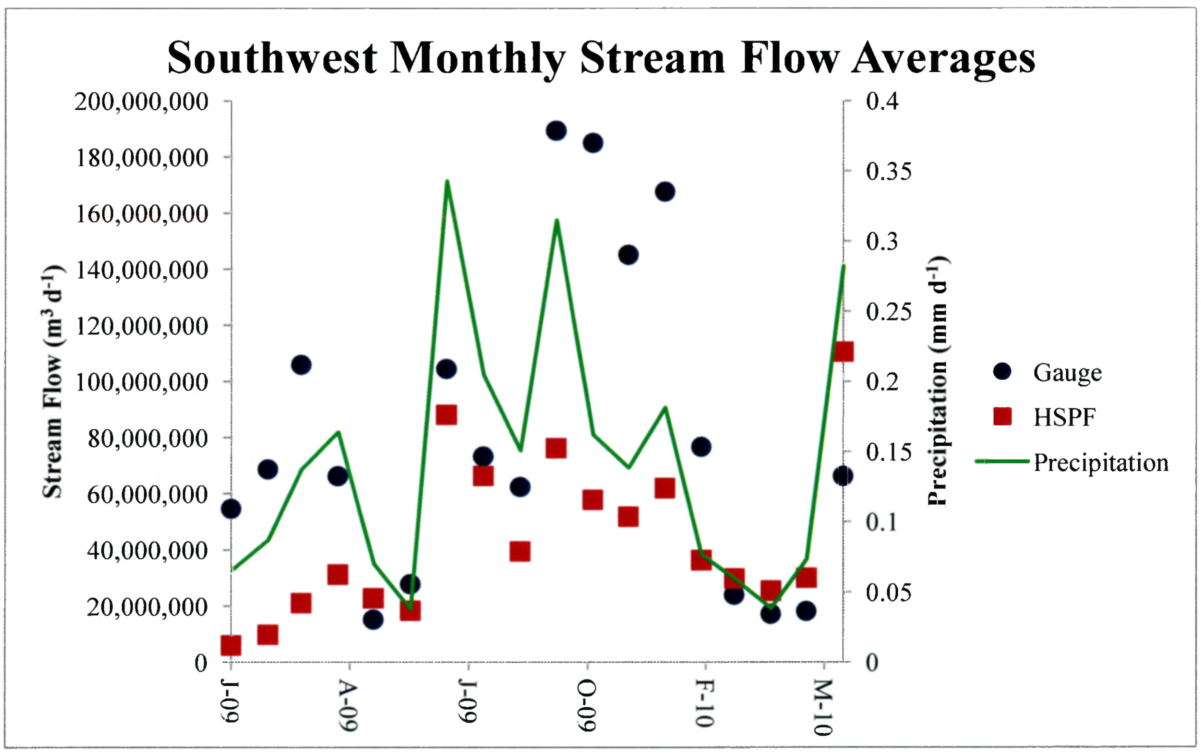

Southwest Monthly Stream Flow Averages
200,000,000
180,000,000
160,000,000
140,000,000
120,000,000
100,000,000
80,000,000
60,000,000
40,000,000
20,000,000
0
Stream Flow (m³ d⁻¹)
0.4
0.35
0.3
0.25
0.2
0.15
0.1
0.05
0
Precipitation (mm d⁻¹)
J-09
A-09
J-09
O-09
F-10
M-10
Gauge
HSPF
Precipitation

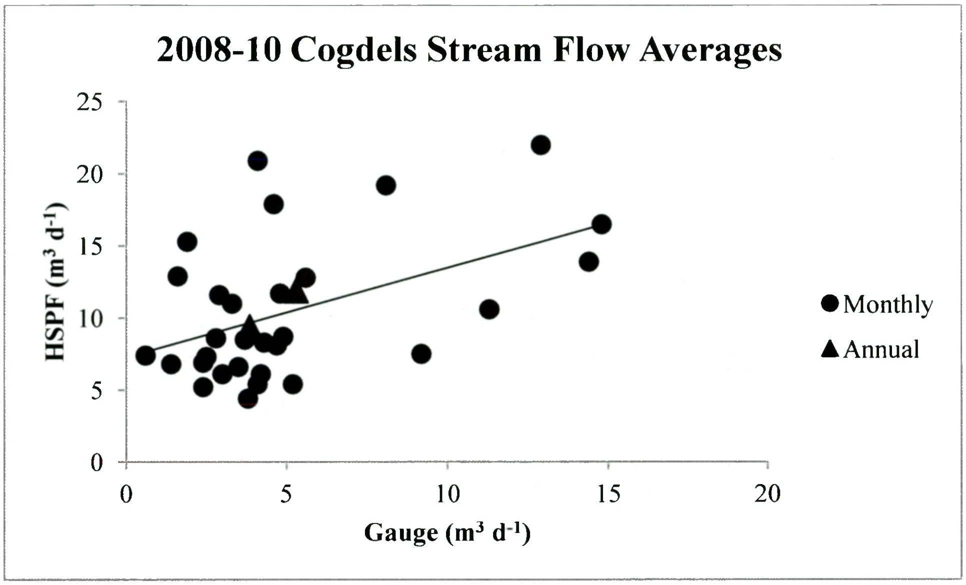
2008-10 Cogdels Stream Flow Averages
HSPF (m³ d⁻¹)
Gauge (m³ d⁻¹)
Monthly
Annual
0
5
10
15
20
25

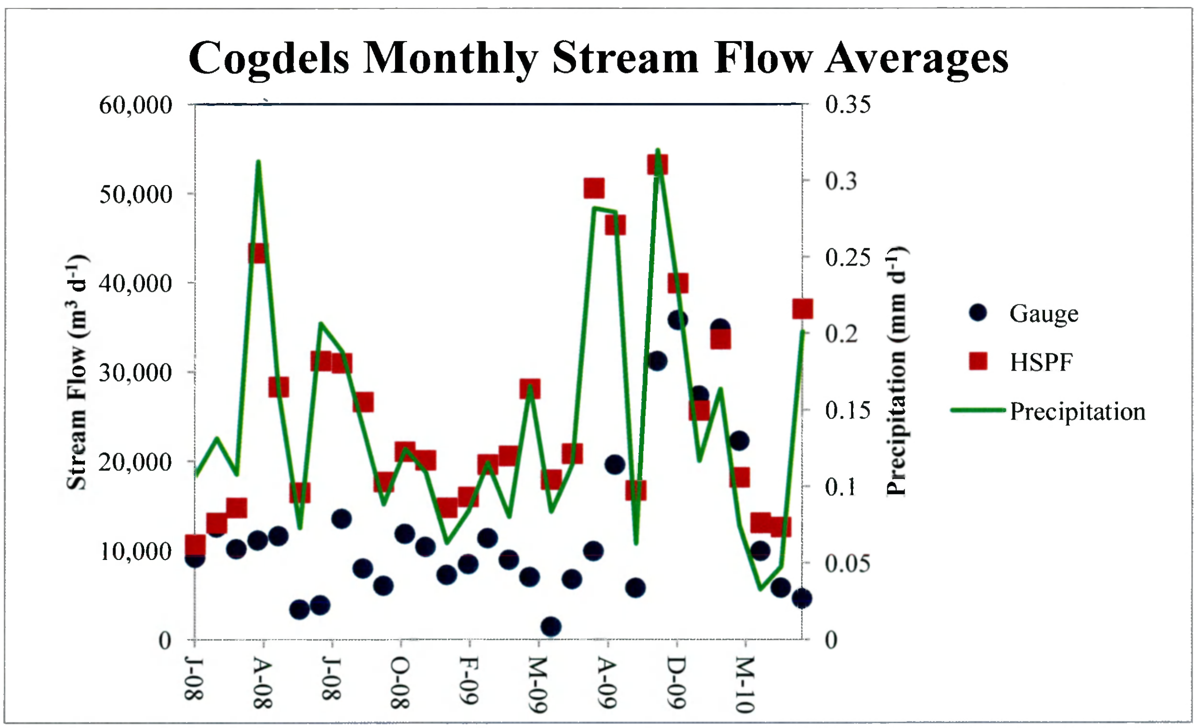
Cogdels Monthly Stream Flow Averages
Stream Flow (m³ d⁻¹)
Precipitation (mm d⁻¹)
Gauge
HSPF
Precipitation
J-08
A-08
J-08
O-08
F-09
M-09
A-09
D-09
M-10

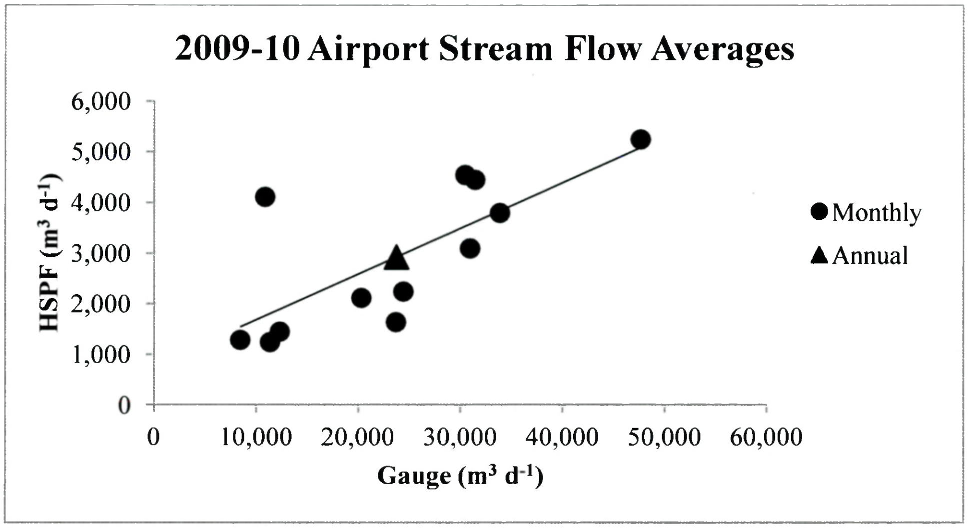
2009-10 Airport Stream Flow Averages
6,000
5,000
4,000
3,000
2,000
1,000
0
HSPF (m³ d⁻¹)
0
10,000
20,000
30,000
40,000
50,000
60,000
Gauge (m³ d⁻¹)
Monthly
Annual

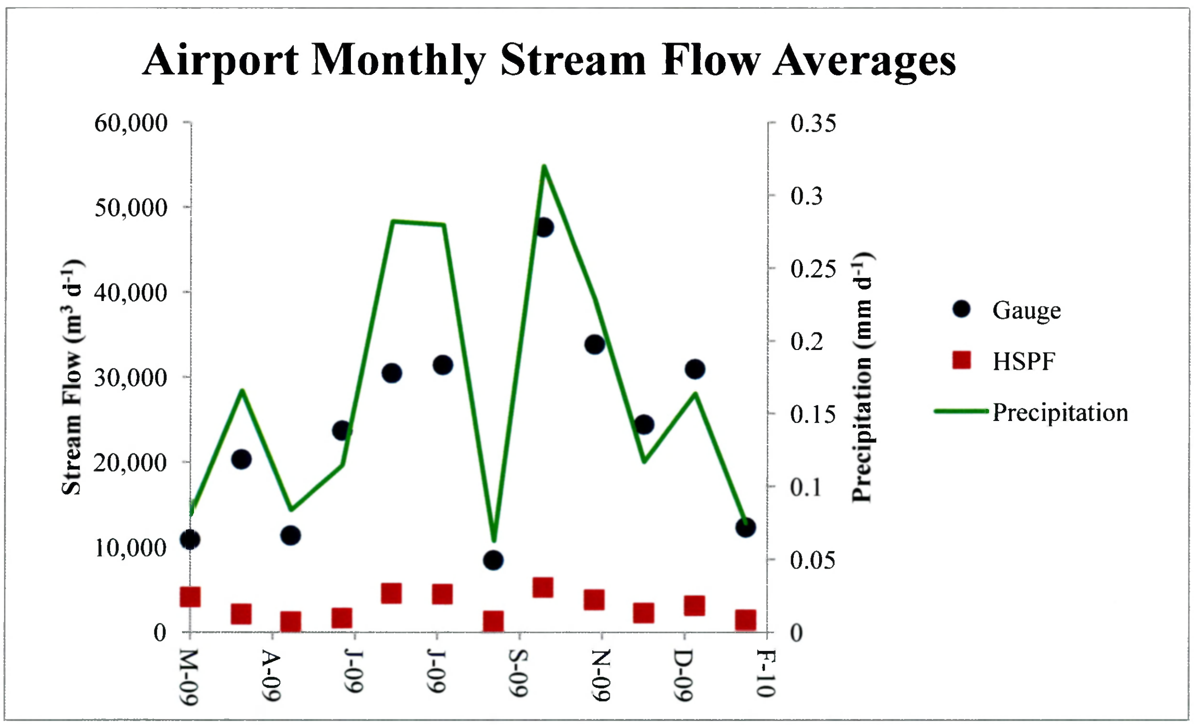
Airport Monthly Stream Flow Averages
60,000
50,000
40,000
30,000
20,000
10,000
0
Stream Flow (m³ d⁻¹)
0.35
0.3
0.25
0.2
0.15
0.1
0.05
0
Precipitation (mm d⁻¹)
M-09
A-09
J-09
J-09
S-09
N-09
D-09
F-10
Gauge
HSPF
Precipitation

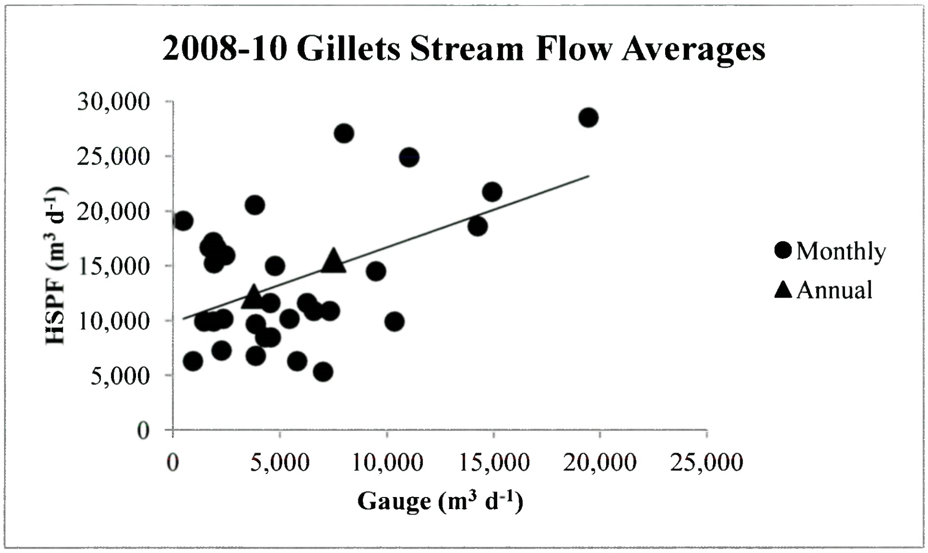

2008-10 Gillets Stream Flow Averages
30,000
25,000
20,000
15,000
10,000
5,000
0
HSPF (m³ d⁻¹)
0
5,000
10,000
15,000
20,000
25,000
Gauge (m³ d⁻¹)
Monthly
Annual

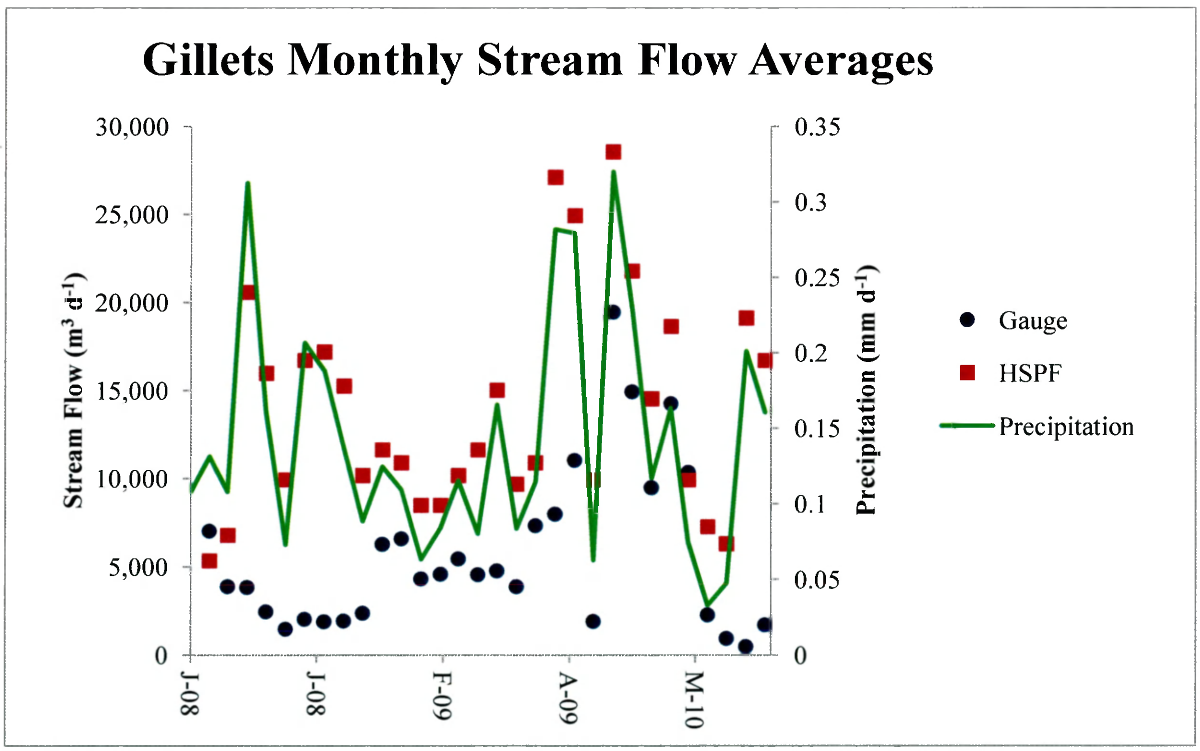

Gillets Monthly Stream Flow Averages
30,000
25,000
20,000
15,000
10,000
5,000
0
Stream Flow (m³ d⁻¹)
0.35
0.3
0.25
0.2
0.15
0.1
0.05
0
Precipitation (mm d⁻¹)
J-08
J-08
F-09
A-09
M-10
Gauge
HSPF
Precipitation

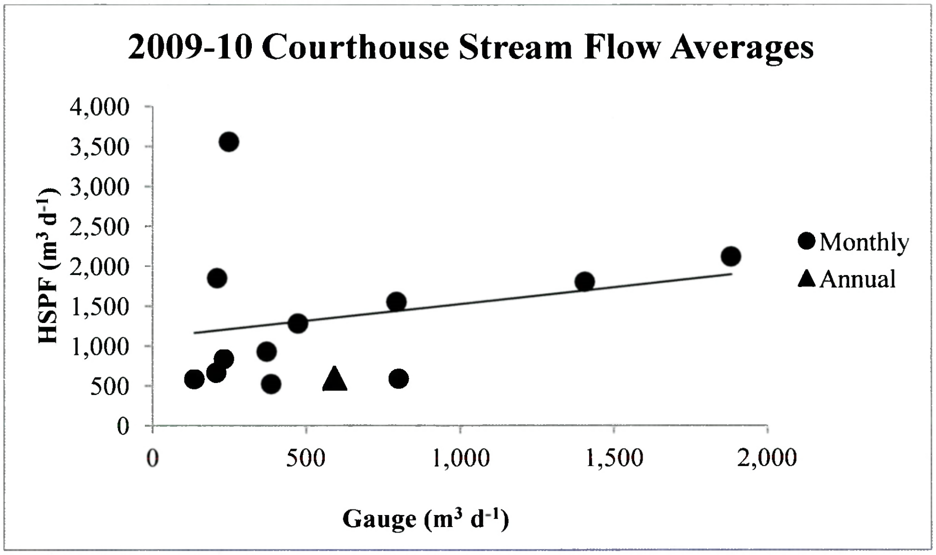
2009-10 Courthouse Stream Flow Averages
4,000
3,500
3,000
2,500
2,000
1,500
1,000
500
0
HSPF (m³ d⁻¹)
0
500
1,000
1,500
2,000
Gauge (m³ d⁻¹)
Monthly
Annual

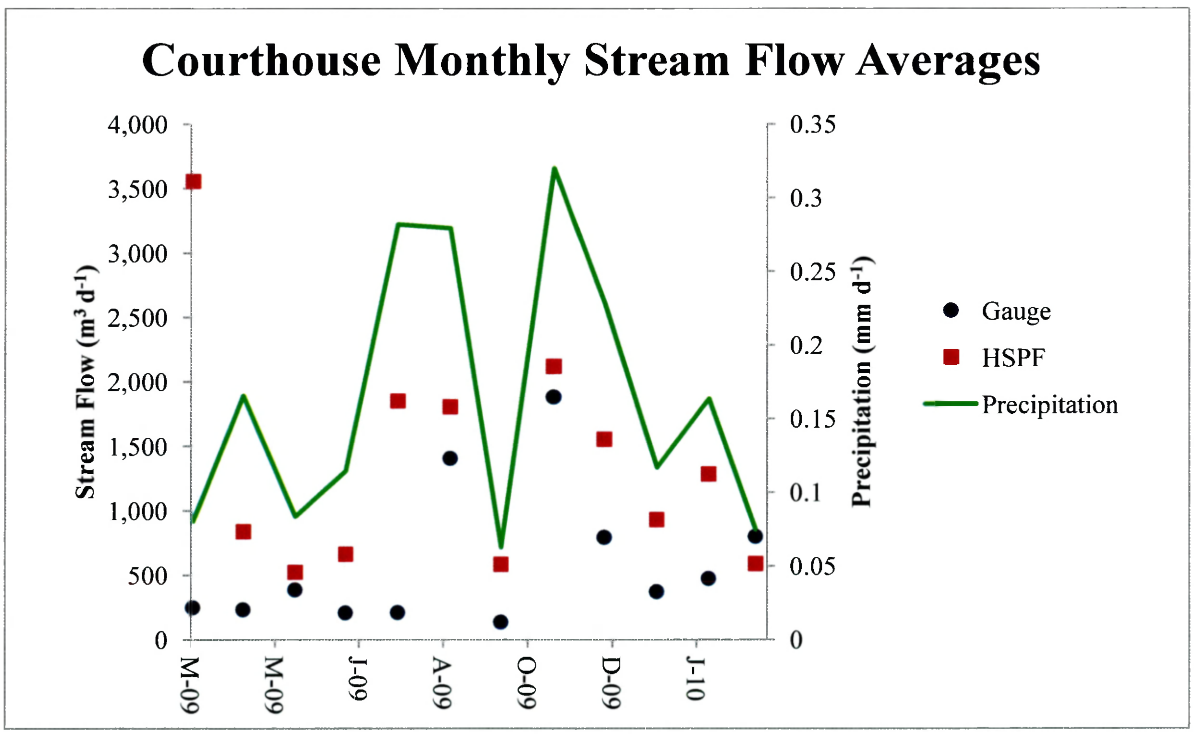
Courthouse Monthly Stream Flow Averages
4,000
3,500
3,000
2,500
2,000
1,500
1,000
500
0
Stream Flow (m³ d⁻¹)
0.35
0.3
0.25
0.2
0.15
0.1
0.05
0
Precipitation (mm d⁻¹)
M-09
M-09
J-09
A-09
O-09
D-09
J-10
Gauge
HSPF
Precipitation

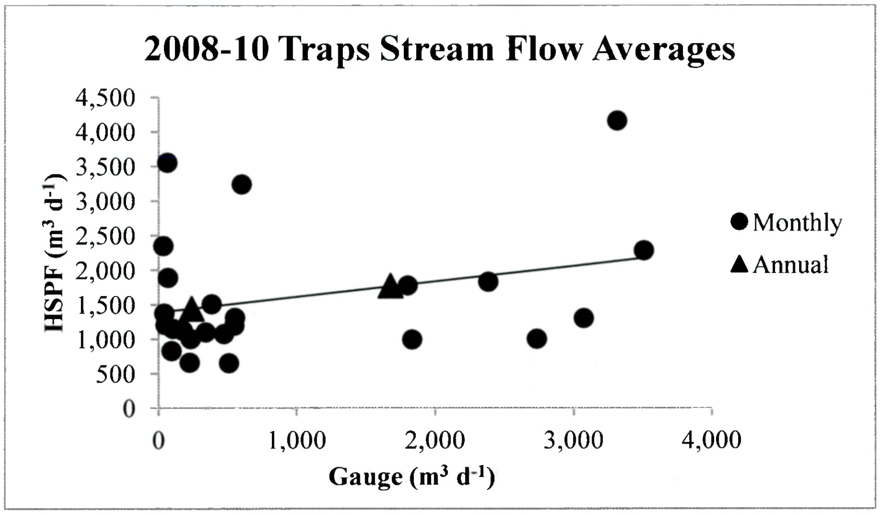
2008-10 Traps Stream Flow Averages
HSPF (m³ d⁻¹)
Gauge (m³ d⁻¹)
Monthly
Annual
4,500
4,000
3,500
3,000
2,500
2,000
1,500
1,000
500
0
1,000
2,000
3,000
4,000

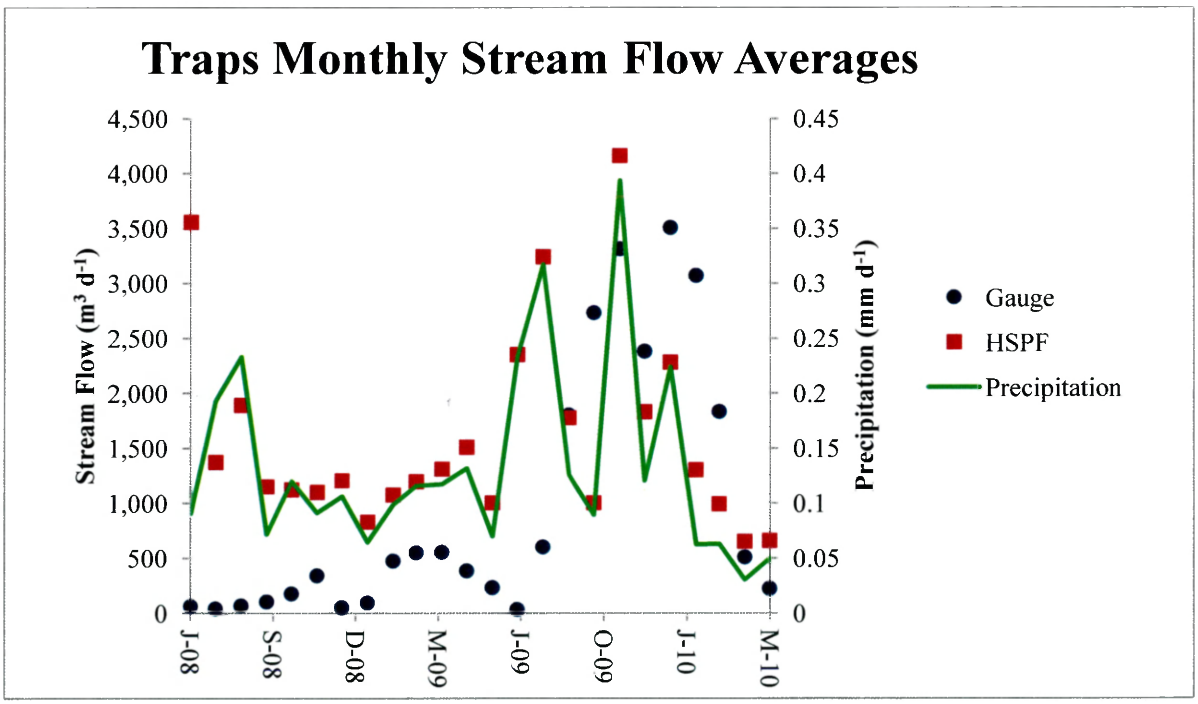
Traps Monthly Stream Flow Averages
Stream Flow (m³ d⁻¹)
Precipitation (mm d⁻¹)
Gauge
HSPF
Precipitation
4,500
4,000
3,500
3,000
2,500
2,000
1,500
1,000
500
0
0.45
0.4
0.35
0.3
0.25
0.2
0.15
0.1
0.05
0
J-08
S-08
D-08
M-09
J-09
O-09
J-10
M-10

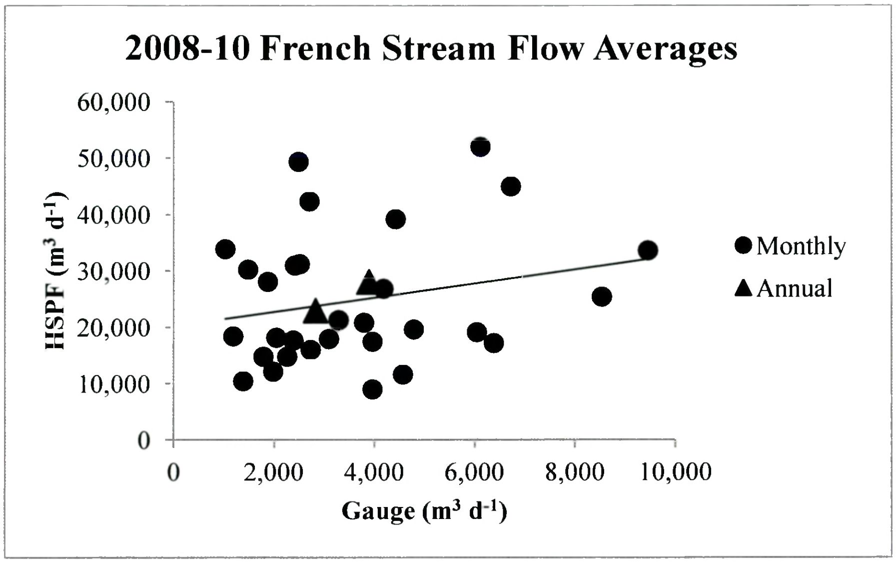
2008-10 French Stream Flow Averages
HSPF (m^3 d^{-1})
60,000
50,000
40,000
30,000
20,000
10,000
0
0
2,000
4,000
6,000
8,000
10,000
Gauge (m^3 d^{-1})
Monthly
Annual

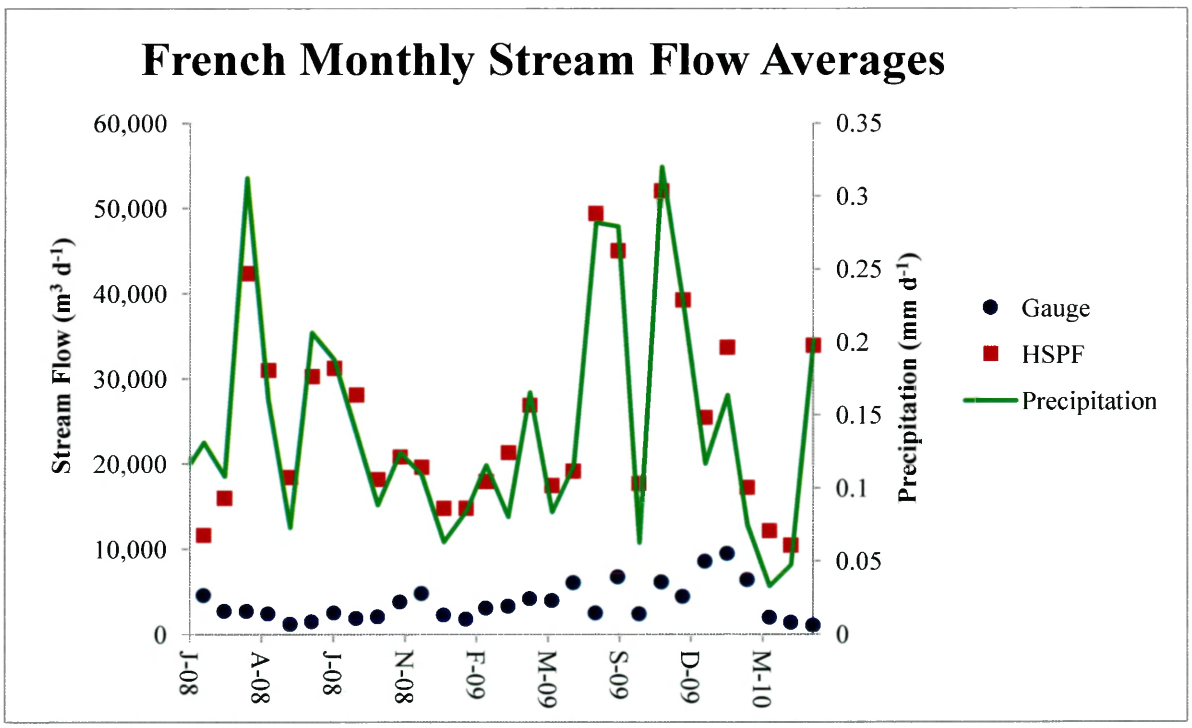
French Monthly Stream Flow Averages
Stream Flow (m^3 d^{-1})
60,000
50,000
40,000
30,000
20,000
10,000
0
Precipitation (mm d^{-1})
0.35
0.3
0.25
0.2
0.15
0.1
0.05
0
J-08
A-08
J-08
N-08
F-09
M-09
S-09
D-09
M-10
Gauge
HSPF
Precipitation

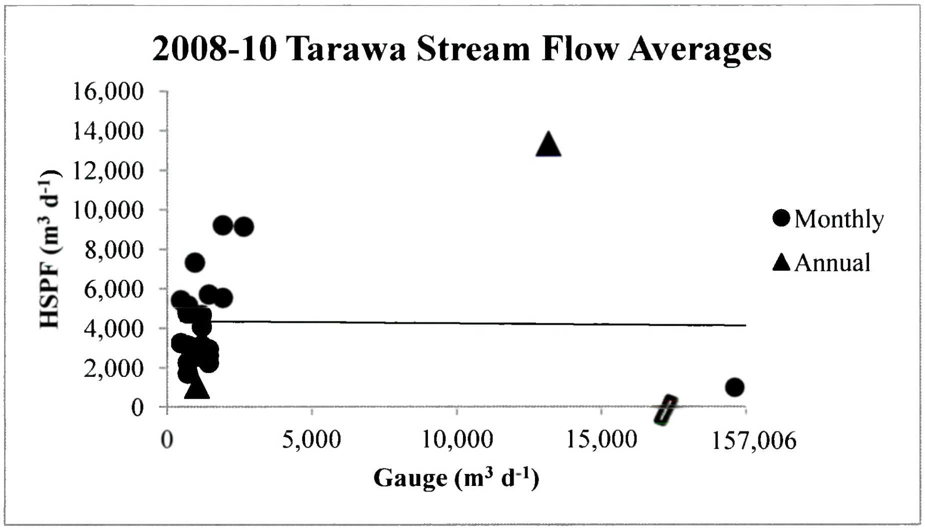
2008-10 Tarawa Stream Flow Averages
16,000
14,000
12,000
10,000
8,000
6,000
4,000
2,000
0
HSPF (m³ d⁻¹)
0
5,000
10,000
15,000
157,006
Gauge (m³ d⁻¹)
Monthly
Annual

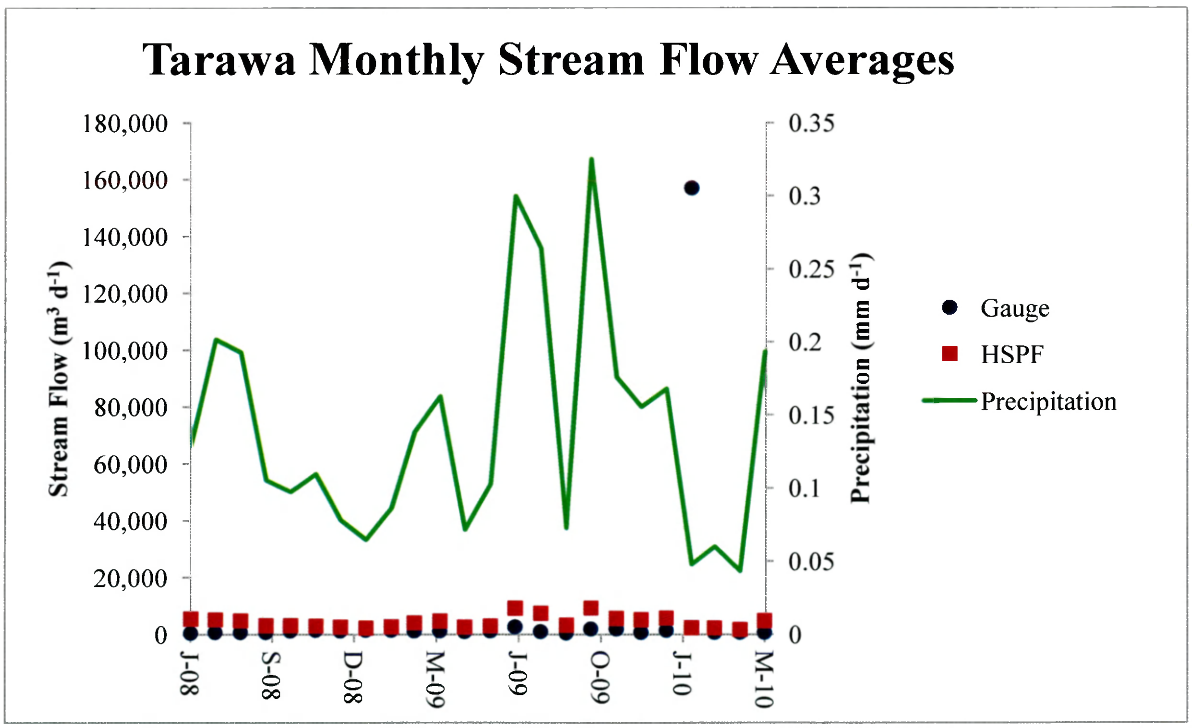
Tarawa Monthly Stream Flow Averages
180,000
160,000
140,000
120,000
100,000
80,000
60,000
40,000
20,000
0
Stream Flow (m³ d⁻¹)
0.35
0.3
0.25
0.2
0.15
0.1
0.05
0
Precipitation (mm d⁻¹)
J-08
S-08
D-08
M-09
J-09
O-09
J-10
M-10
Gauge
HSPF
Precipitation

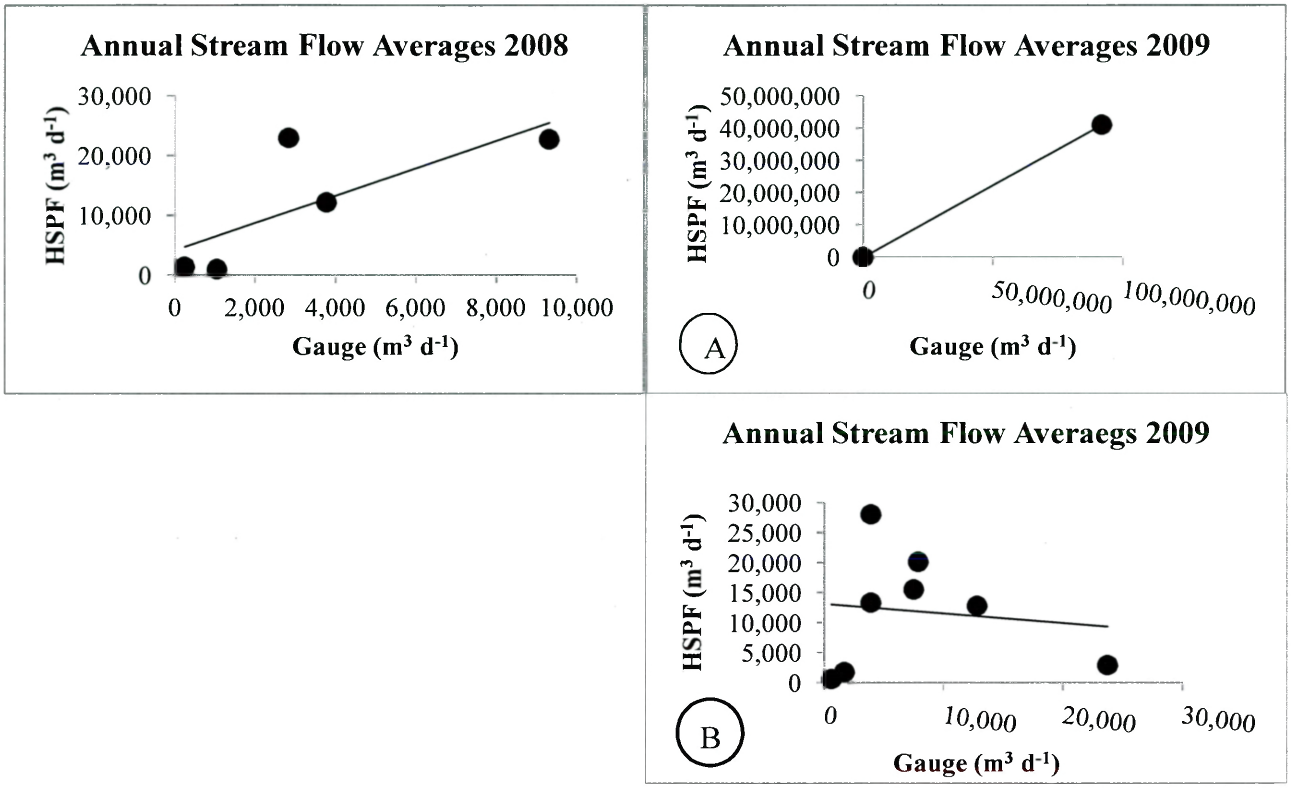

Figure 6. Annual mean observed and modeled stream flow from all sub-watersheds for which an annual cycle of data are available. Panel A of the annual stream flow averages for 2009 gives results for all sub-watersheds (most are clustered around the origin), and panel B removes the outlier (Southwest).

Table 2: Summary statistics for regressions between measured and modeled stream flow ($m^3\ d^{-1}$) from each sub-watershed at the monthly and annual resolution.

	R^2	Slope	Intercept
Monthly			
Freeman	0.50	0.99	12265.41
Southwest	0.25	0.25	2E+07
Cogdel	0.23	0.62	7.29
Airport	0.54	0.09	777.33
Gillets	0.25	0.69	9,846.5
Courthouse	0.07	0.42	1,108.09
Traps	0.08	0.22	1,390.27
French	0.05	1.26	20,196.33
Tarawa	0.04	-0.01	4,364.93
Annual			
2008	0.57	2.29	4,229.85
2009	0.02	-0.16	13,149.54

Sediment Load

Sediment loads to the sub-watersheds also followed the precipitation time series (Fig. 7). Coefficients of determination for monthly loads ranged from 0.0004 in Cogdels to 0.51 in Airport (Table 3). While Cogdels had the lowest R^2, the modeled loads were nevertheless on the same scale as the measured loads and appeared to track the data. Conversely, while Airport had the highest R^2, the model predicted loads nearly one order of magnitude lower than measured loads. The model over-predicted sediment loads to Southwest, Courthouse, Traps, and French, with the latter approximately three orders of magnitude different. HSPF under-predicted sediment loads to Airport and Tarawa, and predicted loads to Cogdels and Gillets in the correct range. The annual averaged daily loads revealed that there was not a general tendency for HSPF to either over or under-estimate sediment loads across the sub-watersheds for both 2008 and 2009 (Fig. 8, Appendix Table 1).

Figure 7. Modeled (HSPF) and observed sediment loads for each MCBCL sub-watershed. Upper panel gives regression results for mean monthly loads across all months where data were available. Annual mean loads are plotted for comparison but are not included in the regression. Lower panel gives the output as a monthly time series with observed precipitation (mean daily values each month). The time span of each plot is dependent on the time frame of gauge data available for each sub-watershed.

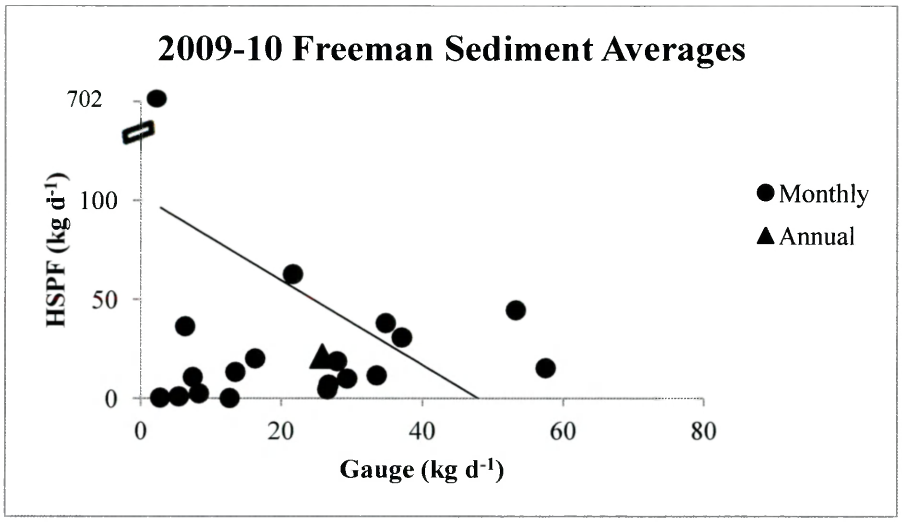

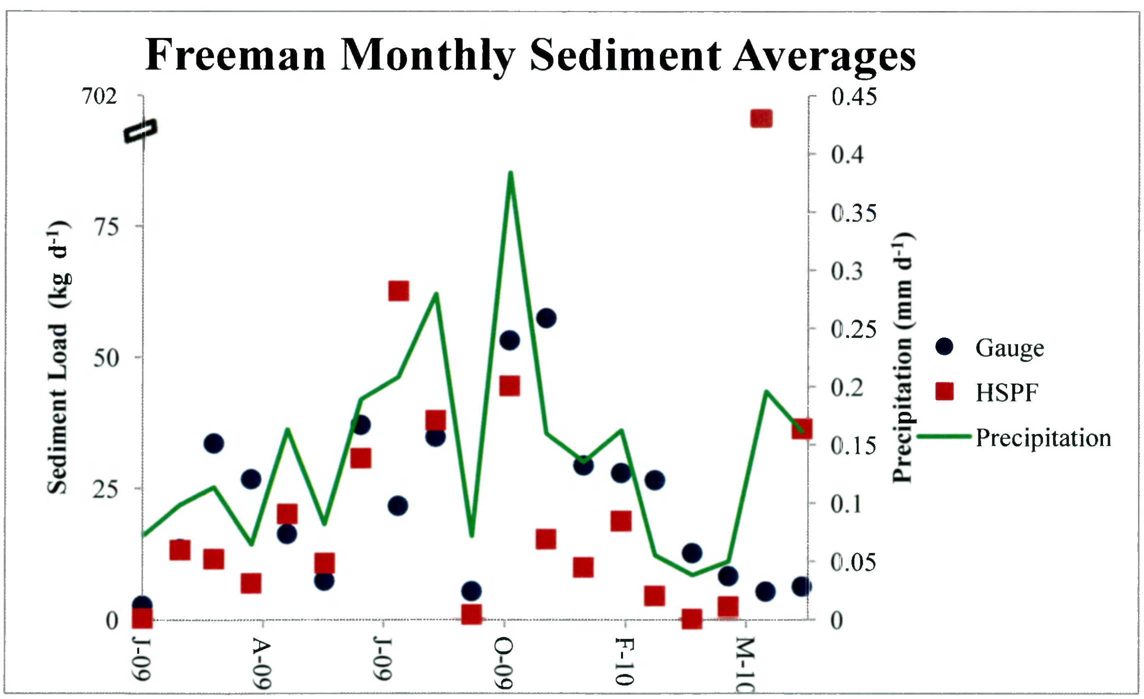

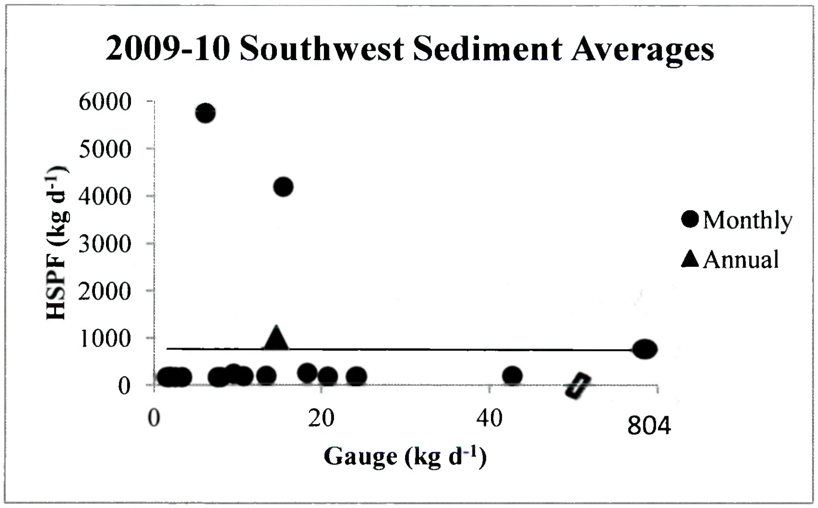
2009-10 Southwest Sediment Averages
6000
5000
4000
3000
2000
1000
0
HSPF (kg d-1)
0
20
40
804
Gauge (kg d-1)
Monthly
Annual

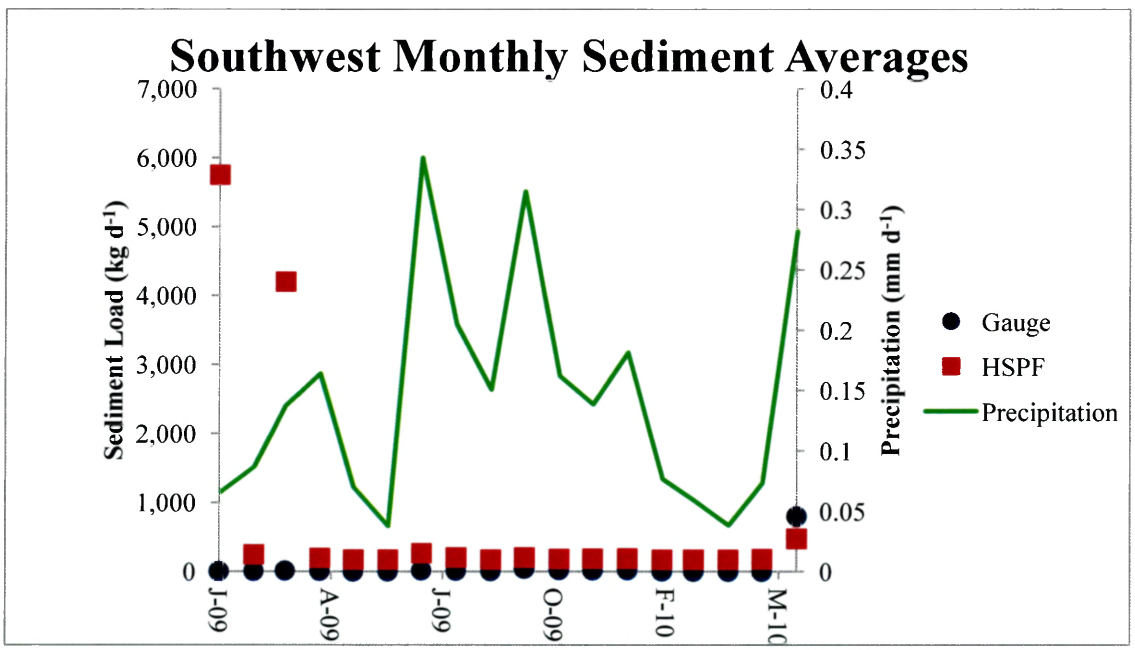
Southwest Monthly Sediment Averages
7,000
6,000
5,000
4,000
3,000
2,000
1,000
0
Sediment Load (kg d-1)
0.4
0.35
0.3
0.25
0.2
0.15
0.1
0.05
0
Precipitation (mm d-1)
J-09
A-09
J-09
O-09
F-10
Gauge
HSPF
Precipitation

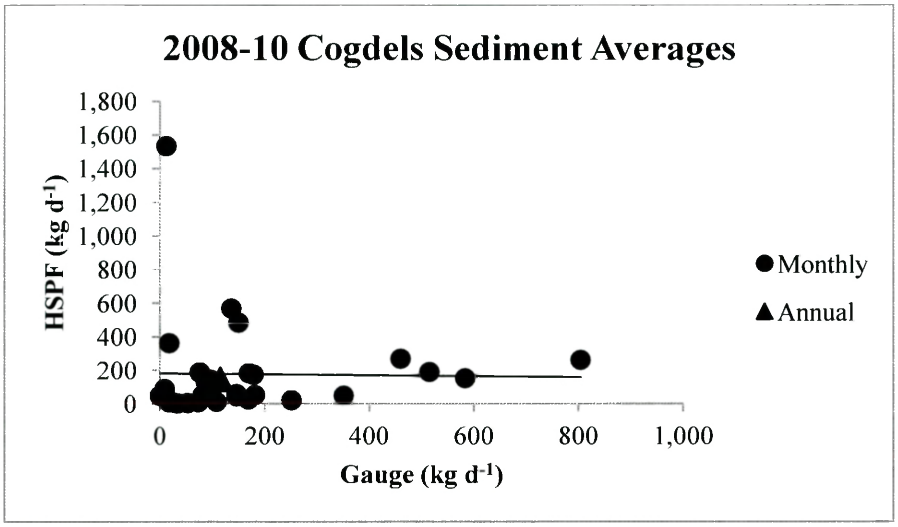

2008-10 Cogdels Sediment Averages
HSPF (kg d-1)
1,800
1,600
1,400
1,200
1,000
800
600
400
200
0
0
200
400
600
800
1,000
Gauge (kg d-1)
Monthly
Annual

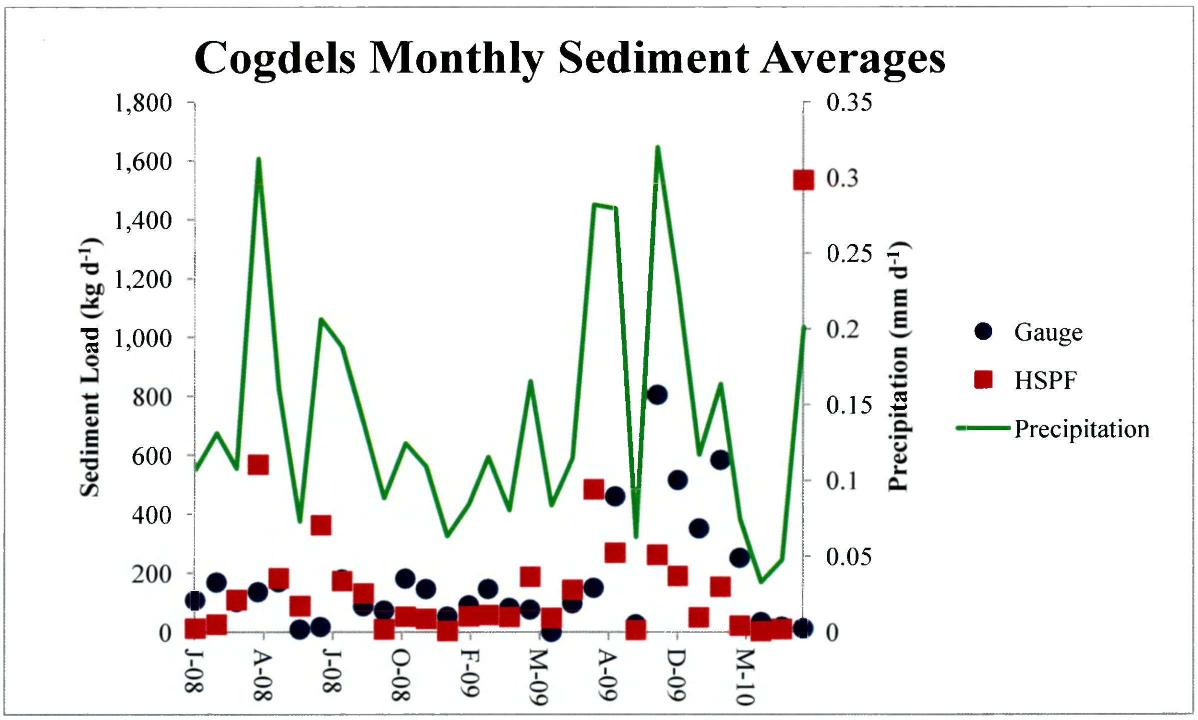

Cogdels Monthly Sediment Averages
Sediment Load (kg d-1)
1,800
1,600
1,400
1,200
1,000
800
600
400
200
0
Precipitation (mm d-1)
0.35
0.3
0.25
0.2
0.15
0.1
0.05
0
J-08
A-08
J-08
O-08
F-09
M-09
A-09
D-09
M-10
Gauge
HSPF
Precipitation

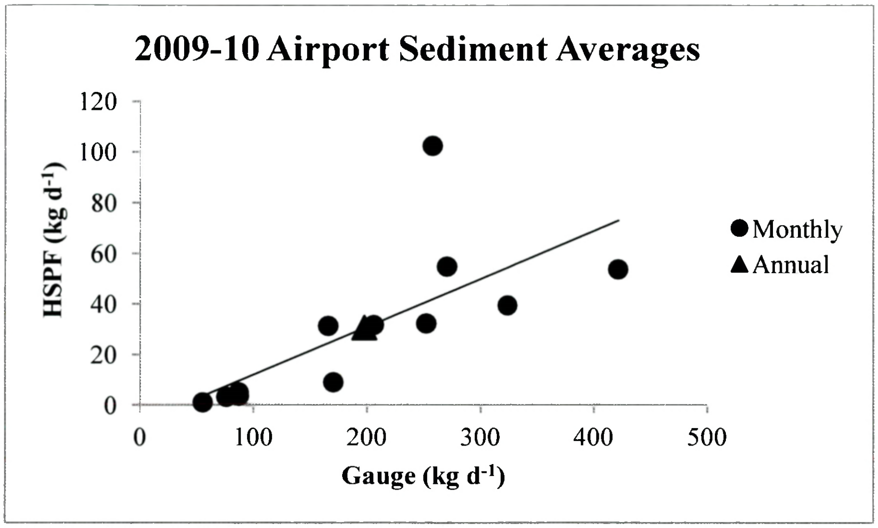
2009-10 Airport Sediment Averages
HSPF (kg d-1)
Gauge (kg d-1)
Monthly
Annual
120
100
80
60
40
20
0
0
100
200
300
400
500

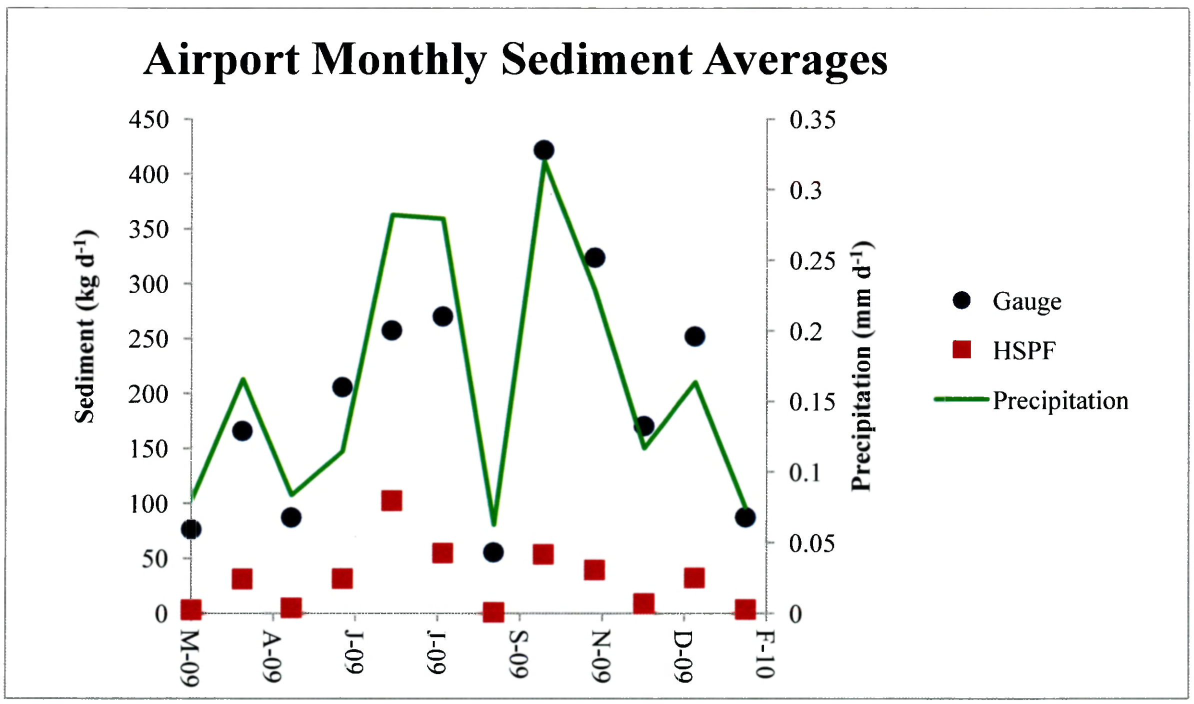
Airport Monthly Sediment Averages
Sediment (kg d-1)
Precipitation (mm d-1)
Gauge
HSPF
Precipitation
450
400
350
300
250
200
150
100
50
0
0.35
0.3
0.25
0.2
0.15
0.1
0.05
0
M-09
A-09
J-09
J-09
S-09
N-09
D-09
F-10

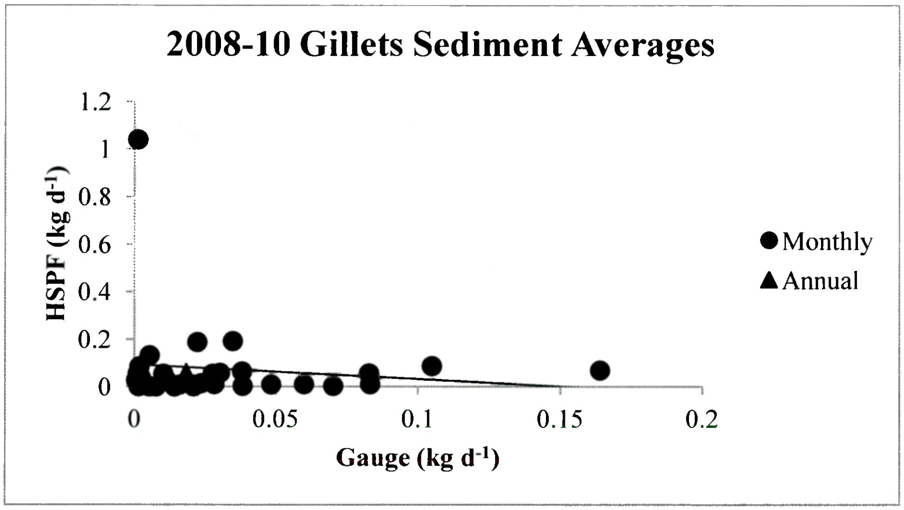

2008-10 Gillets Sediment Averages
HSPF (kg d-1)
1.2
1
0.8
0.6
0.4
0.2
0
0
0.05
0.1
0.15
0.2
Gauge (kg d-1)
Monthly
Annual

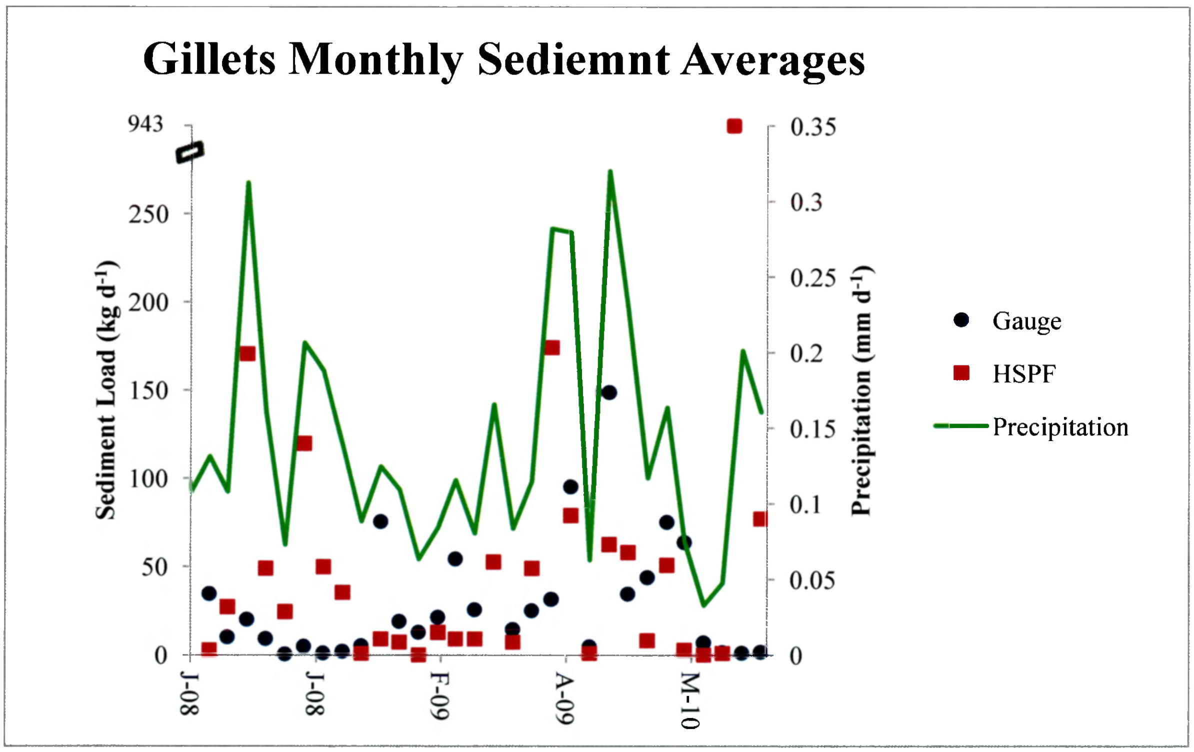

Gillets Monthly Sediemnt Averages
Sediment Load (kg d-1)
943
250
200
150
100
50
0
J-08
J-08
F-09
A-09
M-10
Precipitation (mm d-1)
0.35
0.3
0.25
0.2
0.15
0.1
0.05
0
Gauge
HSPF
Precipitation

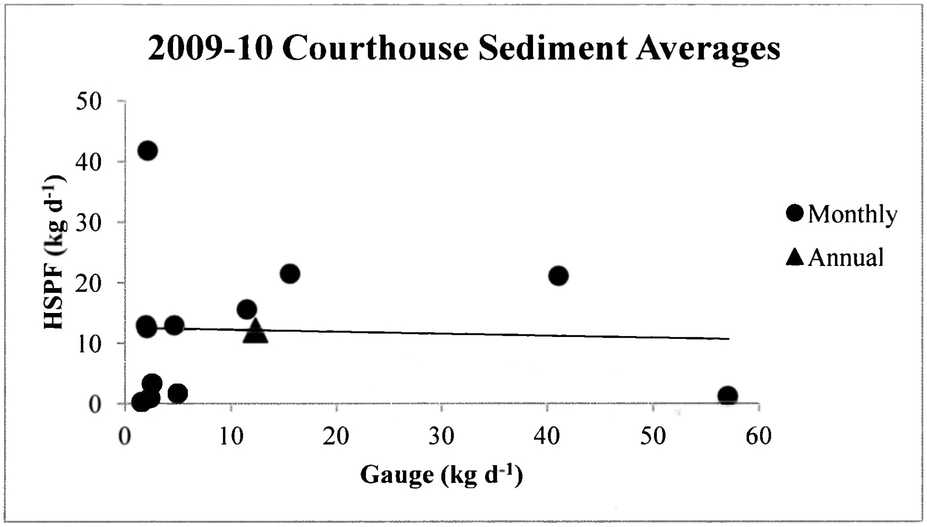
2009-10 Courthouse Sediment Averages
HSPF (kg d-1)
Gauge (kg d-1)
Monthly
Annual
0
10
20
30
40
50
60

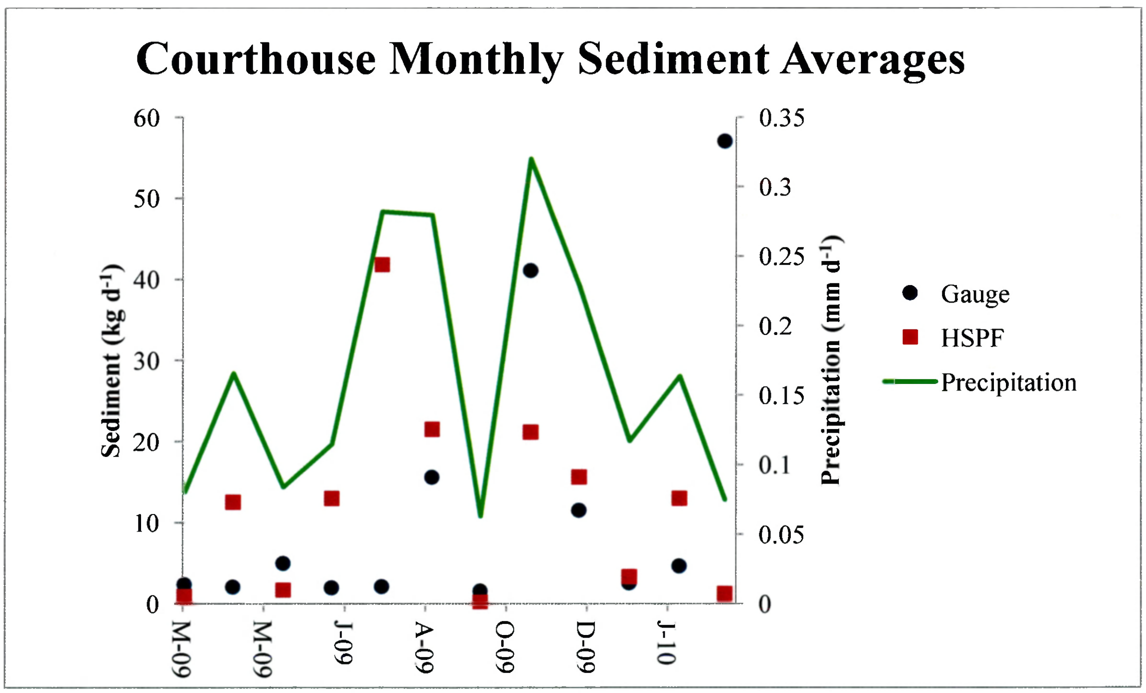
Courthouse Monthly Sediment Averages
Sediment (kg d-1)
Precipitation (mm d-1)
Gauge
HSPF
Precipitation
M-09
M-09
J-09
A-09
O-09
D-09
J-10

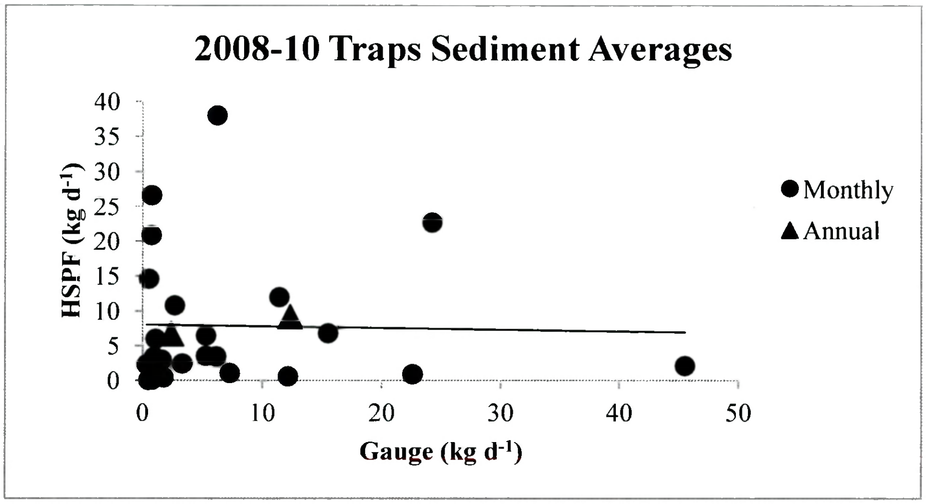
2008-10 Traps Sediment Averages
HSPF (kg d-1)
Gauge (kg d-1)
Monthly
Annual
40
35
30
25
20
15
10
5
0
0
10
20
30
40
50

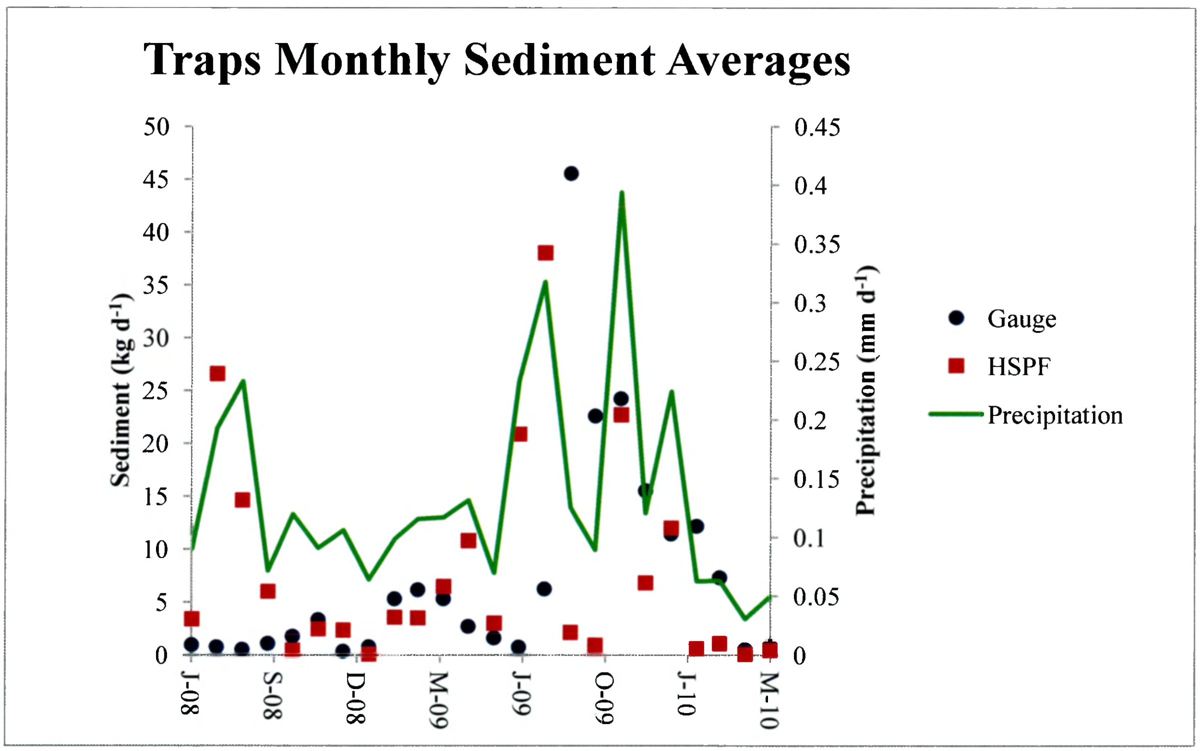
Traps Monthly Sediment Averages
Sediment (kg d-1)
Precipitation (mm d-1)
Gauge
HSPF
Precipitation
50
45
40
35
30
25
20
15
10
5
0
0.45
0.4
0.35
0.3
0.25
0.2
0.15
0.1
0.05
0
J-08
S-08
D-08
M-09
J-09
O-09
J-10
M-10

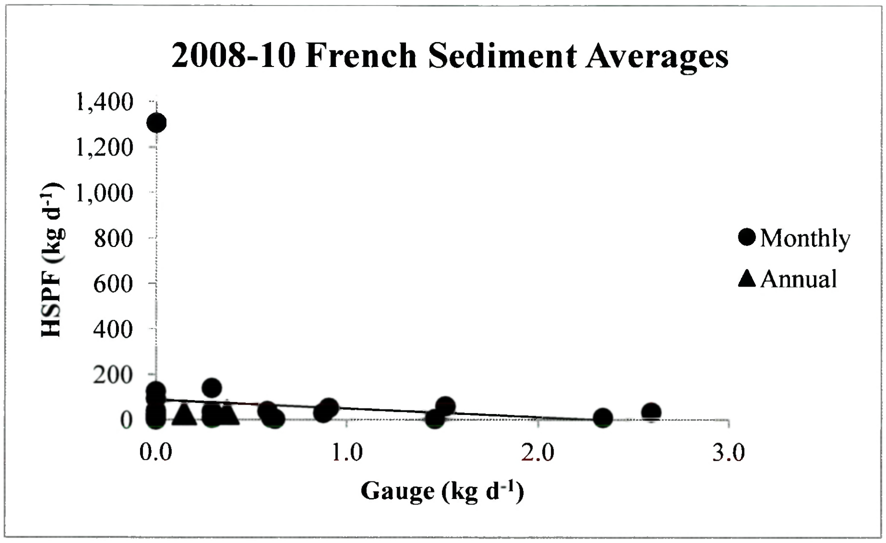

2008-10 French Sediment Averages
HSPF (kg d-1)
Gauge (kg d-1)
Monthly
Annual

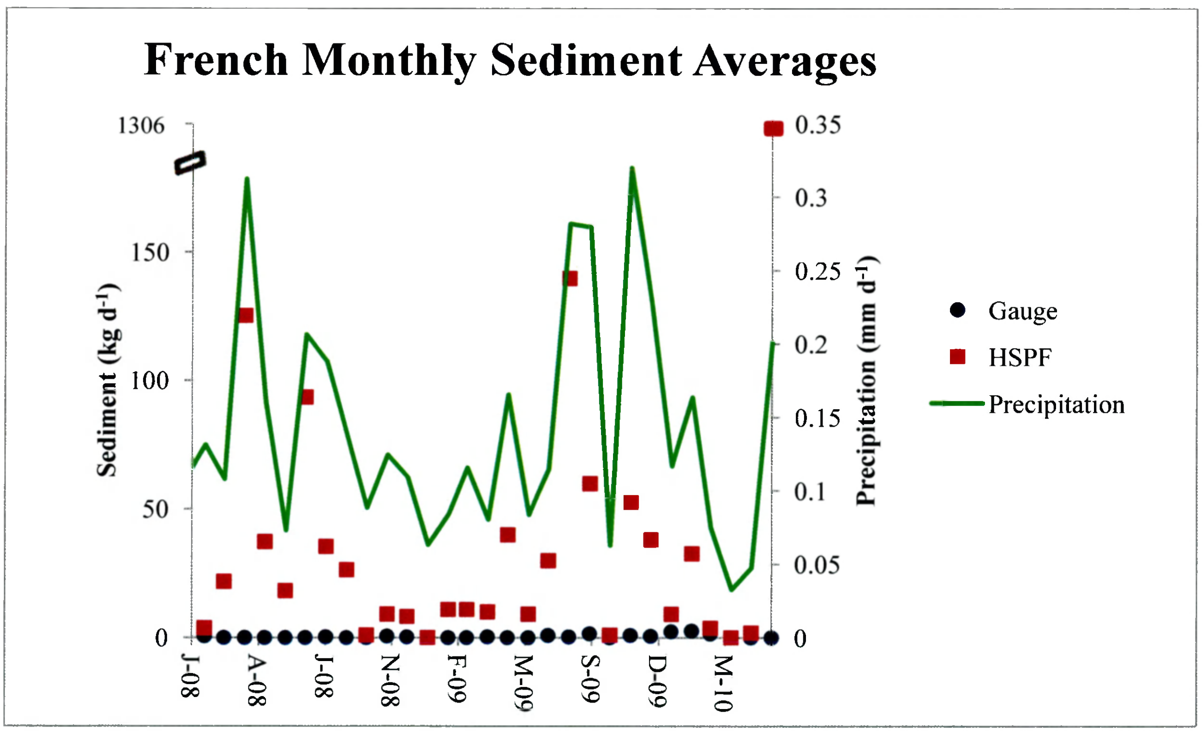

French Monthly Sediment Averages
Sediment (kg d-1)
Precipitation (mm d-1)
Gauge
HSPF
Precipitation

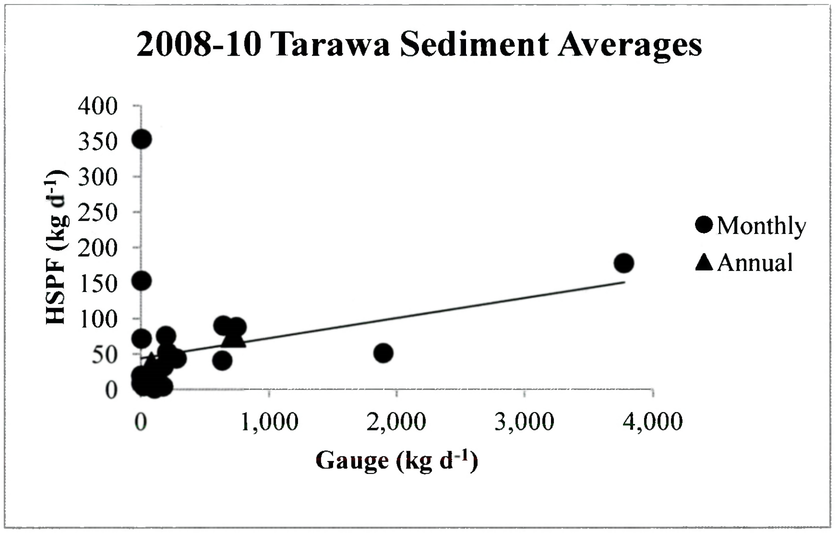
2008-10 Tarawa Sediment Averages
HSPF (kg d-1)
Gauge (kg d-1)
Monthly
Annual
400
350
300
250
200
150
100
50
0
0
1,000
2,000
3,000
4,000

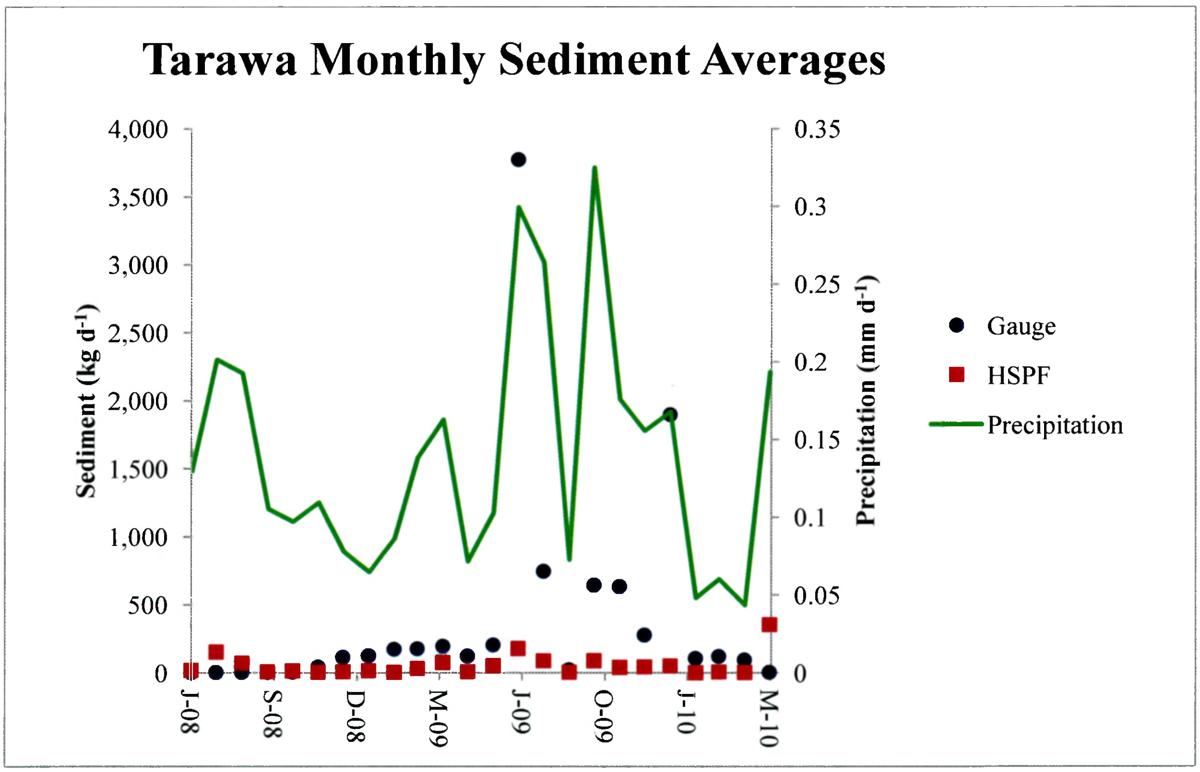
Tarawa Monthly Sediment Averages
Sediment (kg d-1)
Precipitation (mm d-1)
Gauge
HSPF
Precipitation
4,000
3,500
3,000
2,500
2,000
1,500
1,000
500
0
0.35
0.3
0.25
0.2
0.15
0.1
0.05
0
J-08
S-08
D-08
M-09
J-09
O-09
J-10
M-10

Figure 8 Annual mean observed and modeled sediment load from all sub-watersheds for which an annual cycle of data are available.

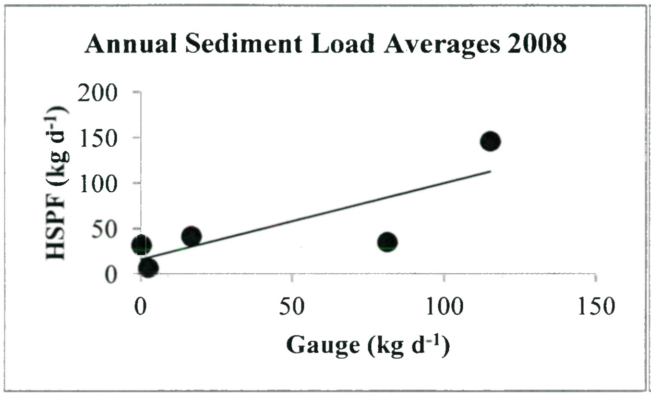

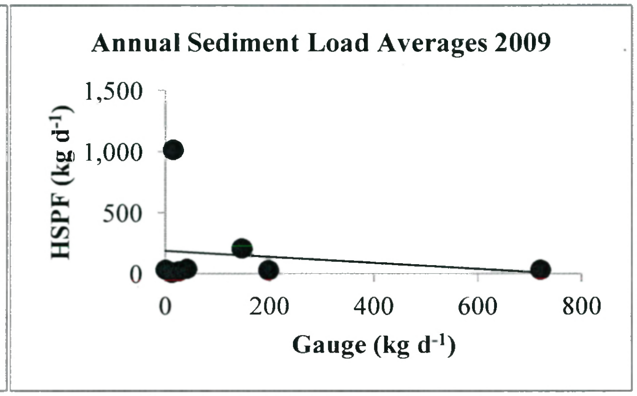

Table 3: Summary statistics for regressions between measured and modeled sediment loads (kg d^{-1}) from each sub-watershed at the monthly and annual resolution.

	R^2	Slope	Intercept
Monthly			
Freeman	0.05	-2.13	102.18
Southwest	0.002	-0.39	762.21
Cogdel	0.0004	-0.03	180.71
Airport	0.51	0.19	-6.91
Gillets	0.01	-0.62	0.09
Courthouse	0.003	-0.03	12.60
Traps	0.0007	-0.02	8.04
French	0.01	-37.79	87.17
Tarawa	0.09	0.03	44.15
Annual			
2008	0.65	0.84	15.98
2009	0.03	-0.24	187.90

NO_x^- and NH_4^+ Loads

HSPF tended to over-predict monthly loads of both NO_x^- and NH_4^+ to the sub-watersheds (Figs. 9, 11; Tables 4-5). HSPF most accurately modeled monthly NO_x^- loads to Southwest, with a coefficient of determination of 0.23. The least accurate simulation was in Traps, with an R^2 of 0.0032. The model most accurately simulated monthly NH_4^+ loads to Courthouse, with an R^2 of 0.39, and least accurately in Gillets, with an R^2 of 0.006. The model over-predicted loads for both nutrients in Southwest, Gillett, and French, and under-predicted loads of both nutrients in Airport and Tarawa. The model over-predicted loads for NO_x^- but under-predicted loads for NH_4^+ in Freeman. In Cogdels, the model predicted NO_x^- and NH_4^+ loads in the correct range, with the exception of late winter 2009 and early spring 2010. In Traps, the model over-predicted loads of NO_x^-, but predicted NH_4^+ loads in the correct range after the first few months.

HSPF had a tendency to over estimated 2008 NOx^- annual average loads, while in 2009 the annual averages were generally in the correct range (Fig. 10, Appendix Table 1). HSPF annual loads of NH_4^+ were within the same range as the data in 2008 and 2009, with no evidence for over or under-estimation (Fig. 12, Appendix Table 1).

Figure 9. Modeled (HSPF) and observed NO_x^- loads for each MCBCL sub-watershed. Upper panel gives regression results for mean monthly loads across all months where data were available. Annual mean loads are plotted for comparison but are not included in the regression. Lower panel gives the output as a monthly time series with observed precipitation (mean daily values each month). The time span of each plot is dependent on the time frame of gauge data available for each sub-watershed.

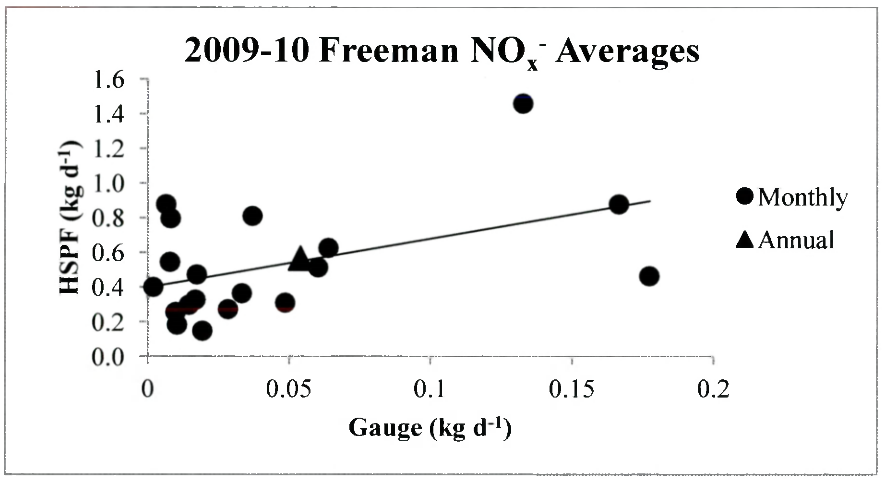

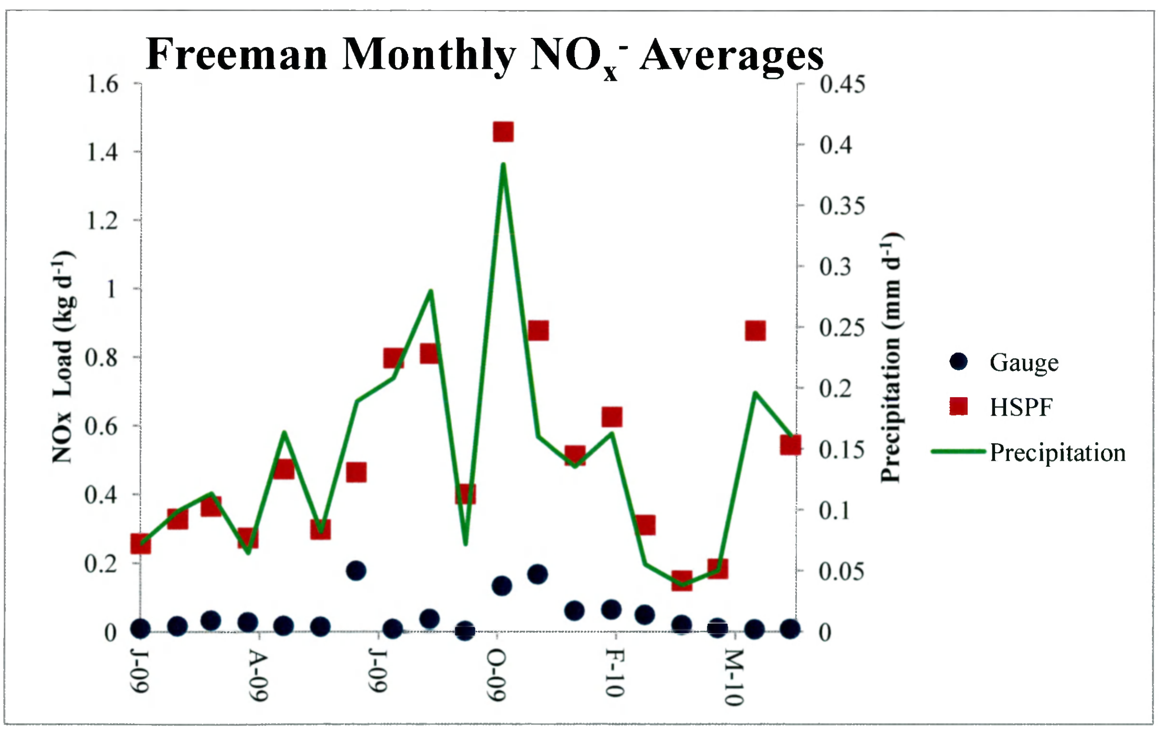

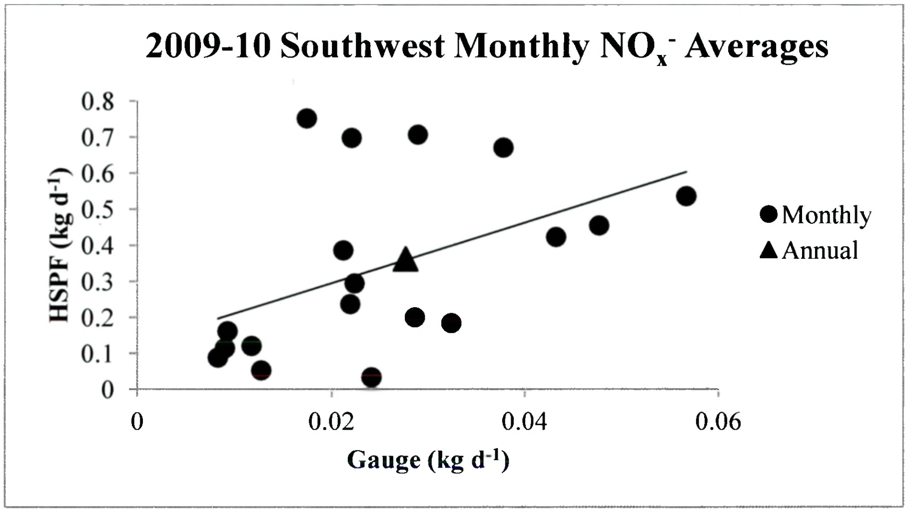
2009-10 Southwest Monthly NOx- Averages
HSPF (kg d-1)
Gauge (kg d-1)
Monthly
Annual
0.8
0.7
0.6
0.5
0.4
0.3
0.2
0.1
0
0
0.02
0.04
0.06

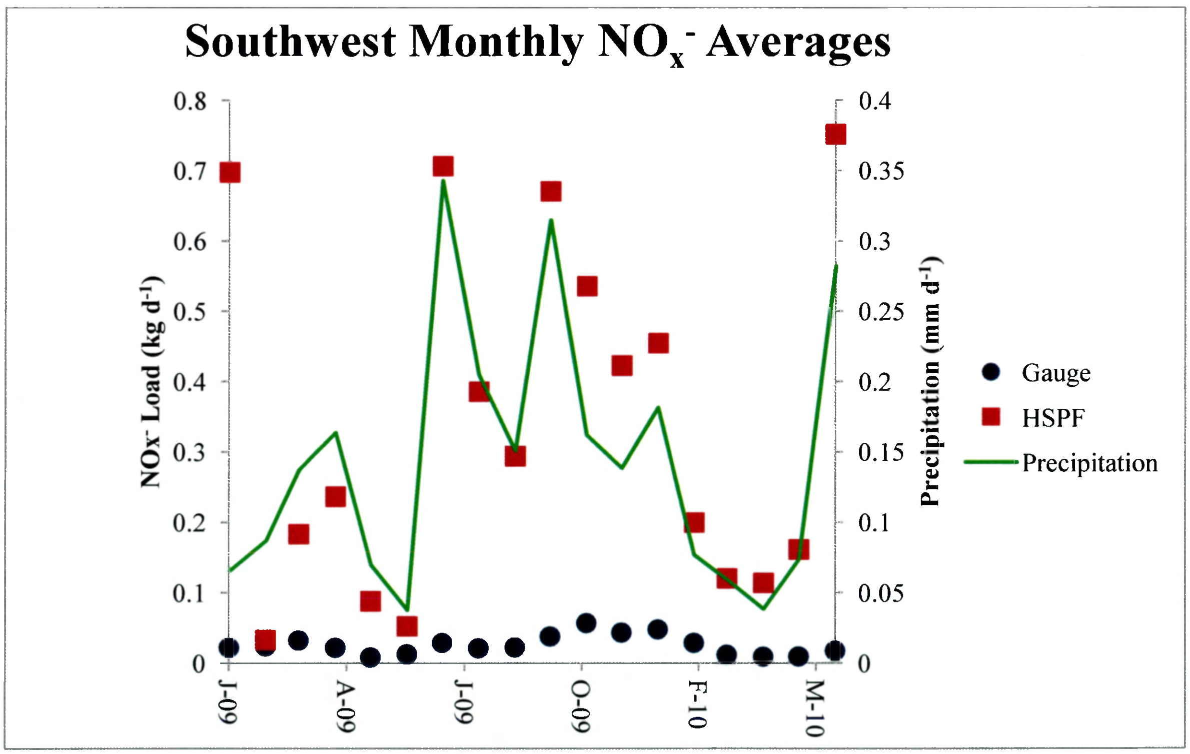
Southwest Monthly NOx- Averages
NOx- Load (kg d-1)
Precipitation (mm d-1)
Gauge
HSPF
Precipitation
J-09
A-09
J-09
O-09
F-10
M-10

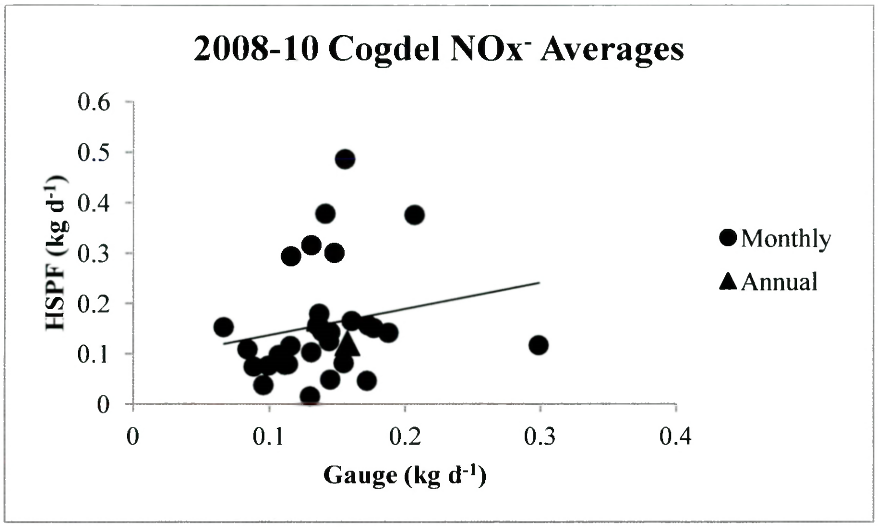
2008-10 Cogdel NOx- Averages
HSPF (kg d-1)
Gauge (kg d-1)
0.6
0.5
0.4
0.3
0.2
0.1
0
0
0.1
0.2
0.3
0.4
Monthly
Annual

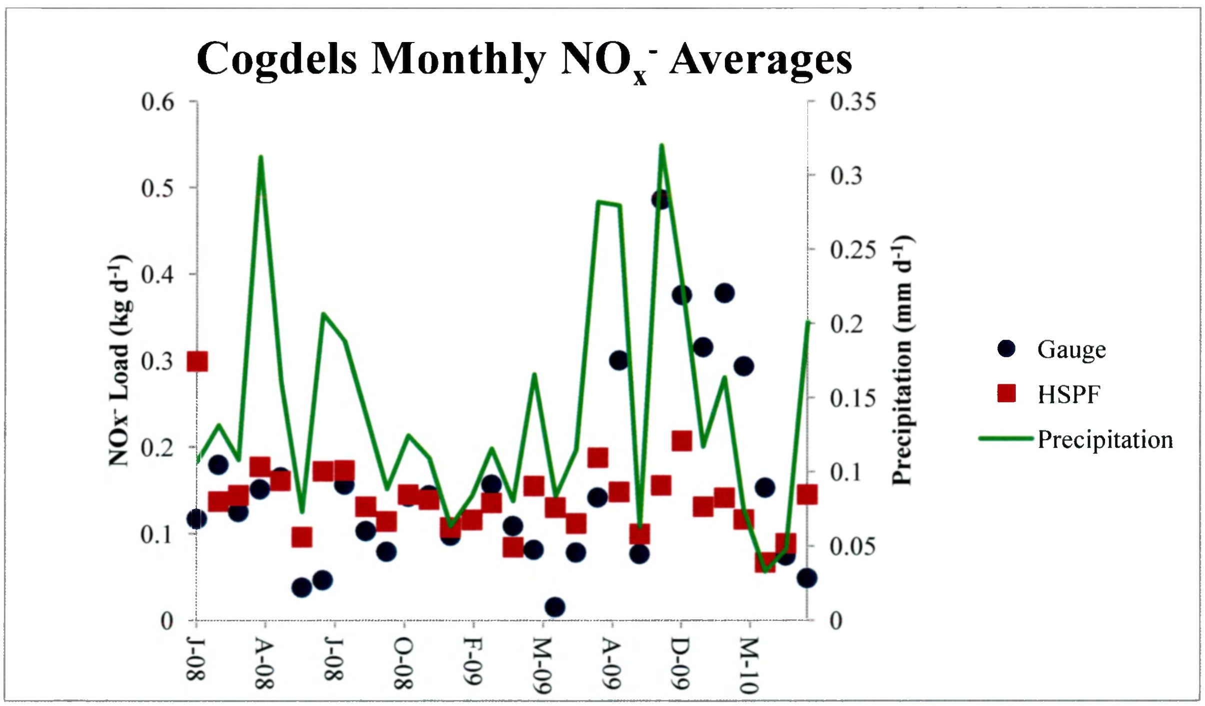
Cogdels Monthly NOx- Averages
NOx- Load (kg d-1)
Precipitation (mm d-1)
0.6
0.5
0.4
0.3
0.2
0.1
0
0.35
0.3
0.25
0.2
0.15
0.1
0.05
0
J-08
A-08
J-08
O-08
F-09
M-09
A-09
D-09
M-10
Gauge
HSPF
Precipitation

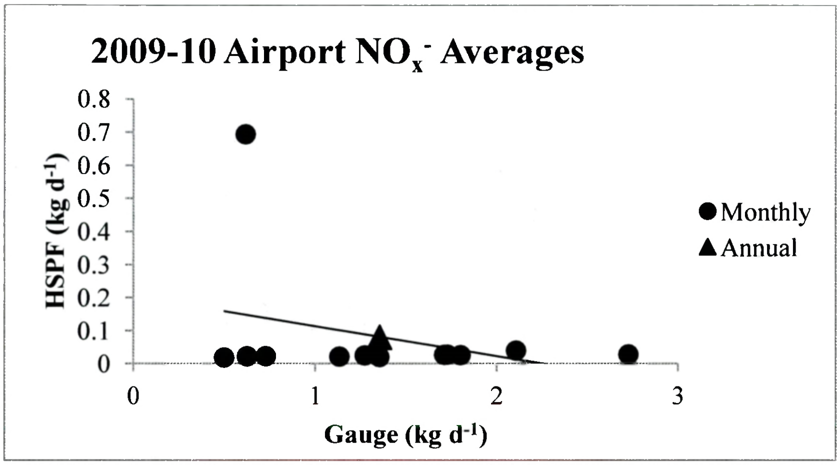

2009-10 Airport NO_x^- Averages
HSPF (kg d-1)
Gauge (kg d-1)
0.8
0.7
0.6
0.5
0.4
0.3
0.2
0.1
0
0
1
2
3
Monthly
Annual

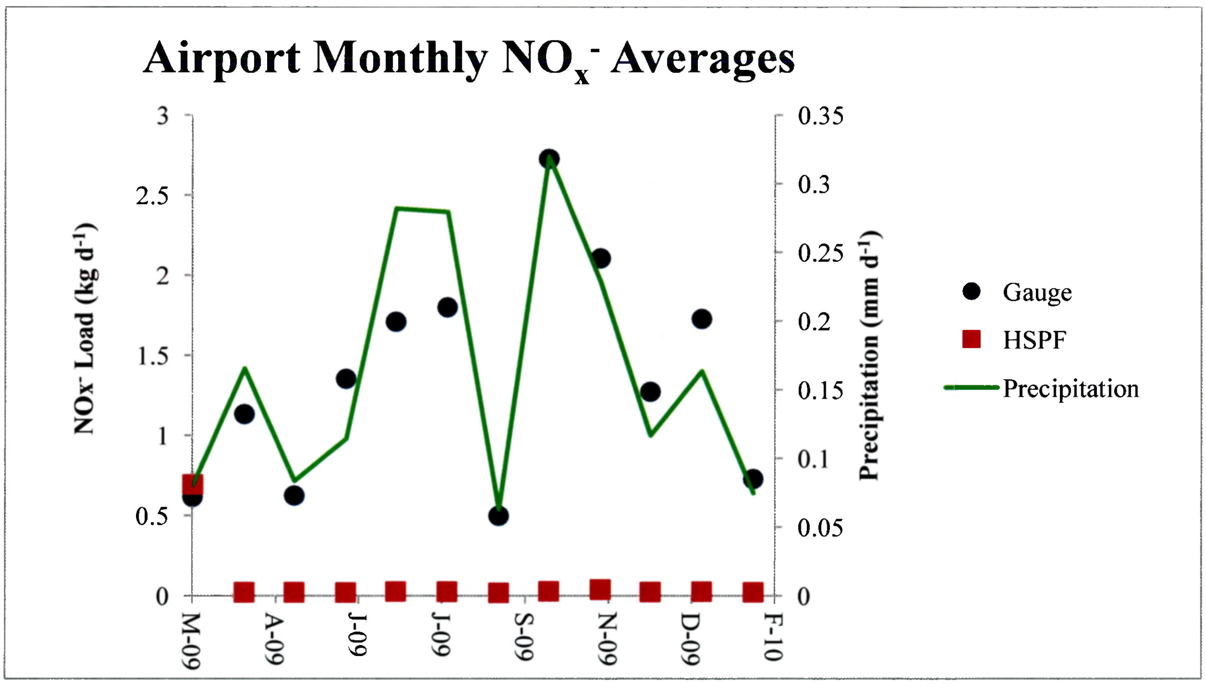

Airport Monthly NO_x^- Averages
NOx- Load (kg d-1)
Precipitation (mm d-1)
3
2.5
2
1.5
1
0.5
0
0.35
0.3
0.25
0.2
0.15
0.1
0.05
0
M-09
A-09
J-09
J-09
S-09
N-09
D-09
F-10
Gauge
HSPF
Precipitation

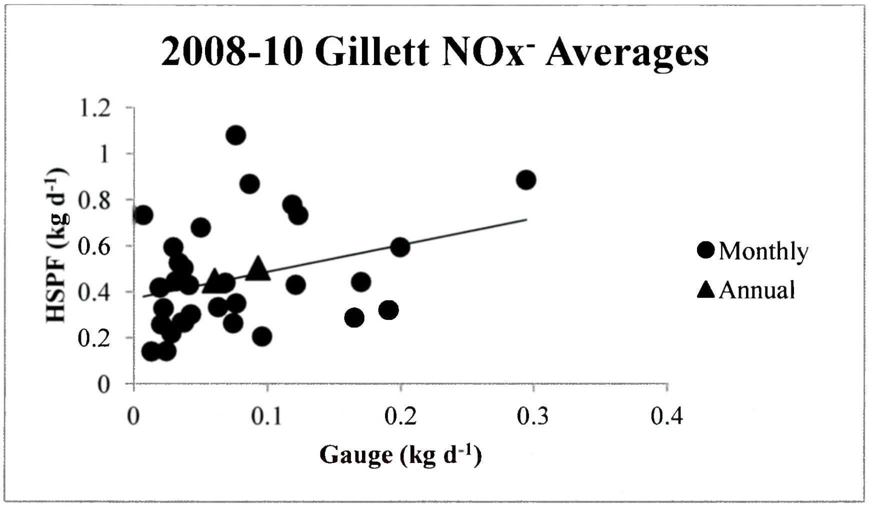
2008-10 Gillett NOx- Averages
HSPF (kg d-1)
Gauge (kg d-1)
Monthly
Annual
1.2
1
0.8
0.6
0.4
0.2
0
0
0.1
0.2
0.3
0.4

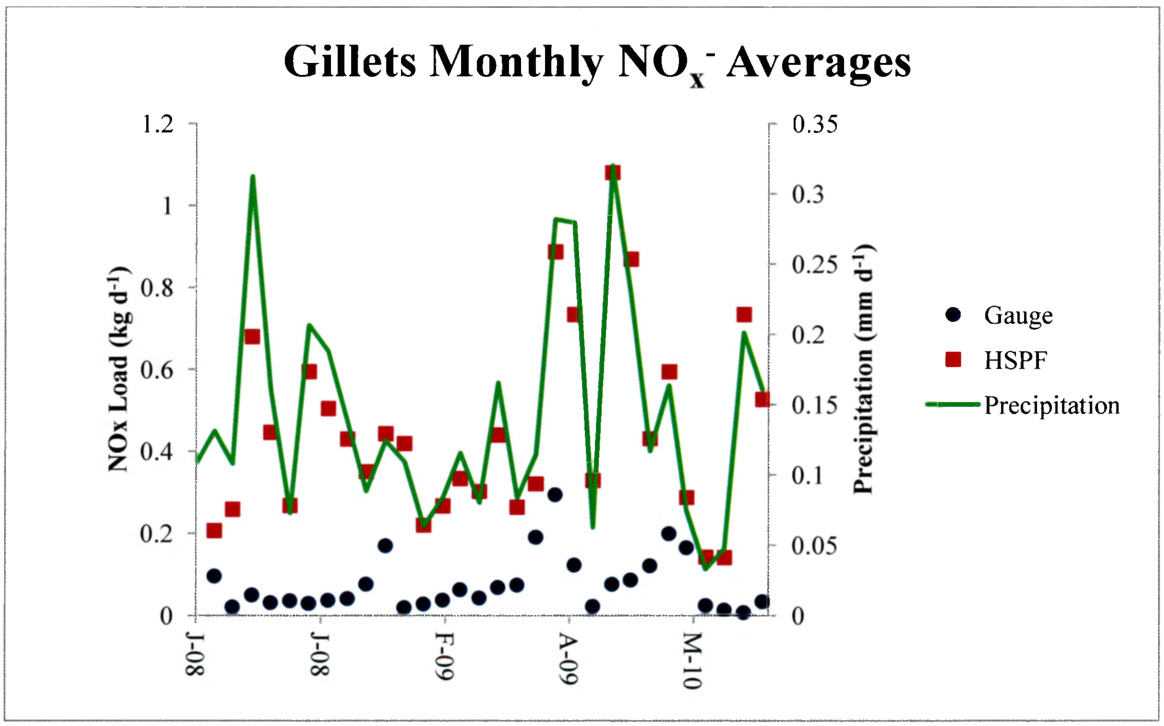
Gillets Monthly NOx- Averages
NOx Load (kg d-1)
Precipitation (mm d-1)
Gauge
HSPF
Precipitation
1.2
1
0.8
0.6
0.4
0.2
0
0.35
0.3
0.25
0.2
0.15
0.1
0.05
0
J-08
J-08
F-09
A-09
M-10

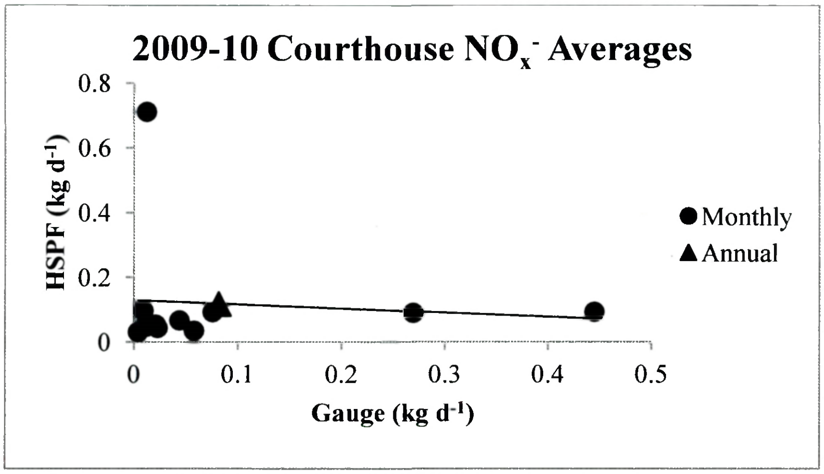

2009-10 Courthouse NOx- Averages
HSPF (kg d-1)
Gauge (kg d-1)
Monthly
Annual
0.8
0.6
0.4
0.2
0
0.1
0.2
0.3
0.4
0.5

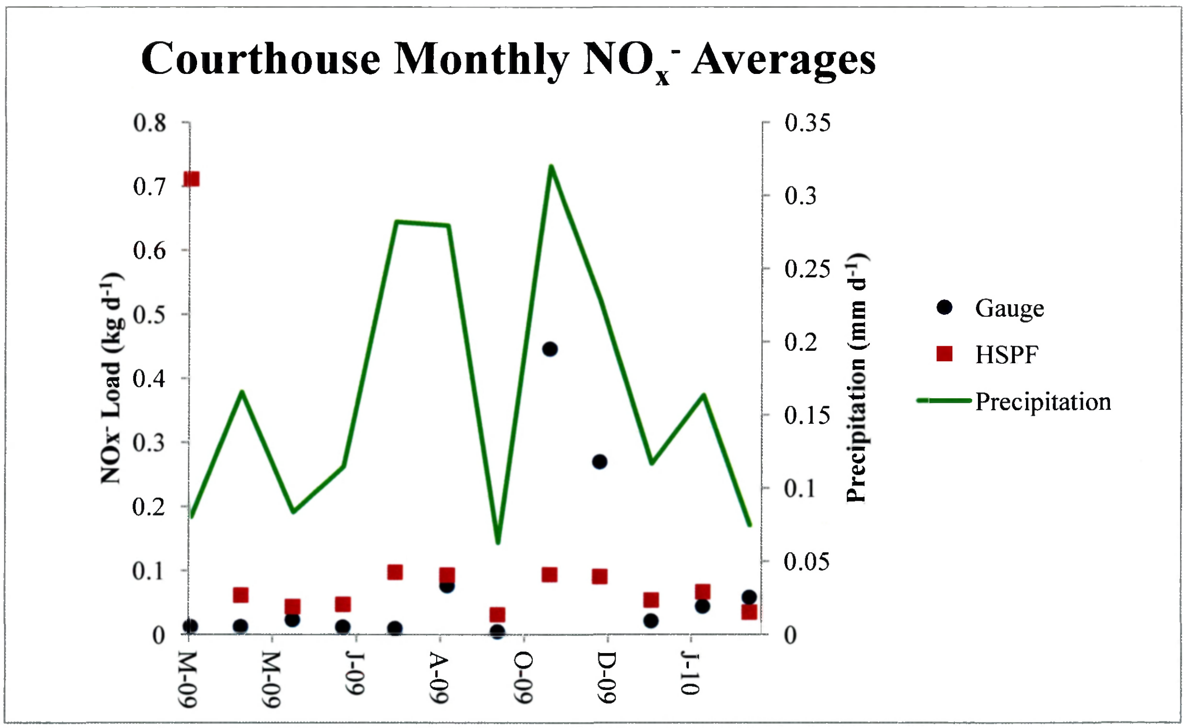

Courthouse Monthly NOx- Averages
NOx- Load (kg d-1)
Precipitation (mm d-1)
Gauge
HSPF
Precipitation
M-09
M-09
J-09
A-09
O-09
D-09
J-10

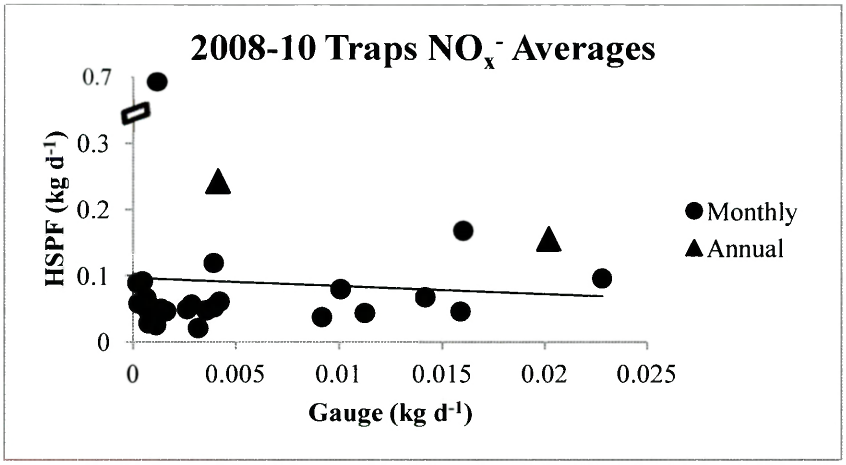

2008-10 Traps NO$_x^-$ Averages
HSPF (kg d^{-1})
Gauge (kg d^{-1})
0.7
0.3
0.2
0.1
0
0
0.005
0.01
0.015
0.02
0.025
Monthly
Annual

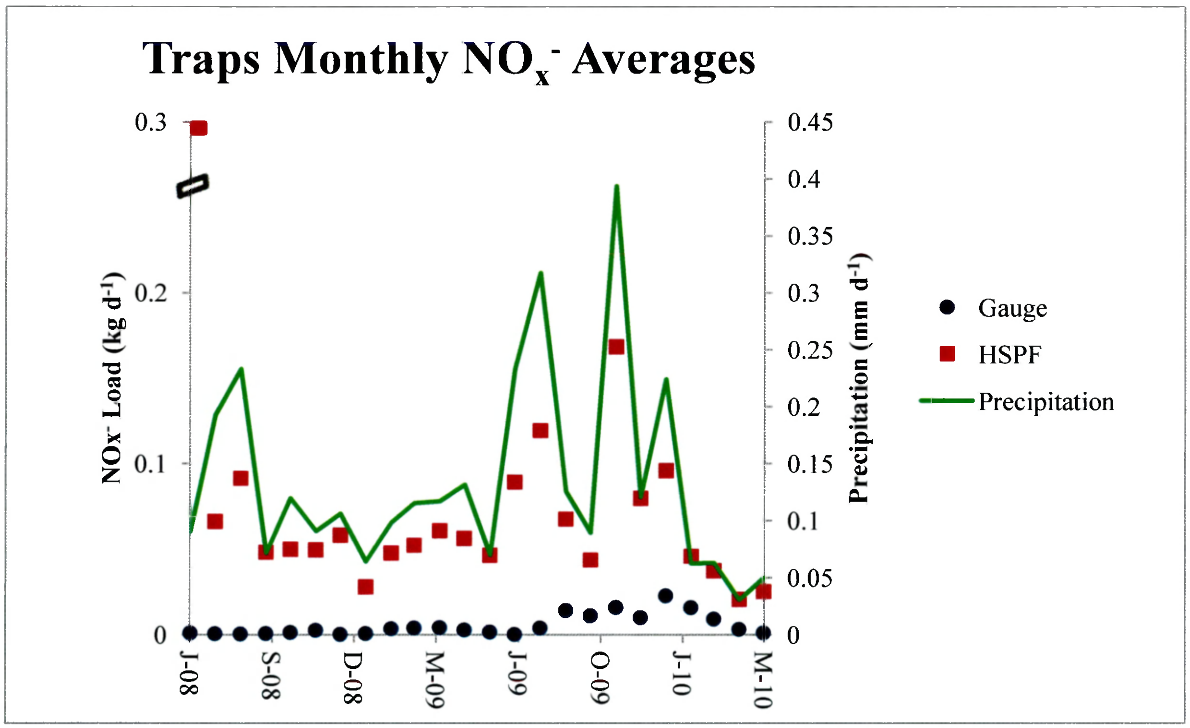

Traps Monthly NO$_x^-$ Averages
NOx$^-$ Load (kg d^{-1})
Precipitation (mm d^{-1})
0.3
0.2
0.1
0
0.45
0.4
0.35
0.3
0.25
0.2
0.15
0.1
0.05
0
J-08
S-08
D-08
M-09
J-09
O-09
J-10
M-10
Gauge
HSPF
Precipitation

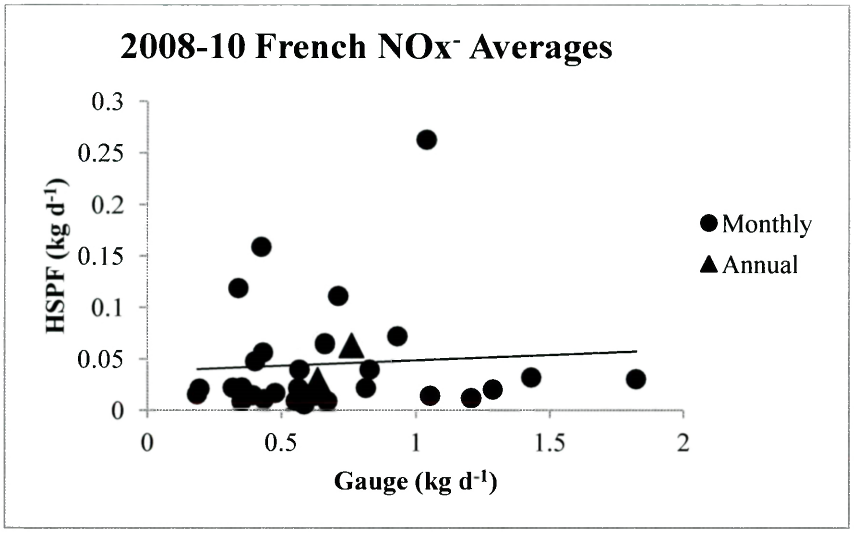

2008-10 French NOx- Averages
HSPF (kg d-1)
Gauge (kg d-1)
Monthly
Annual
0
0.05
0.1
0.15
0.2
0.25
0.3
0
0.5
1
1.5
2

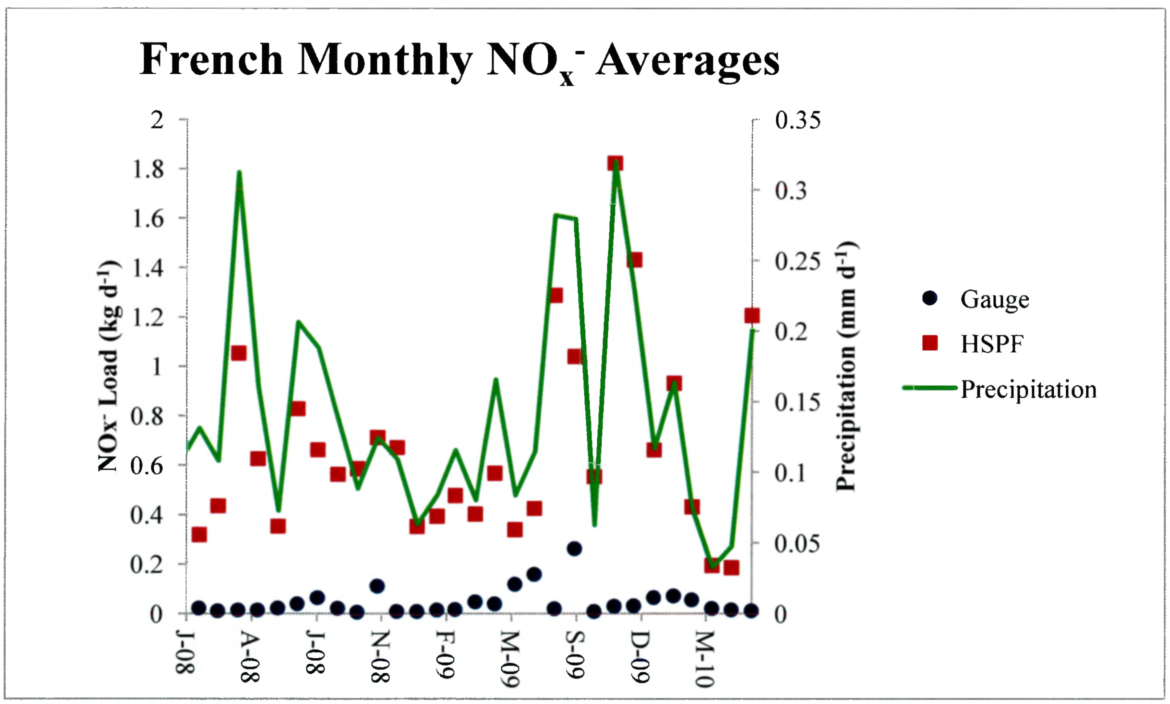

French Monthly NOx- Averages
NOx- Load (kg d-1)
Precipitation (mm d-1)
Gauge
HSPF
Precipitation
0
0.2
0.4
0.6
0.8
1
1.2
1.4
1.6
1.8
2
0
0.05
0.1
0.15
0.2
0.25
0.3
0.35
J-08
A-08
J-08
N-08
F-09
M-09
S-09
D-09
M-10

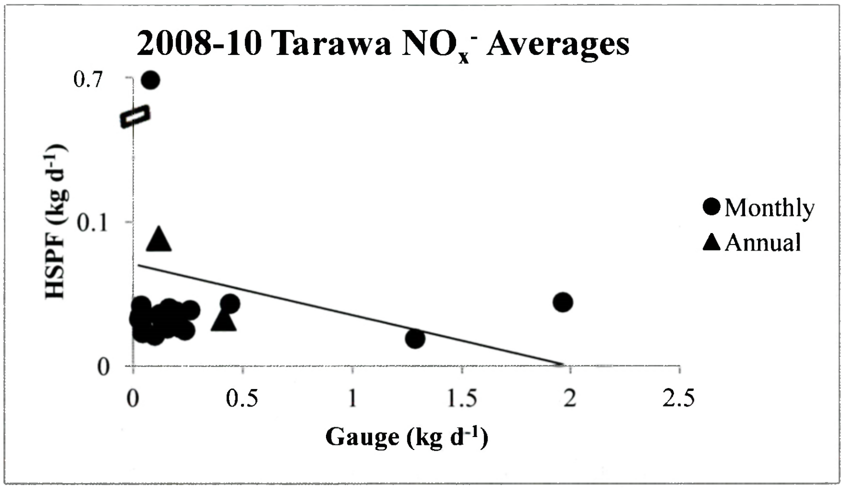

2008-10 Tarawa NO_x^- Averages
0.7
0.1
0
HSPF (kg d-1)
0
0.5
1
1.5
2
2.5
Gauge (kg d-1)
Monthly
Annual

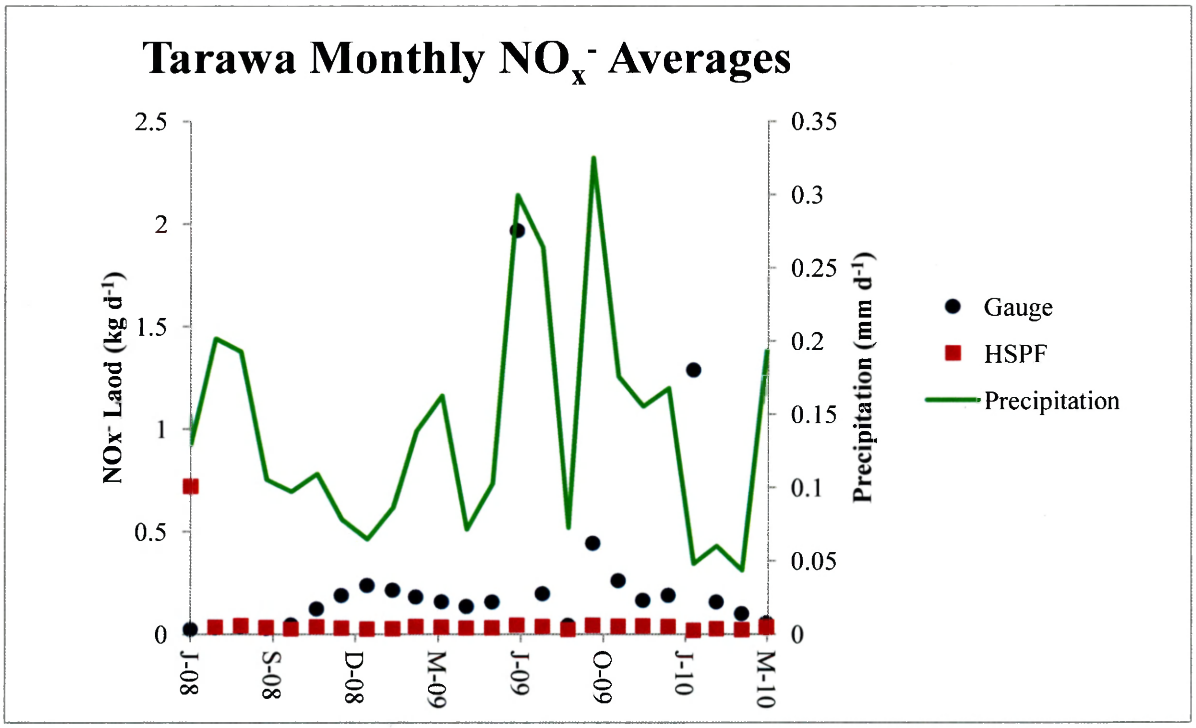

Tarawa Monthly NO_x^- Averages
2.5
2
1.5
1
0.5
0
NOx- Laod (kg d-1)
0.35
0.3
0.25
0.2
0.15
0.1
0.05
0
Precipitation (mm d-1)
J-08
S-08
D-08
M-09
J-09
O-09
J-10
M-10
Gauge
HSPF
Precipitation

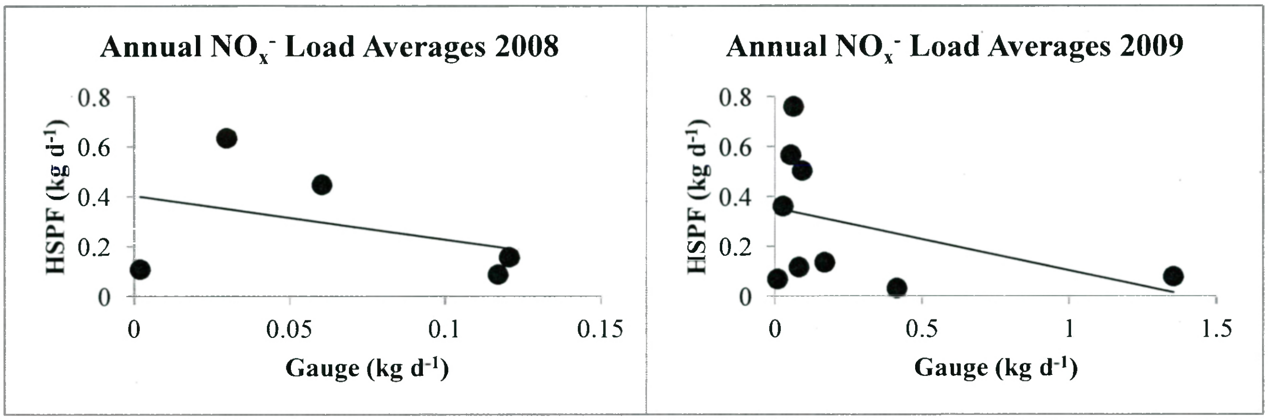

Figure 10. Annual mean observed and modeled stream flow from all sub-watersheds for which an annual cycle of data are available.

Table 4: Summary statistics for regressions between measured and modeled NO_x^- loads (kg d^{-1}) from each sub-watershed at the monthly and annual resolution.

	R^2	Slope	Intercept
Monthly			
Freeman	0.22	2.80	0.40
Southwest	0.23	8.40	0.13
Cogdel	0.04	0.52	0.08
Airport	0.10	-0.09	0.20
Gillets	0.11	1.16	0.37
Courthouse	0.008	-0.13	0.13
Traps	0.003	-1.22	0.10
French	0.005	0.01	0.04
Tarawa	0.01	-0.04	0.07
Annual			
2008	0.14	-1.75	0.40
2009	0.17	-0.25	0.36

Figure 11. Modeled (HSPF) and observed NH_4^+ loads for each MCBCL sub-watershed. Upper panel gives regression results for mean monthly loads across all months where data were available. Annual mean loads are plotted for comparison but are not included in the regression. Lower panel gives the output as a monthly time series with observed precipitation (mean daily values each month). The time span of each plot is dependent on the time frame of gauge data available for each sub-watershed.

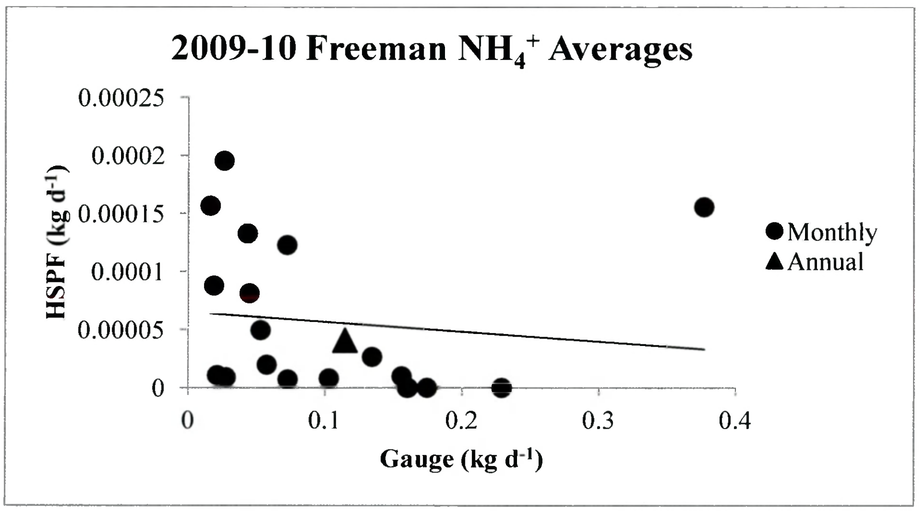

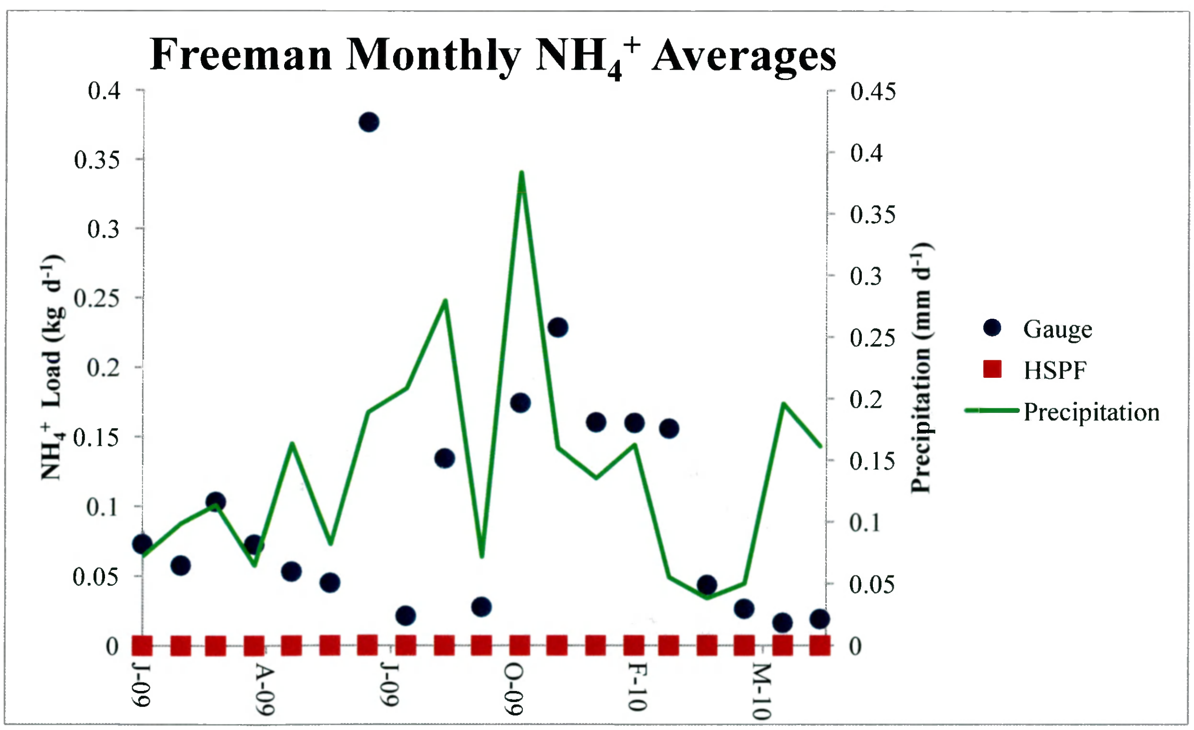

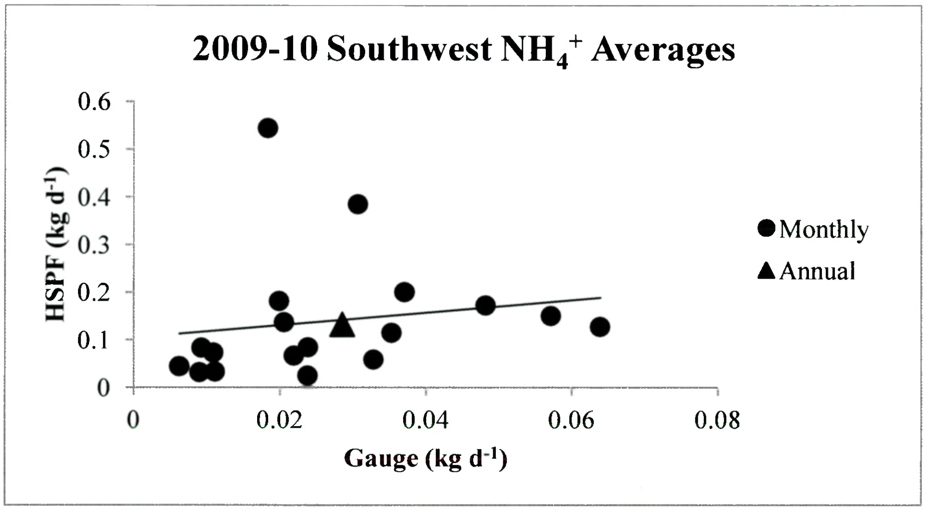
2009-10 Southwest NH_4^+ Averages
HSPF (kg d-1)
Gauge (kg d-1)
0.6
0.5
0.4
0.3
0.2
0.1
0
0
0.02
0.04
0.06
0.08
Monthly
Annual

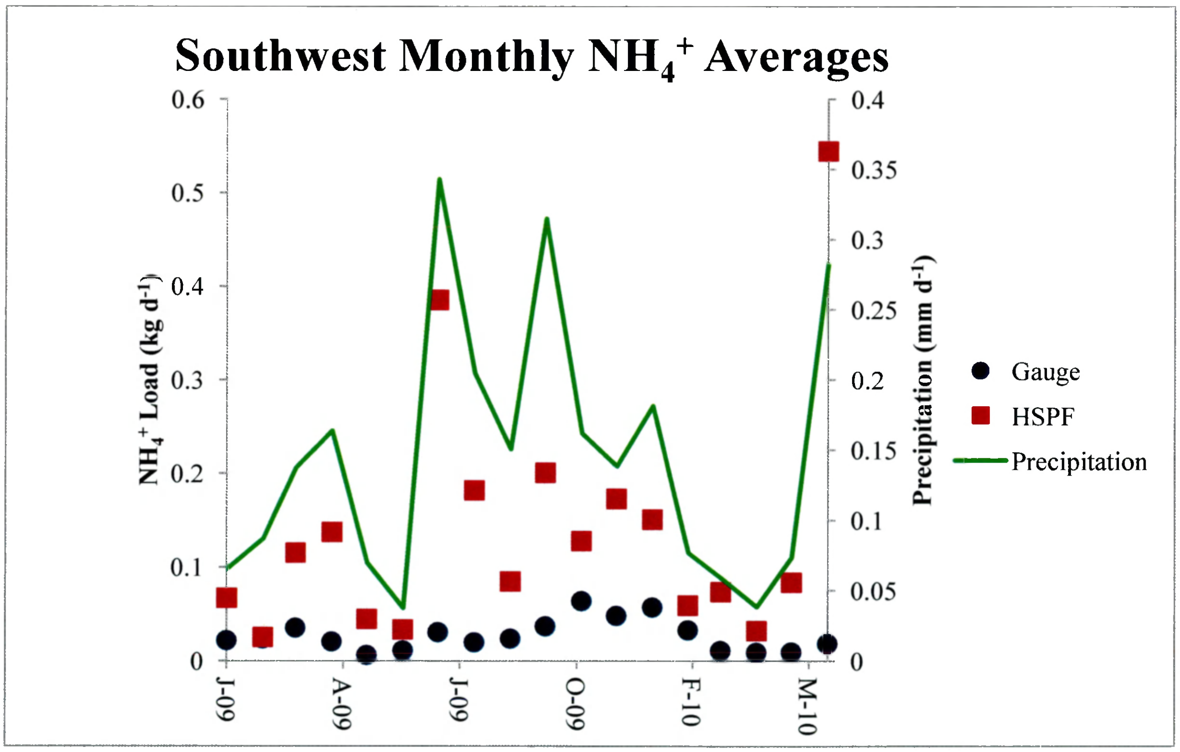
Southwest Monthly NH_4^+ Averages
NH_4^+ Load (kg d-1)
Precipitation (mm d-1)
0.6
0.5
0.4
0.3
0.2
0.1
0
0.4
0.35
0.3
0.25
0.2
0.15
0.1
0.05
0
J-09
A-09
J-09
O-09
F-10
M-10
Gauge
HSPF
Precipitation

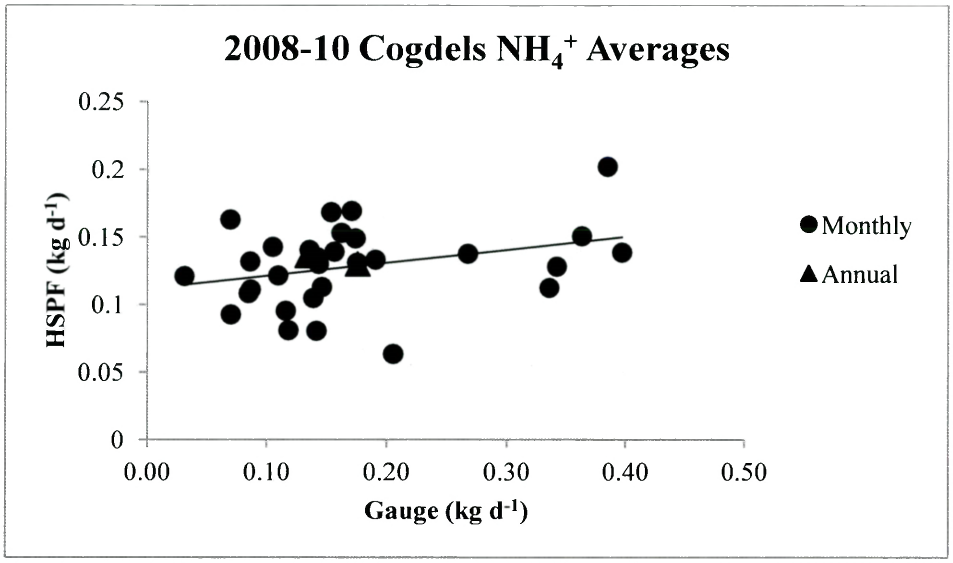
2008-10 Cogdels NH_4^+ Averages
0.25
0.2
0.15
0.1
0.05
0
HSPF (kg d^{-1})
0.00
0.10
0.20
0.30
0.40
0.50
Gauge (kg d^{-1})
Monthly
Annual

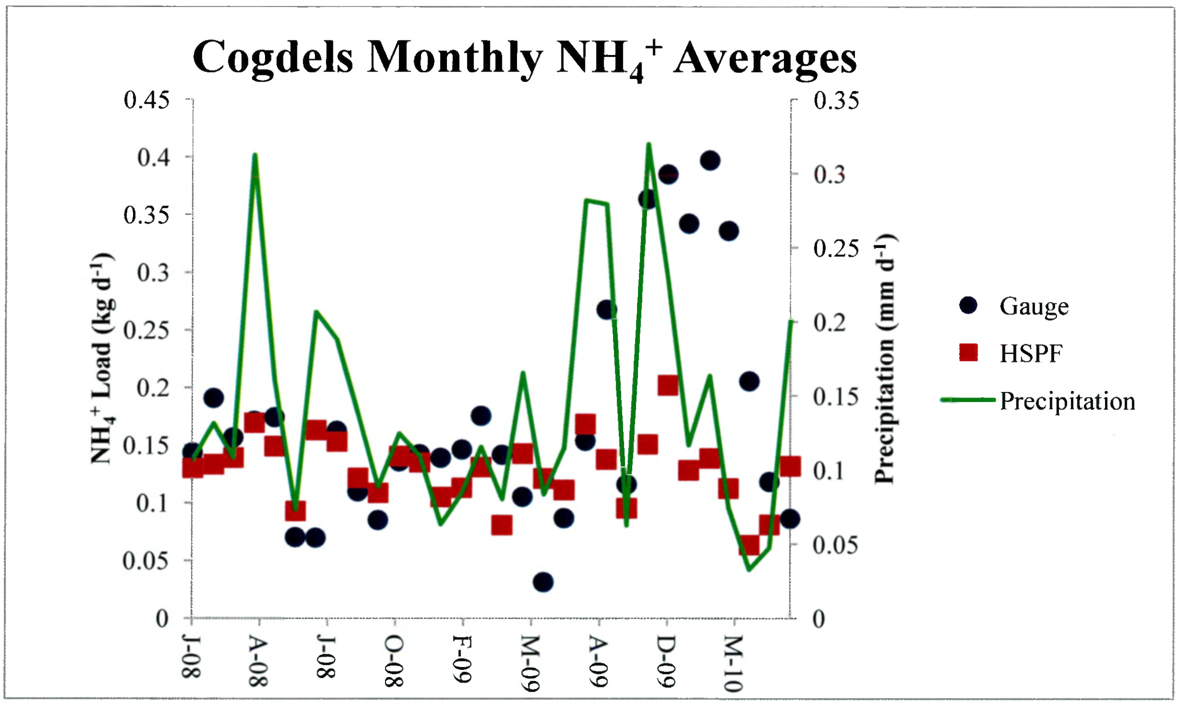
Cogdels Monthly NH_4^+ Averages
0.45
0.4
0.35
0.3
0.25
0.2
0.15
0.1
0.05
0
NH_4^+ Load (kg d^{-1})
0.35
0.3
0.25
0.2
0.15
0.1
0.05
0
Precipitation (mm d^{-1})
J-08
A-08
J-08
O-08
F-09
M-09
A-09
D-09
M-10
Gauge
HSPF
Precipitation

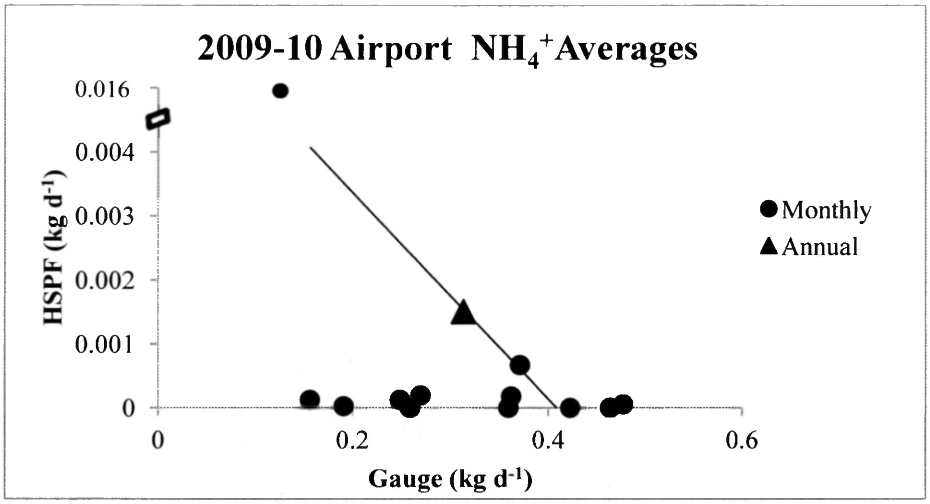
2009-10 Airport NH4+Averages
HSPF (kg d-1)
0.016
0.004
0.003
0.002
0.001
0
0
0.2
0.4
0.6
Gauge (kg d-1)
Monthly
Annual

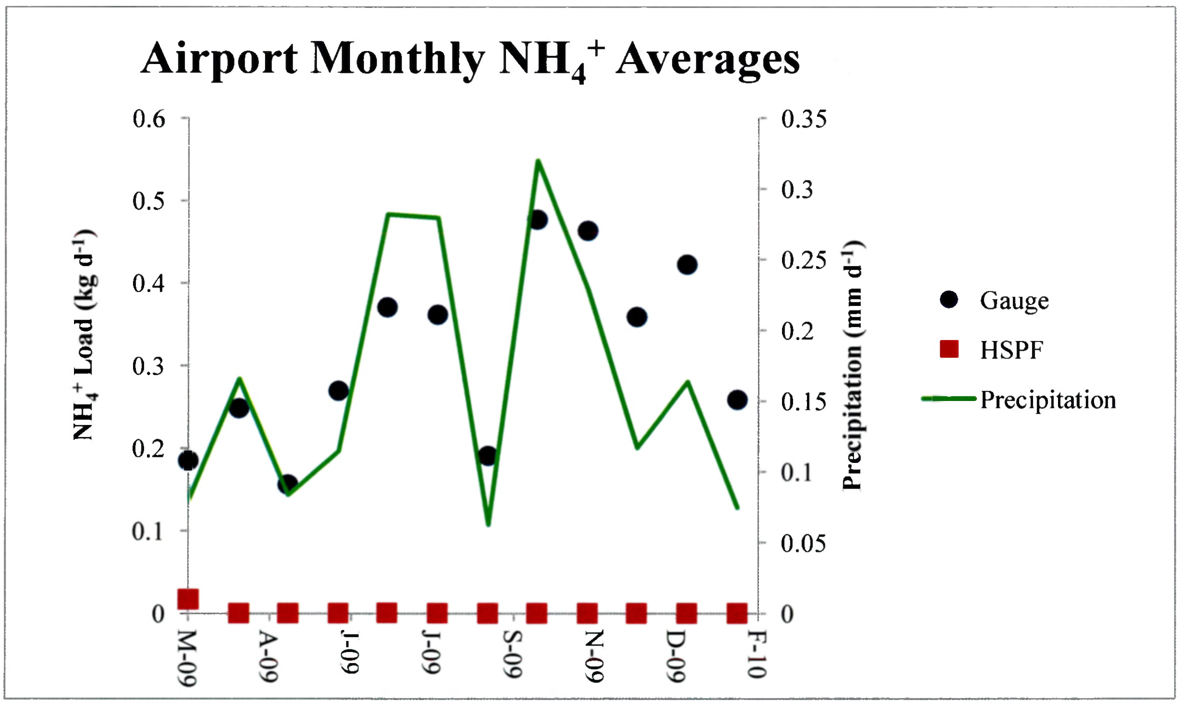
Airport Monthly NH4+ Averages
NH4+ Load (kg d-1)
0.6
0.5
0.4
0.3
0.2
0.1
0
Precipitation (mm d-1)
0.35
0.3
0.25
0.2
0.15
0.1
0.05
0
M-09
A-09
J-09
J-09
S-09
N-09
D-09
F-10
Gauge
HSPF
Precipitation

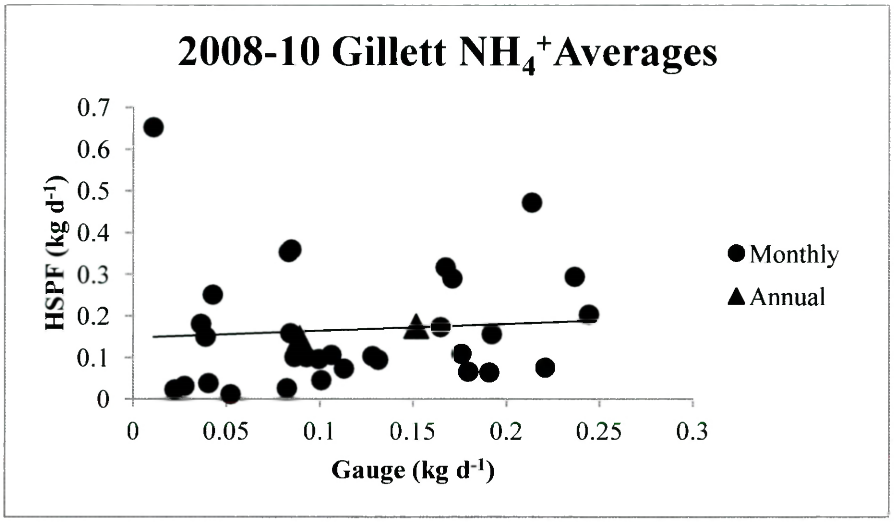
2008-10 Gillett NH4+Averages
HSPF (kg d-1)
Gauge (kg d-1)
Monthly
Annual
0.7
0.6
0.5
0.4
0.3
0.2
0.1
0
0.05
0.1
0.15
0.2
0.25
0.3

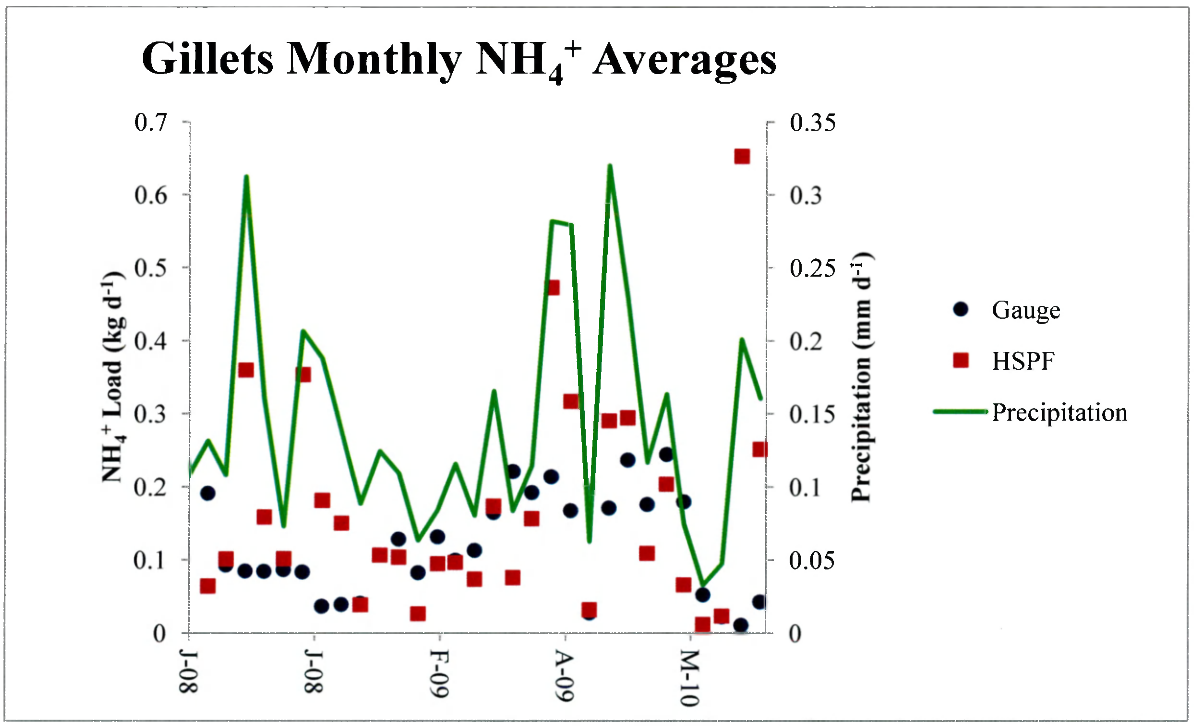
Gillets Monthly NH4+ Averages
NH4+ Load (kg d-1)
Precipitation (mm d-1)
Gauge
HSPF
Precipitation
J-08
J-08
F-09
A-09
M-10

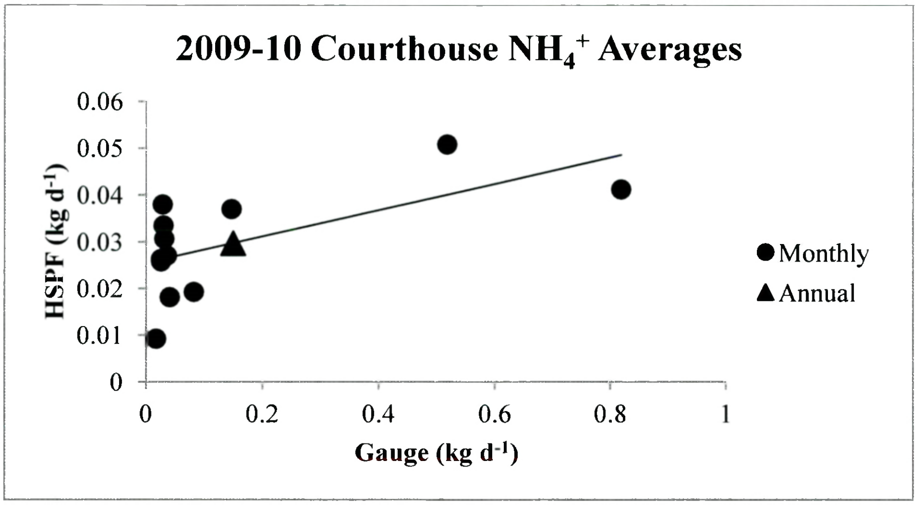
2009-10 Courthouse NH4+ Averages
HSPF (kg d-1)
Gauge (kg d-1)
0.06
0.05
0.04
0.03
0.02
0.01
0
0
0.2
0.4
0.6
0.8
1
Monthly
Annual

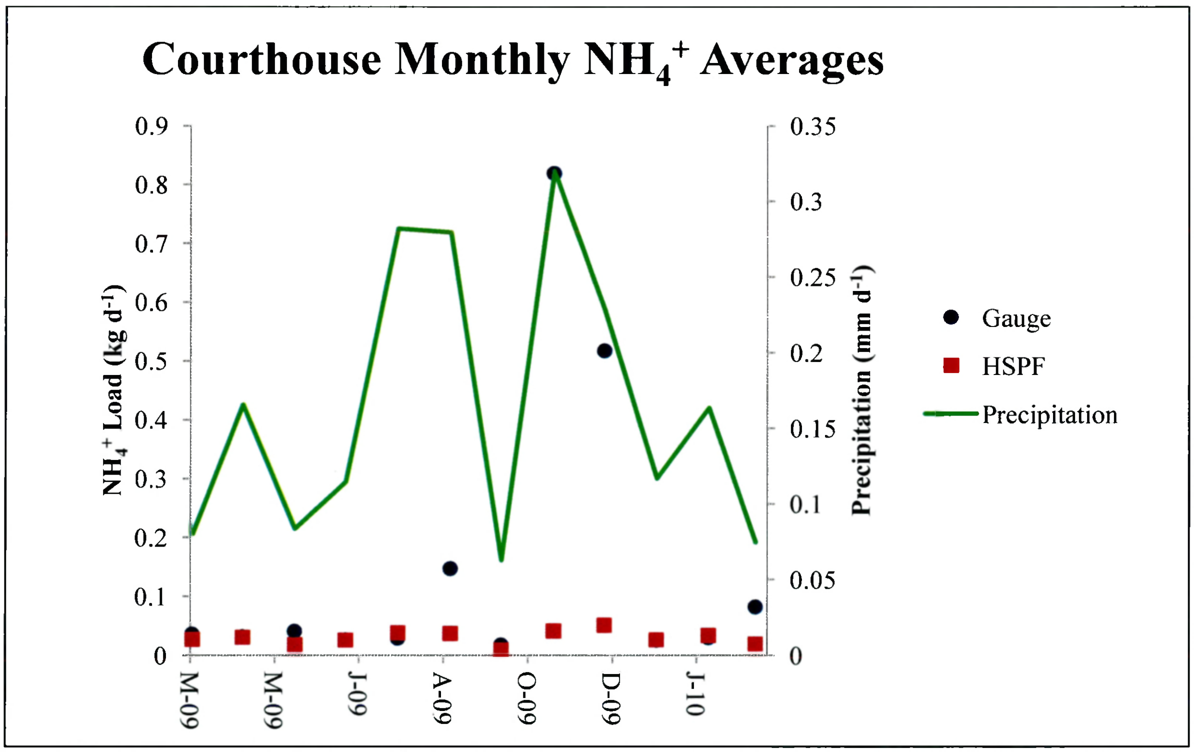
Courthouse Monthly NH4+ Averages
NH4+ Load (kg d-1)
Precipitation (mm d-1)
0.9
0.8
0.7
0.6
0.5
0.4
0.3
0.2
0.1
0
0.35
0.3
0.25
0.2
0.15
0.1
0.05
0
M-09
M-09
J-09
A-09
O-09
D-09
J-10
Gauge
HSPF
Precipitation

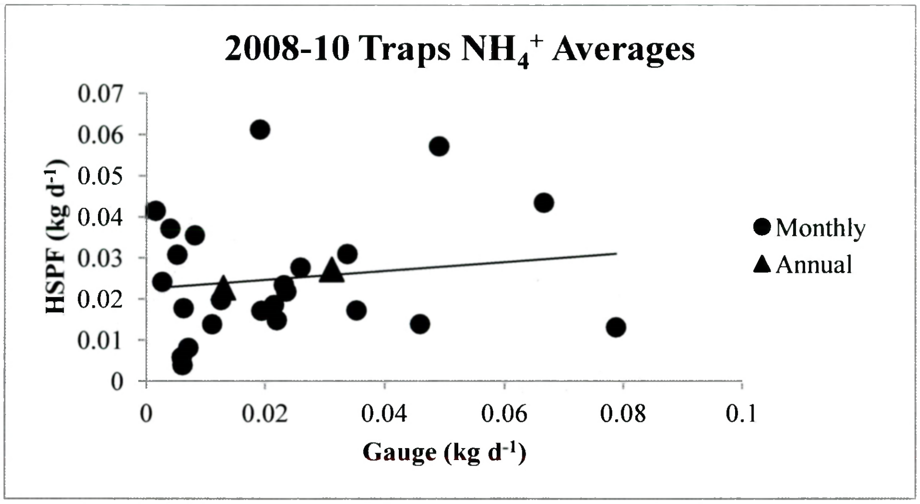
2008-10 Traps NH_4^+ Averages
HSPF (kg d^{-1})
Gauge (kg d^{-1})
0.07
0.06
0.05
0.04
0.03
0.02
0.01
0
0.02
0.04
0.06
0.08
0.1
Monthly
Annual

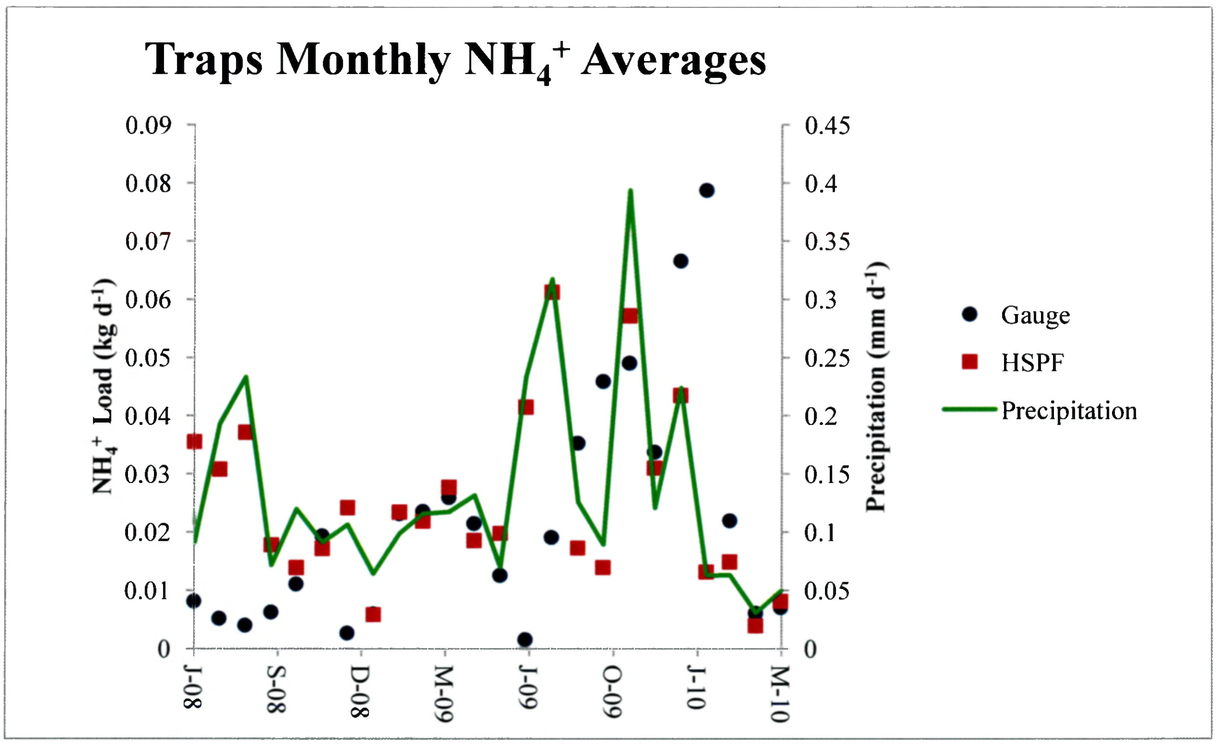
Traps Monthly NH_4^+ Averages
NH_4^+ Load (kg d^{-1})
Precipitation (mm d^{-1})
0.09
0.08
0.07
0.06
0.05
0.04
0.03
0.02
0.01
0
0.45
0.4
0.35
0.3
0.25
0.2
0.15
0.1
0.05
J-08
S-08
D-08
M-09
J-09
O-09
J-10
M-10
Gauge
HSPF
Precipitation

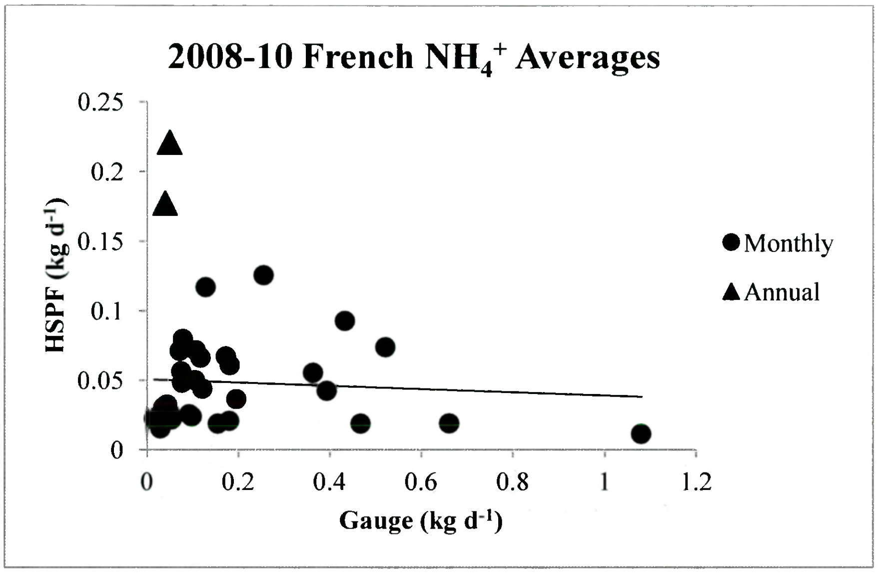

2008-10 French NH_4^+ Averages
0.25
0.2
0.15
0.1
0.05
0
HSPF (kg d-1)
Monthly
Annual
0
0.2
0.4
0.6
0.8
1
1.2
Gauge (kg d-1)

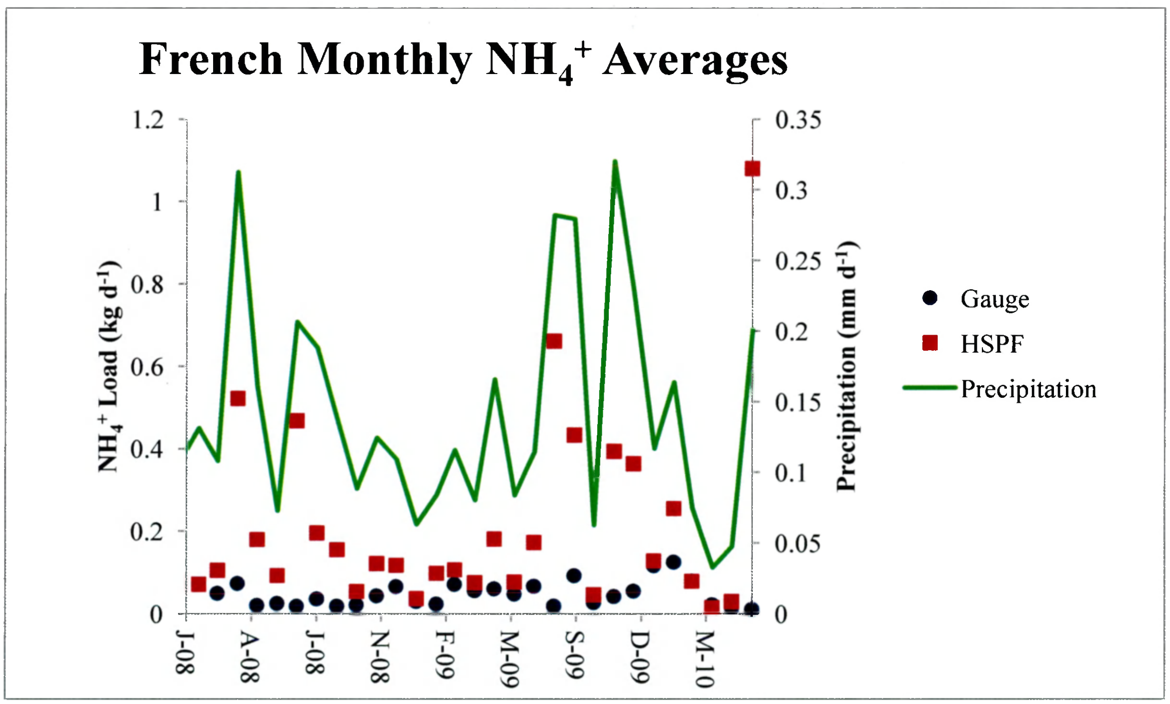

French Monthly NH_4^+ Averages
1.2
1
0.8
0.6
0.4
0.2
0
NH_4^+ Load (kg d-1)
0.35
0.3
0.25
0.2
0.15
0.1
0.05
0
Precipitation (mm d-1)
J-08
A-08
J-08
N-08
F-09
M-09
S-09
D-09
M-10
Gauge
HSPF
Precipitation

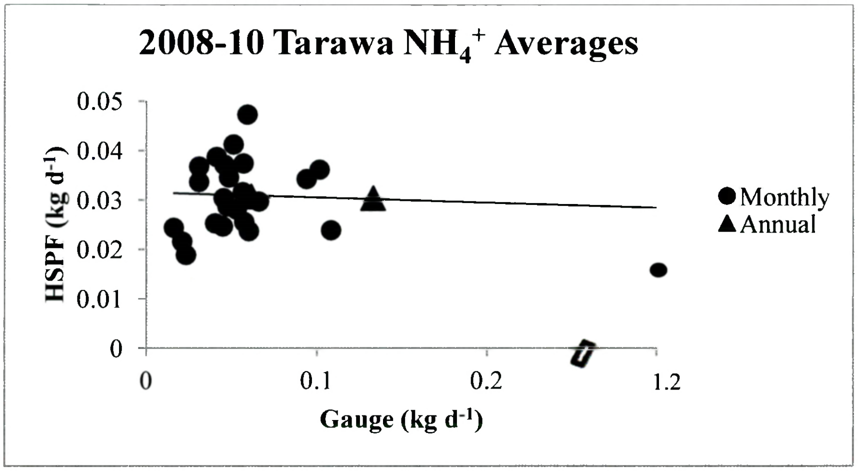
2008-10 Tarawa NH4+ Averages
0.05
0.04
0.03
0.02
0.01
0
HSPF (kg d-1)
0
0.1
0.2
1.2
Gauge (kg d-1)
Monthly
Annual

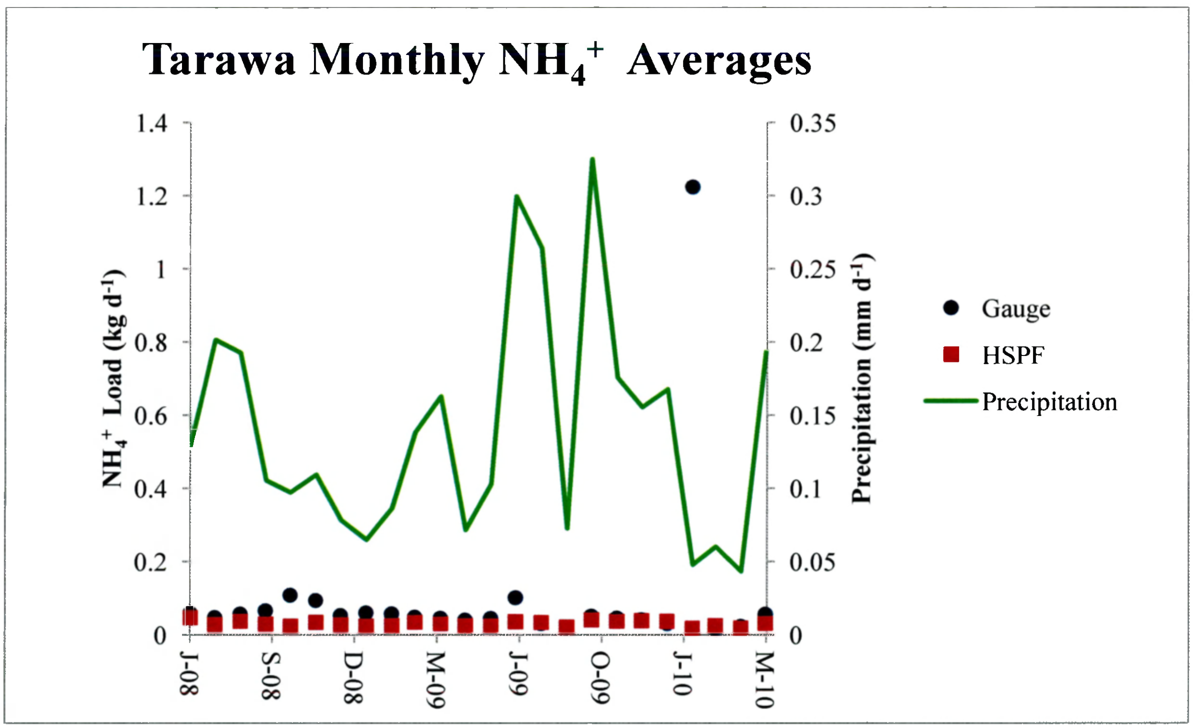
Tarawa Monthly NH4+ Averages
1.4
1.2
1
0.8
0.6
0.4
0.2
0
NH4+ Load (kg d-1)
0.35
0.3
0.25
0.2
0.15
0.1
0.05
0
Precipitation (mm d-1)
J-08
S-08
D-08
M-09
J-09
O-09
J-10
M-10
Gauge
HSPF
Precipitation

Figure 12 Annual mean observed and modeled stream flow from all sub-watersheds for which an annual cycle of data are available.

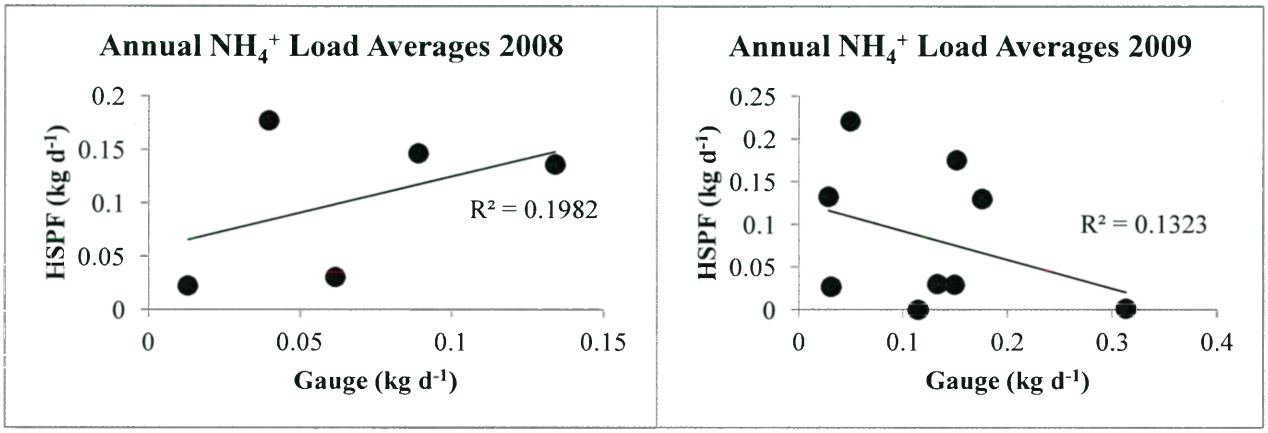

Table 5: Summary statistics for regressions between measured and modeled NH_4^+ loads (kg d^{-1}) from each sub-watershed at the monthly and annual resolution.

	R^2	Slope	Intercept
Monthly			
Freeman	0.01	-9E-05	7E-05
Southwest	0.03	1.31	0.10
Cogdel	0.10	0.10	0.11
Airport	0.13	-0.02	0.007
Gillets	0.01	0.16	0.15
Courthouse	0.39	0.03	0.03
Traps	0.02	0.11	0.02
French	0.008	-0.01	0.05
Tarawa	0.11	-0.01	0.03
Annual			
2008	0.20	0.68	0.06
2009	0.13	-0.34	0.13

PO_4^{3-} Load

Modeled PO_4^{3-} loads to the sub-watersheds again followed the trends in precipitation, and followed observed loads more closely than for NO_x^- and NH_4^+ (Fig. 13, Table 6). Coefficients of determination for monthly loads ranged from 0.012 in French to 0.31 in Courthouse. The model over-predicted loads to Gillets, Courthouse, Traps, and French and under-predicted loads to Airport. The model slightly over-predicted loads to Cogdels and Courthouse, except in late 2009 and early 2010 when loads were under-predicted despite greater precipitation. The model did fairly well estimating loads to Tarawa when the highest observed value was removed, except in late 2008 when loads were slightly under-predicted. The model reproduced loads in the correct range in Freeman and Southwest. Annual average loads were slightly over-predicted in 2008, while the annual averages in 2009 were within the correct range (Fig. 14, Appendix Table 1).

Figure 13. Modeled (HSPF) and observed PO_4^{3-} loads for each MCBCL sub-watershed. Upper panel gives regression results for mean monthly loads across all months where data were available. Annual mean loads are plotted for comparison but are not included in the regression. Lower panel gives the output as a monthly time series with observed precipitation (mean daily values each month). The time span of each plot is dependent on the time frame of gauge data available for each sub-watershed.

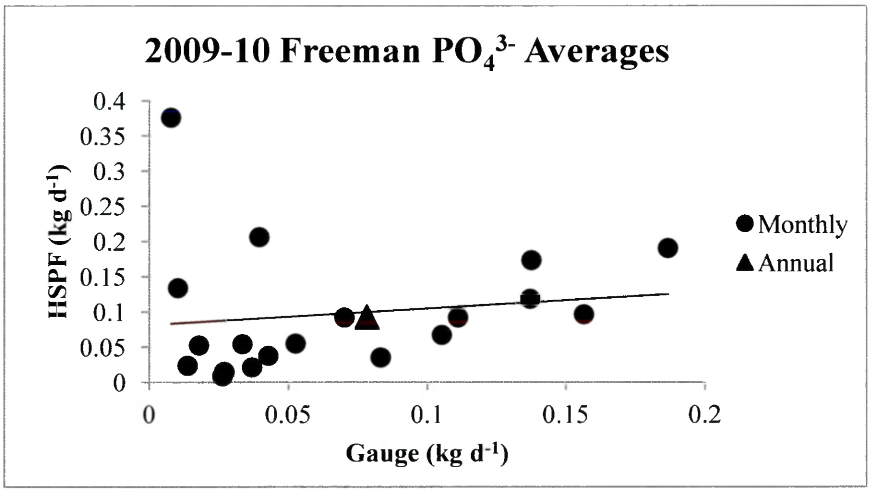

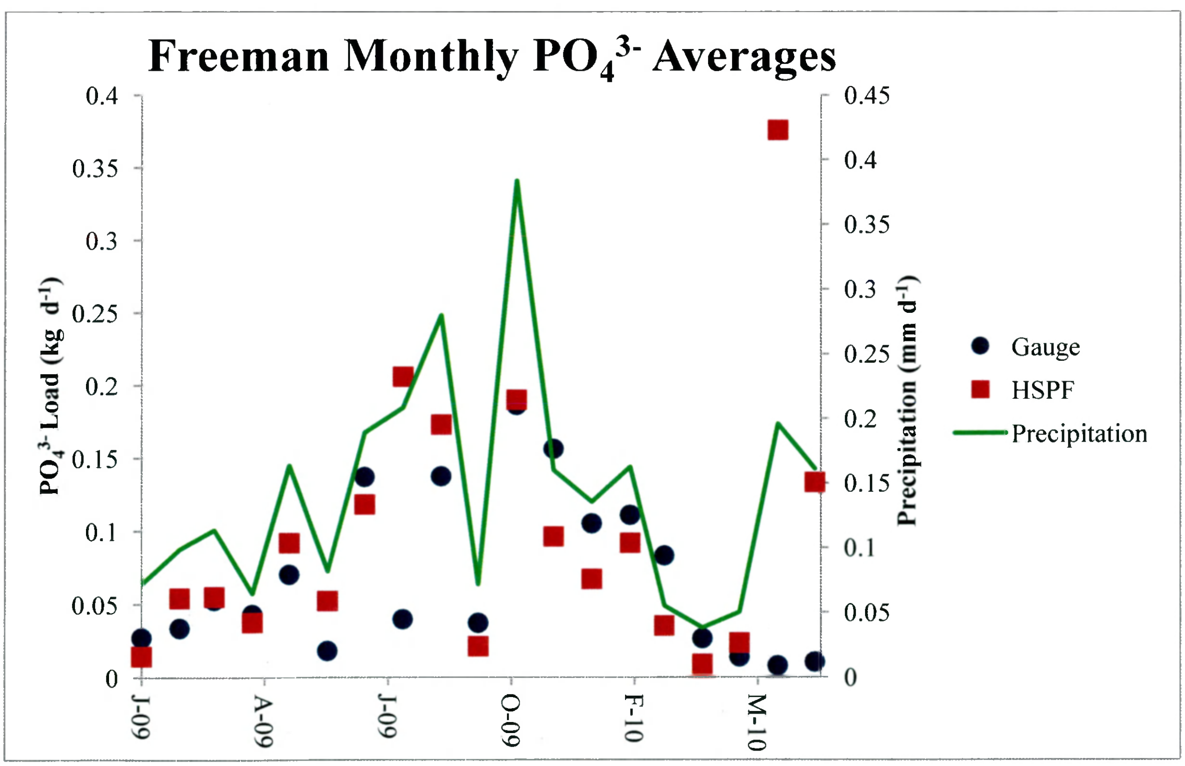

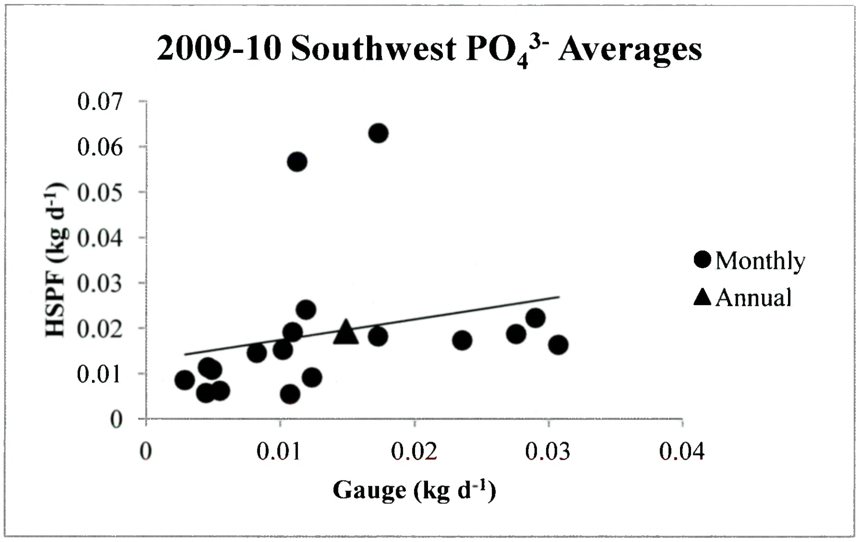
2009-10 Southwest PO_4^{3-} Averages
HSPF (kg d-1)
Gauge (kg d-1)
Monthly
Annual
0.07
0.06
0.05
0.04
0.03
0.02
0.01
0
0
0.01
0.02
0.03
0.04

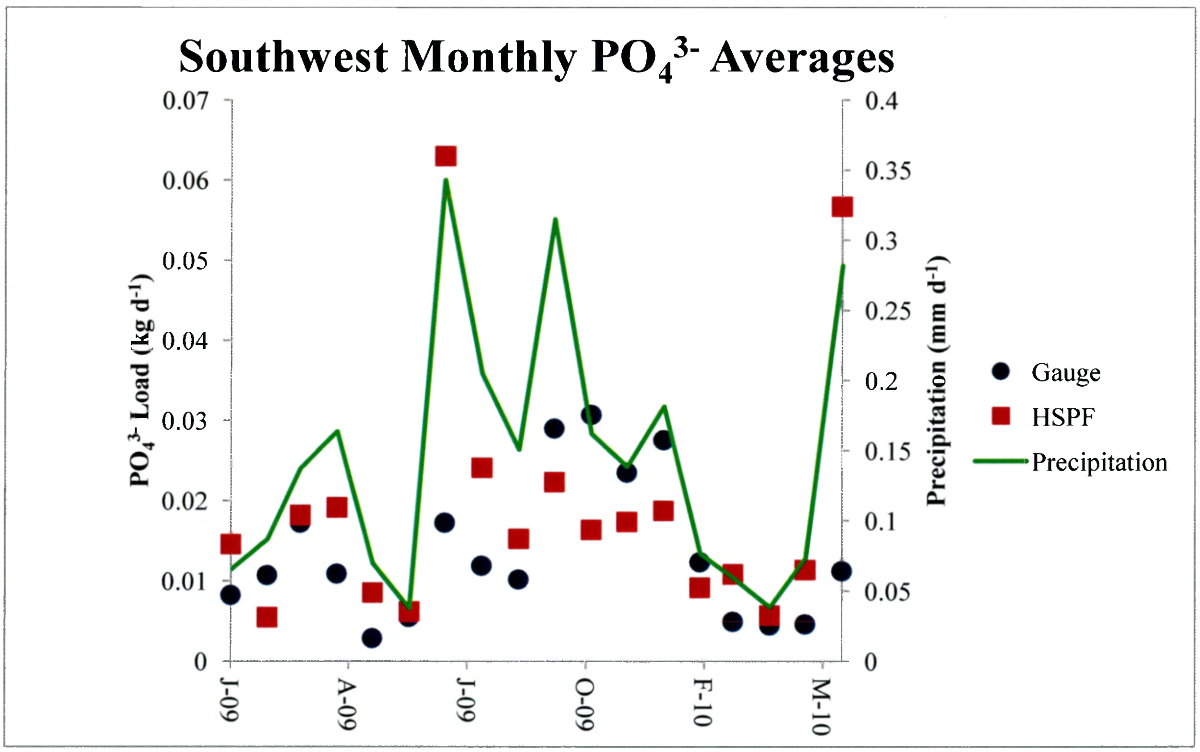
Southwest Monthly PO_4^{3-} Averages
PO_4^{3-} Load (kg d-1)
Precipitation (mm d-1)
Gauge
HSPF
Precipitation
J-09
A-09
J-09
O-09
F-10
M-10

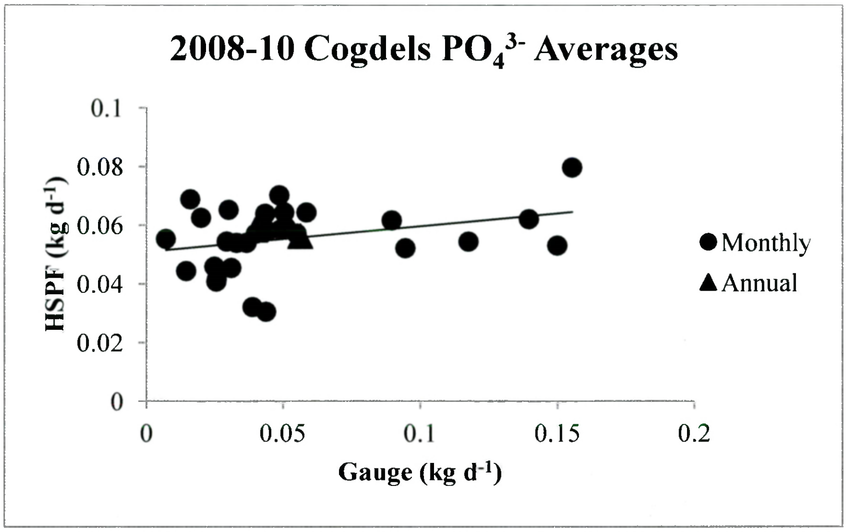
2008-10 Cogdels PO_4^{3-} Averages
HSPF (kg d^{-1})
Gauge (kg d^{-1})
0
0.02
0.04
0.06
0.08
0.1
0.05
0.15
0.2
Monthly
Annual

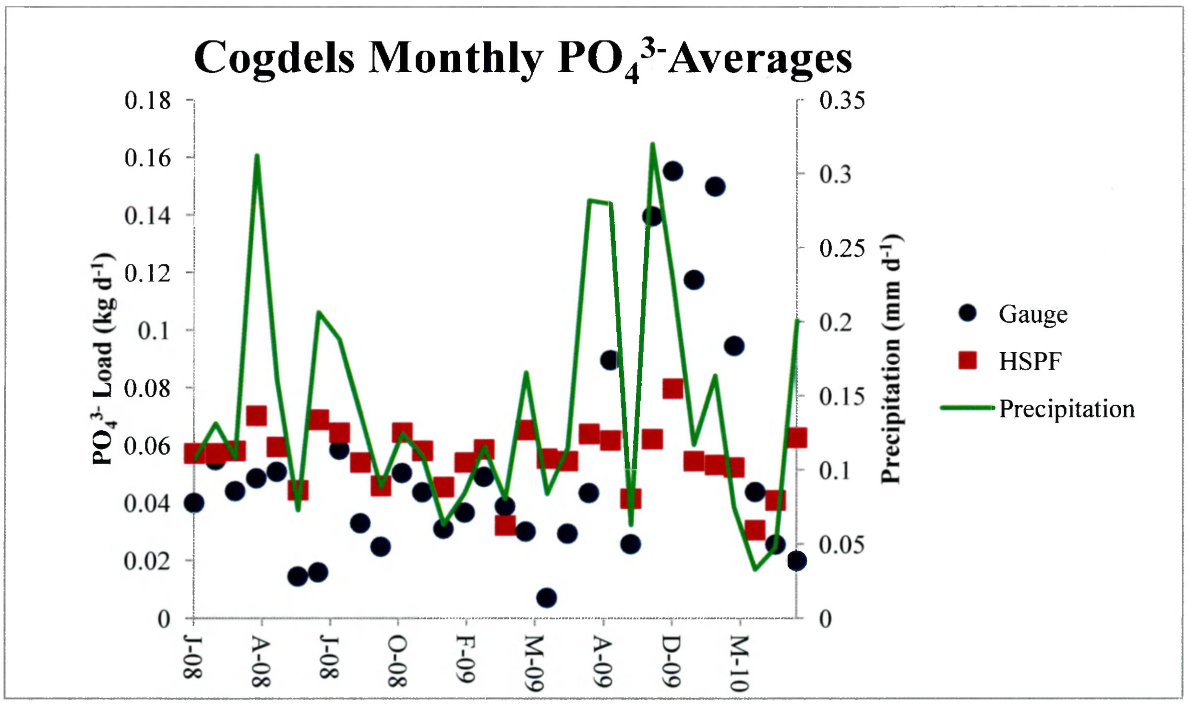
Cogdels Monthly PO_4^{3-} Averages
PO_4^{3-} Load (kg d^{-1})
Precipitation (mm d^{-1})
0
0.02
0.04
0.06
0.08
0.1
0.12
0.14
0.16
0.18
0.05
0.15
0.2
0.25
0.3
0.35
J-08
A-08
J-08
O-08
F-09
M-09
A-09
D-09
M-10
Gauge
HSPF
Precipitation

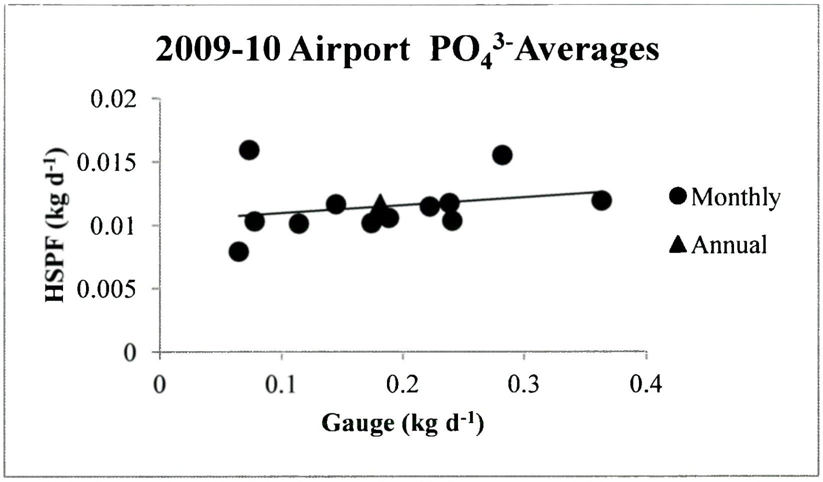

2009-10 Airport PO4 3- Averages
0.02
0.015
0.01
0.005
0
HSPF (kg d-1)
0
0.1
0.2
0.3
0.4
Gauge (kg d-1)
Monthly
Annual

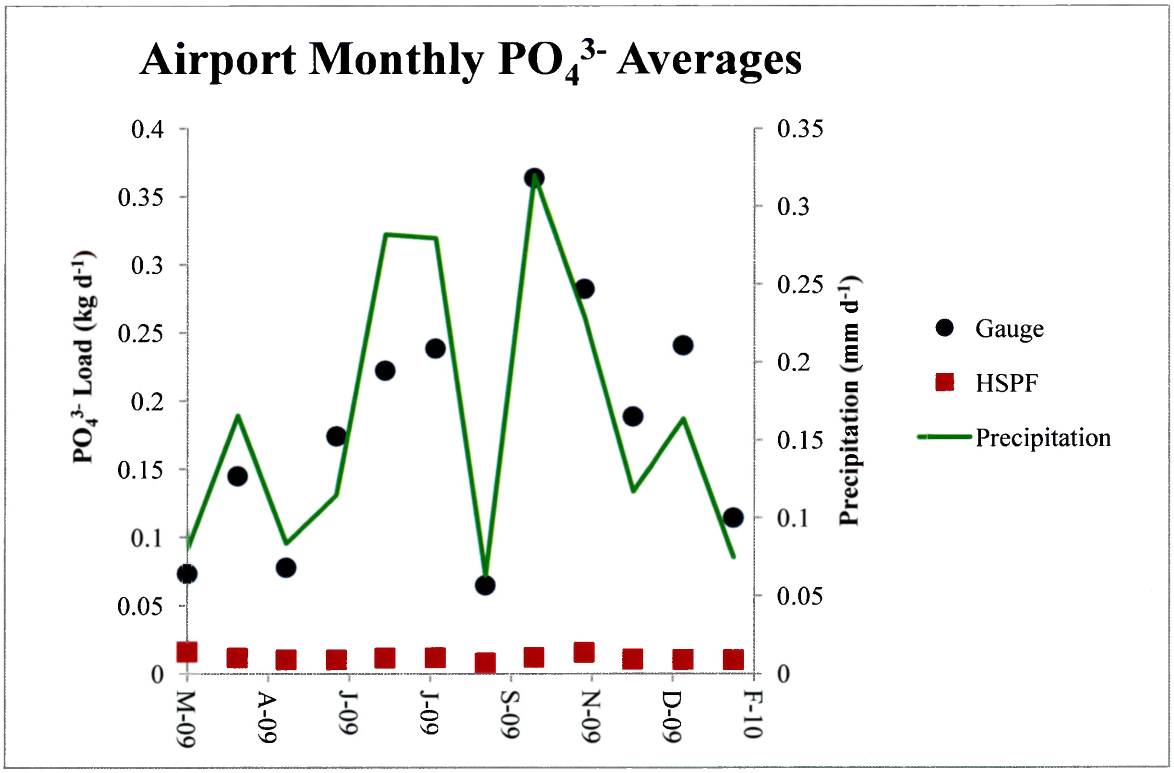

Airport Monthly PO4 3- Averages
0.4
0.35
0.3
0.25
0.2
0.15
0.1
0.05
0
PO4 3- Load (kg d-1)
0.35
0.3
0.25
0.2
0.15
0.1
0.05
0
Precipitation (mm d-1)
M-09
A-09
J-09
J-09
S-09
N-09
D-09
F-10
Gauge
HSPF
Precipitation

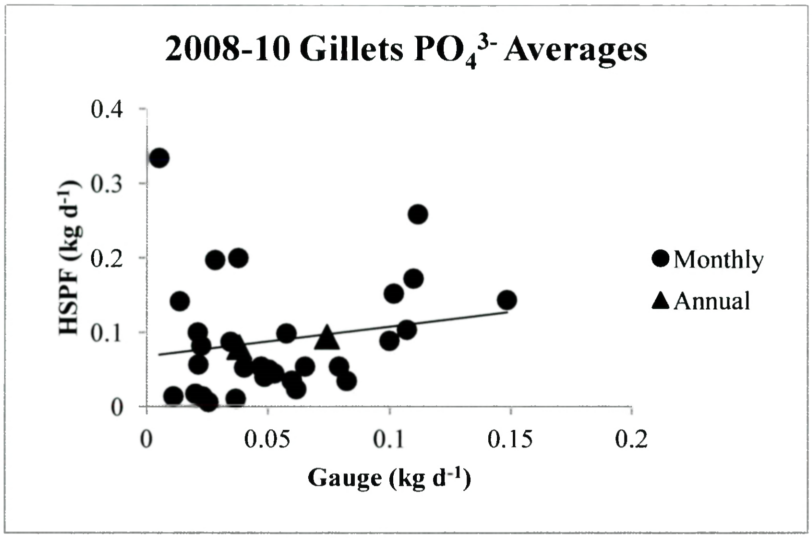
2008-10 Gillets PO_4^{3-} Averages
HSPF (kg d-1)
Gauge (kg d-1)
Monthly
Annual
0.4
0.3
0.2
0.1
0
0
0.05
0.1
0.15
0.2

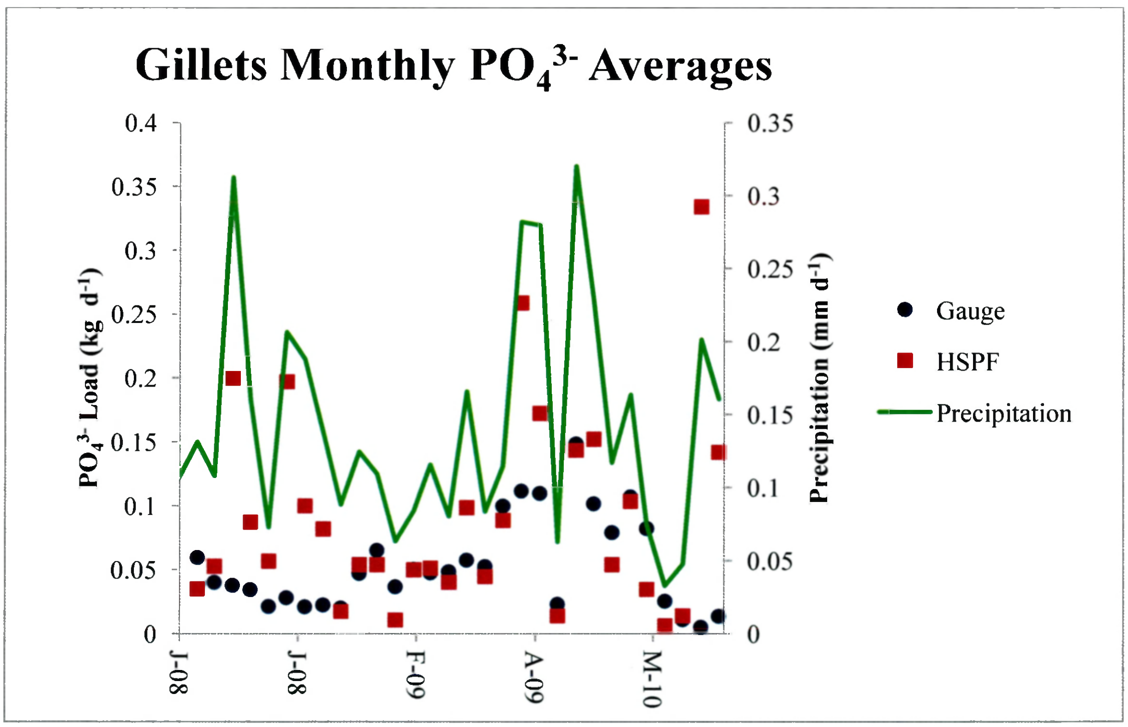
Gillets Monthly PO_4^{3-} Averages
PO_4^{3-} Load (kg d-1)
Precipitation (mm d-1)
Gauge
HSPF
Precipitation
J-08
J-08
F-09
A-09
M-10

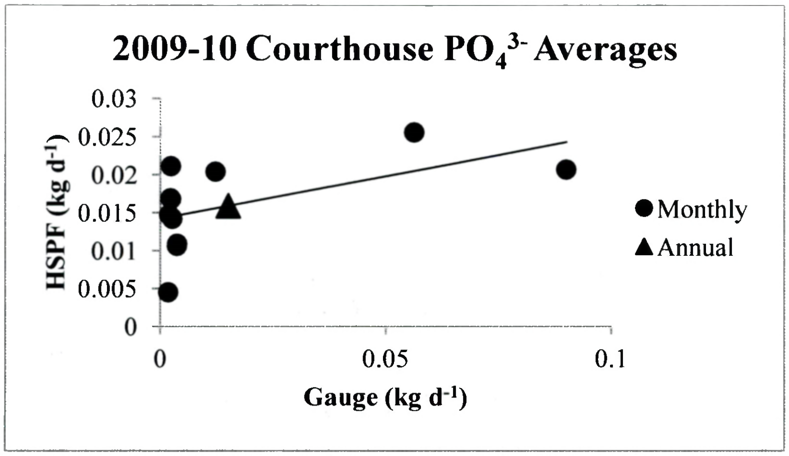

2009-10 Courthouse PO_4^{3-} Averages
0.03
0.025
0.02
0.015
0.01
0.005
0
HSPF (kg d-1)
0
0.05
0.1
Gauge (kg d-1)
Monthly
Annual

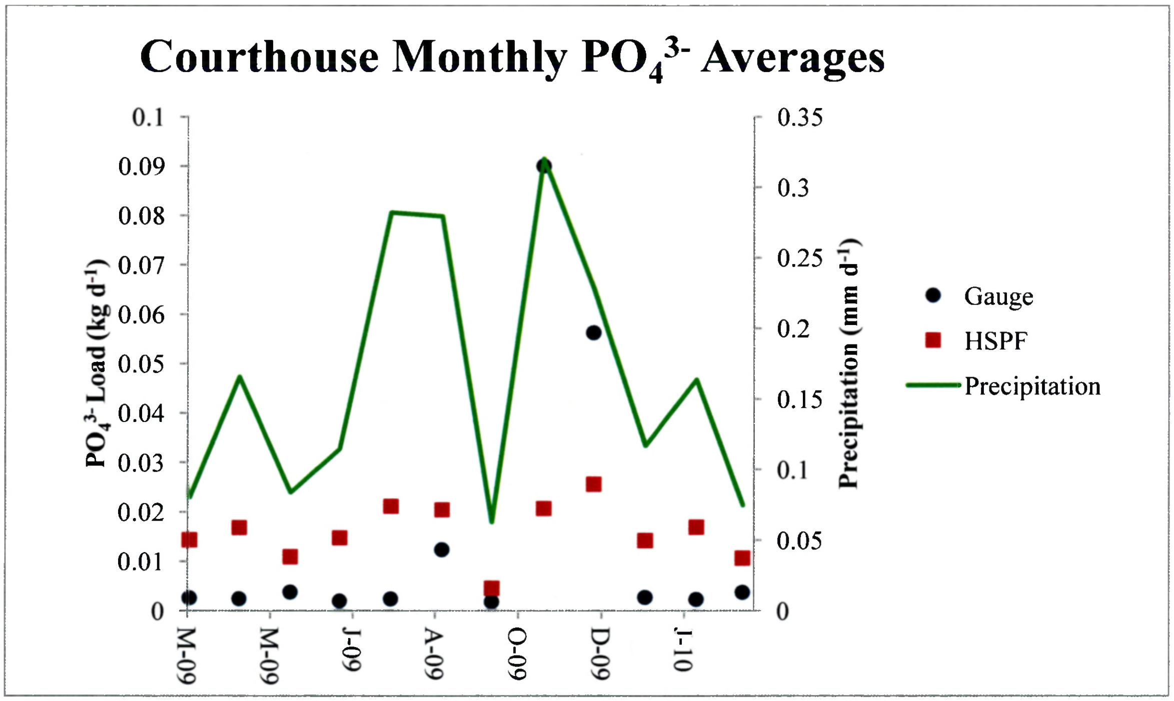

Courthouse Monthly PO_4^{3-} Averages
0.1
0.09
0.08
0.07
0.06
0.05
0.04
0.03
0.02
0.01
0
PO_4^{3-} Load (kg d-1)
0.35
0.3
0.25
0.2
0.15
0.1
0.05
0
Precipitation (mm d-1)
M-09
M-09
J-09
A-09
O-09
D-09
J-10
Gauge
HSPF
Precipitation

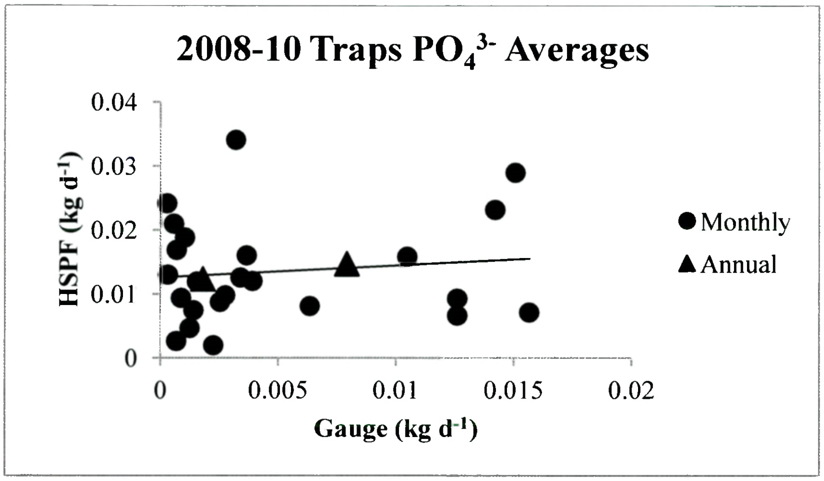

2008-10 Traps PO_4^{3-} Averages
0.04
0.03
0.02
0.01
0
HSPF (kg d-1)
0
0.005
0.01
0.015
0.02
Gauge (kg d-1)
Monthly
Annual

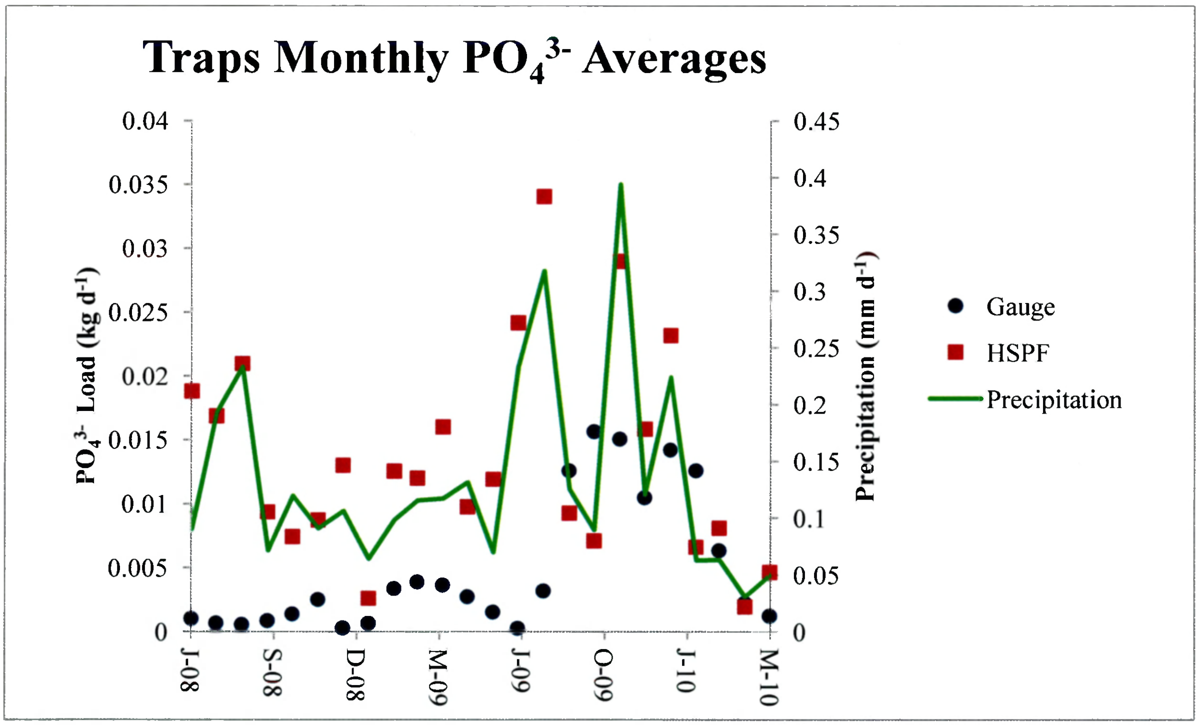

Traps Monthly PO_4^{3-} Averages
0.04
0.035
0.03
0.025
0.02
0.015
0.01
0.005
0
PO_4^{3-} Load (kg d-1)
0.45
0.4
0.35
0.3
0.25
0.2
0.15
0.1
0.05
0
Precipitation (mm d-1)
J-08
S-08
D-08
M-09
J-09
O-09
J-10
M-10
Gauge
HSPF
Precipitation

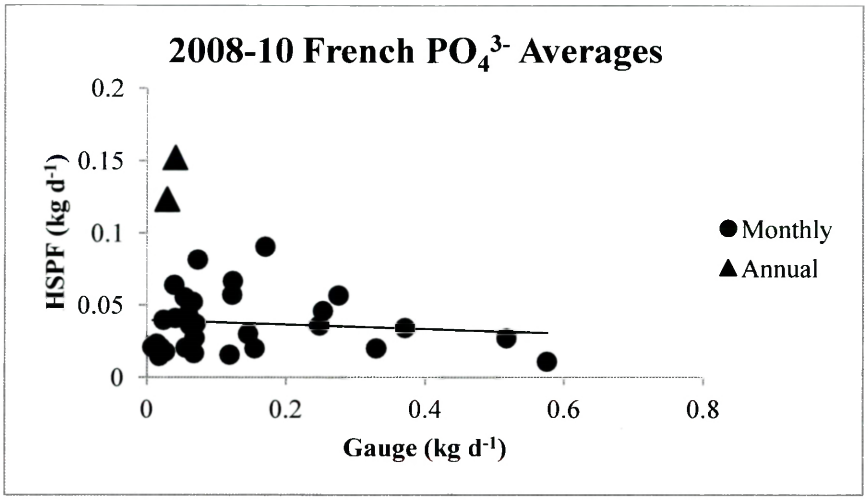

2008-10 French PO$_4^{3-}$ Averages
0.2
0.15
0.1
0.05
0
HSPF (kg d^{-1})
0
0.2
0.4
0.6
0.8
Gauge (kg d^{-1})
Monthly
Annual

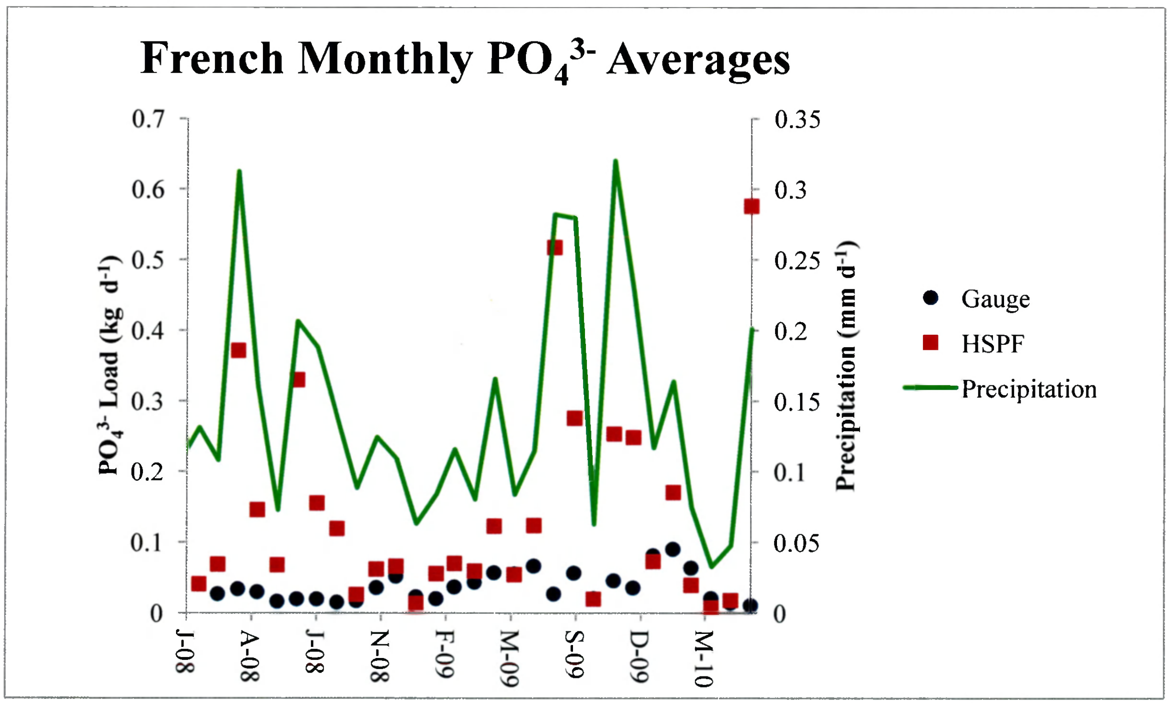

French Monthly PO$_4^{3-}$ Averages
0.7
0.6
0.5
0.4
0.3
0.2
0.1
0
PO$_4^{3-}$ Load (kg d^{-1})
0.35
0.3
0.25
0.2
0.15
0.1
0.05
0
Precipitation (mm d^{-1})
J-08
A-08
J-08
N-08
F-09
M-09
S-09
D-09
M-10
Gauge
HSPF
Precipitation

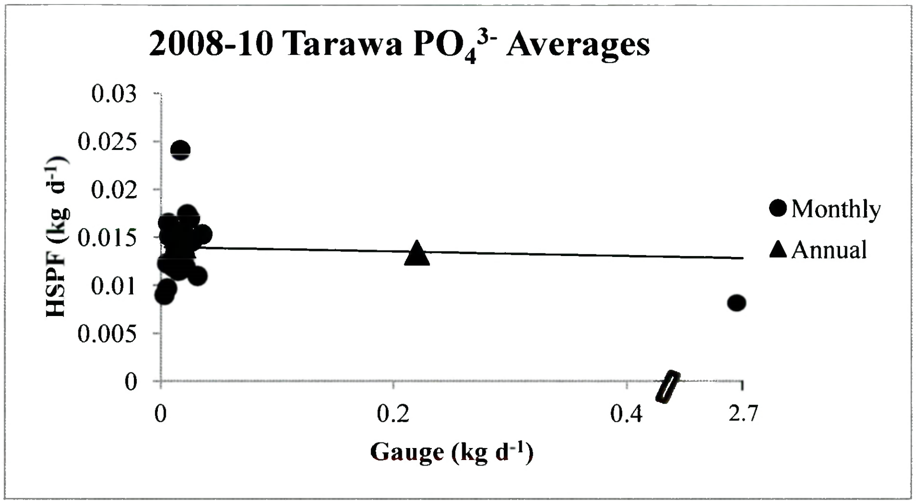
2008-10 Tarawa PO_4^{3-} Averages
HSPF (kg d-1)
Gauge (kg d-1)
Monthly
Annual
0.03
0.025
0.02
0.015
0.01
0.005
0
0
0.2
0.4
2.7

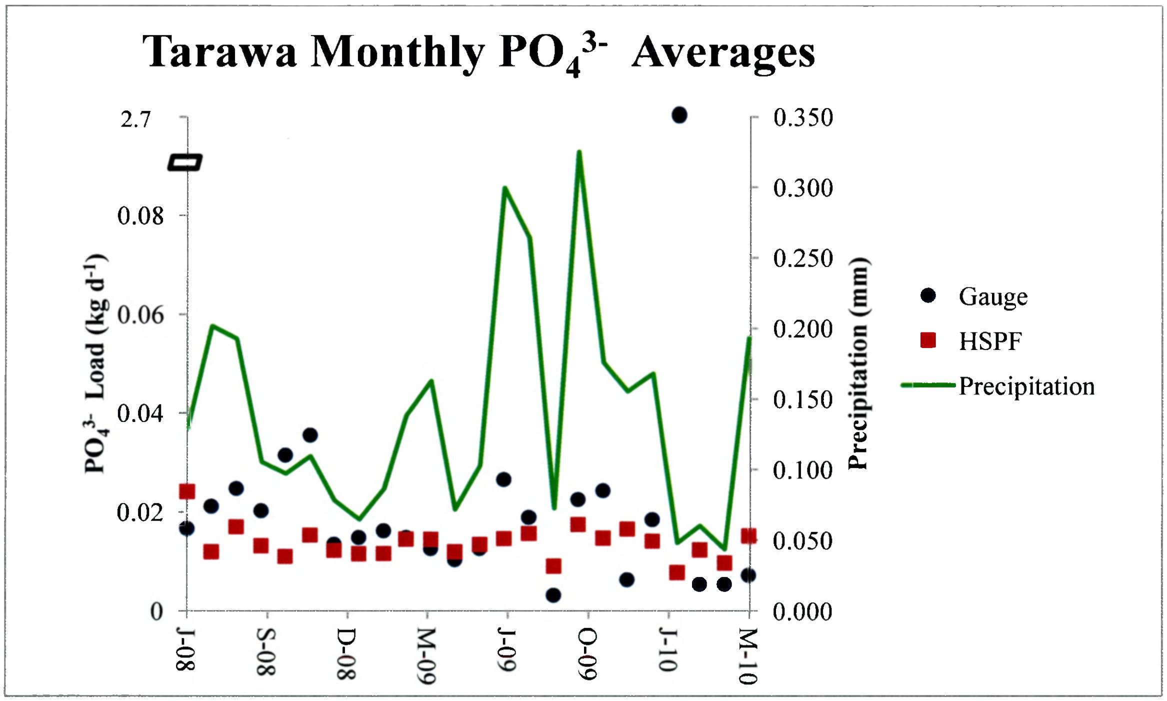
Tarawa Monthly PO_4^{3-} Averages
PO_4^{3-} Load (kg d-1)
Precipitation (mm)
Gauge
HSPF
Precipitation
2.7
0.08
0.06
0.04
0.02
0
0.350
0.300
0.250
0.200
0.150
0.100
0.050
0.000
J-08
S-08
D-08
M-09
J-09
O-09
J-10
M-10

Figure 14. Annual mean observed and modeled stream flow from all sub-watersheds for which an annual cycle of data are available.

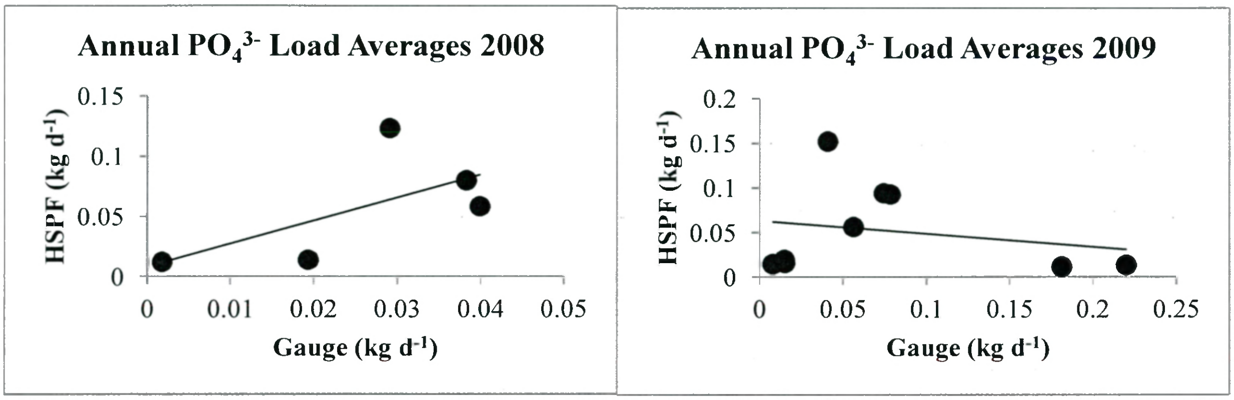

Table 7: Summary statistics for regressions between measured and modeled PO_4^{3-} loads (kg d^{-1}) from each sub-watershed at the monthly and annual resolution.

	R^2	Slope	Intercept
Monthly			
Freeman	0.02	0.23	0.08
Southwest	0.06	0.46	0.01
Cogdel	0.10	0.09	0.05
Airport	0.06	0.01	0.01
Gillets	0.03	0.40	0.07
Courthouse	0.31	0.11	0.01
Traps	0.01	0.19	0.01
French	0.01	-0.02	0.04
Tarawa	0.14	-0.0023	0.01
Annual			
2008	0.41	1.91	0.01
2009	0.05	-0.15	0.06

PLOAD Model

The PLOAD model predicted loads that were positively correlated with observed loads across the nine MCBCL sub-watersheds for TSS, TN, and PO_4^{3-} (Figs. 15-17 and Appendix Table 2). Predicted loads for 2008 were more closely correlated with the observations than for 2009. Generally, PLOAD was able to predict TSS loads within the range of the data for 2009, while TSS loads were under-estimated in 2008. PLOAD was able to estimate 2008 and 2009 TN loads fairly well, where all estimates were within the same range as the gauge loads. Overall, PO_4^{3-} loads were not well predicted, with PLOAD over-estimating loads in both 2008 and 2009.

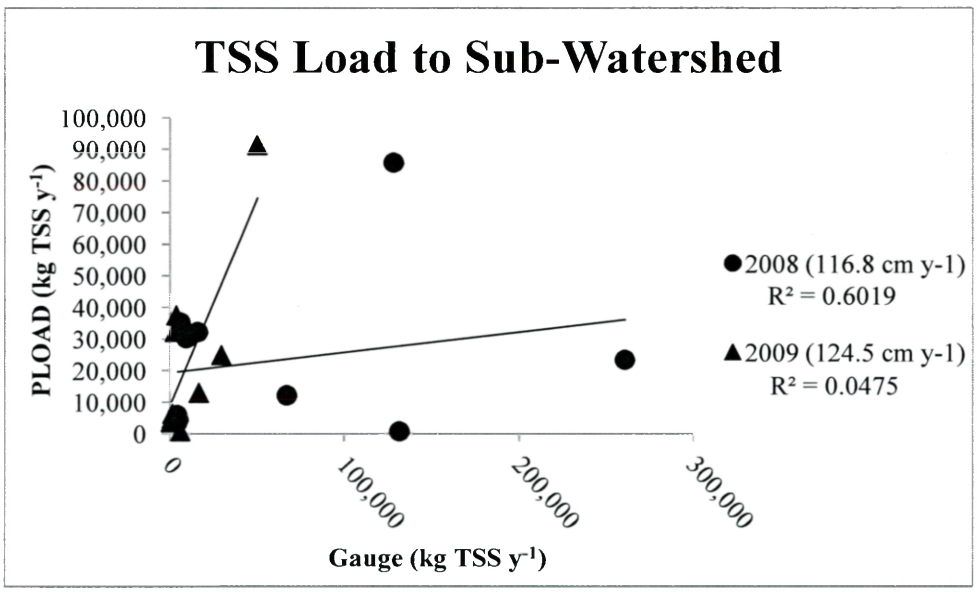

Figure 15. Modeled (PLOAD) and observed annual loading of total suspended solids across all nine MCBCL sub-watersheds. Rainfall totals were adjusted for each run of the model, and are indicated in the legend. The year 2008 represents the time frame of July 2008-June 2009 and the year 2009 represents the time frame of July 2009-June 2010.

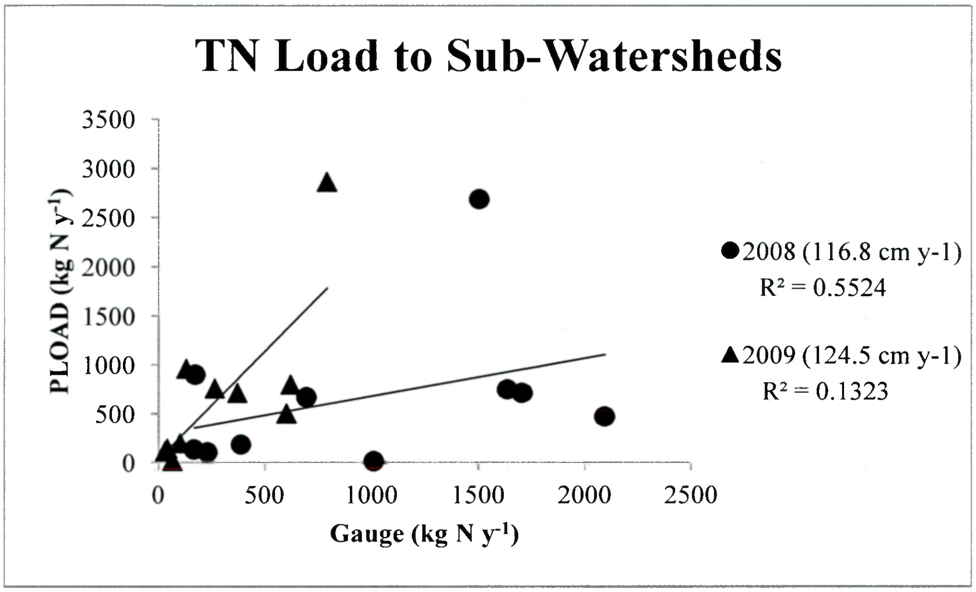

Figure 16. As for Fig. 15, but for loads of total nitrogen.

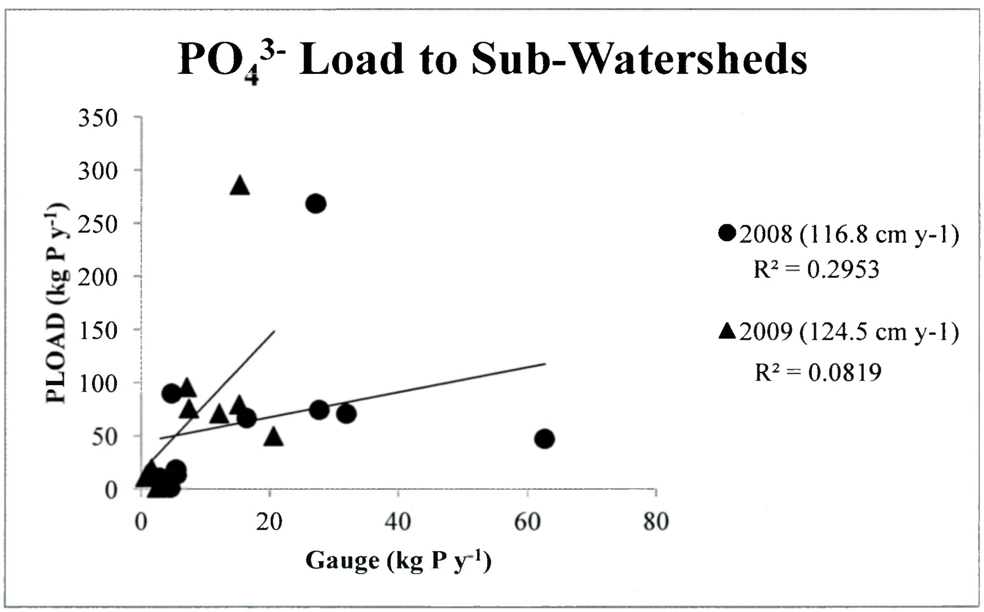

Figure 17. As for Fig. 15, but for loads of orthophosphate.

Model Scale-up to MCBCL

A major focus of DCERP has been to quantify the importance of external sources of TN to the NRE given that phytoplankton production in the estuary is nitrogen-limited (Paerl and Reckhow, 2012; Mallin et al. 2005). HSPF and PLOAD predicted TN loads originating from that portion of the NRE watershed impacted by MCBCL were combined with estimates of loads from the other major sources of TN to the New River Estuary determined by Brush (2012) and Anderson et al. (2012) (Fig.18). The analysis confirms the results from other DCERP watershed models (Brush,2012) that the TN load coming from MCBCL is much lower than loads coming from off-base portions of the watershed.

Figure 18. Model comparison of the contribution of major external sources to the total TN load entering the New River Estuary. MCBCL loads were estimated with a variety of models including HSPF and PLOAD as part of this study. Other sources were quantified by Brush (2012) and Anderson et al. (2012). Briefly, the off-base load was scaled up from USGS data at its Gum Branch station, MCBCL wastewater treatment facility (WWTF) loads were computed from data provided by MCBCL, atmospheric deposition was computed from local NADPP and EPA CastNet stations, and the load from Onslow Bay was computed from published offshore nitrogen concentrations and model estimates of advective inputs of water from offshore.

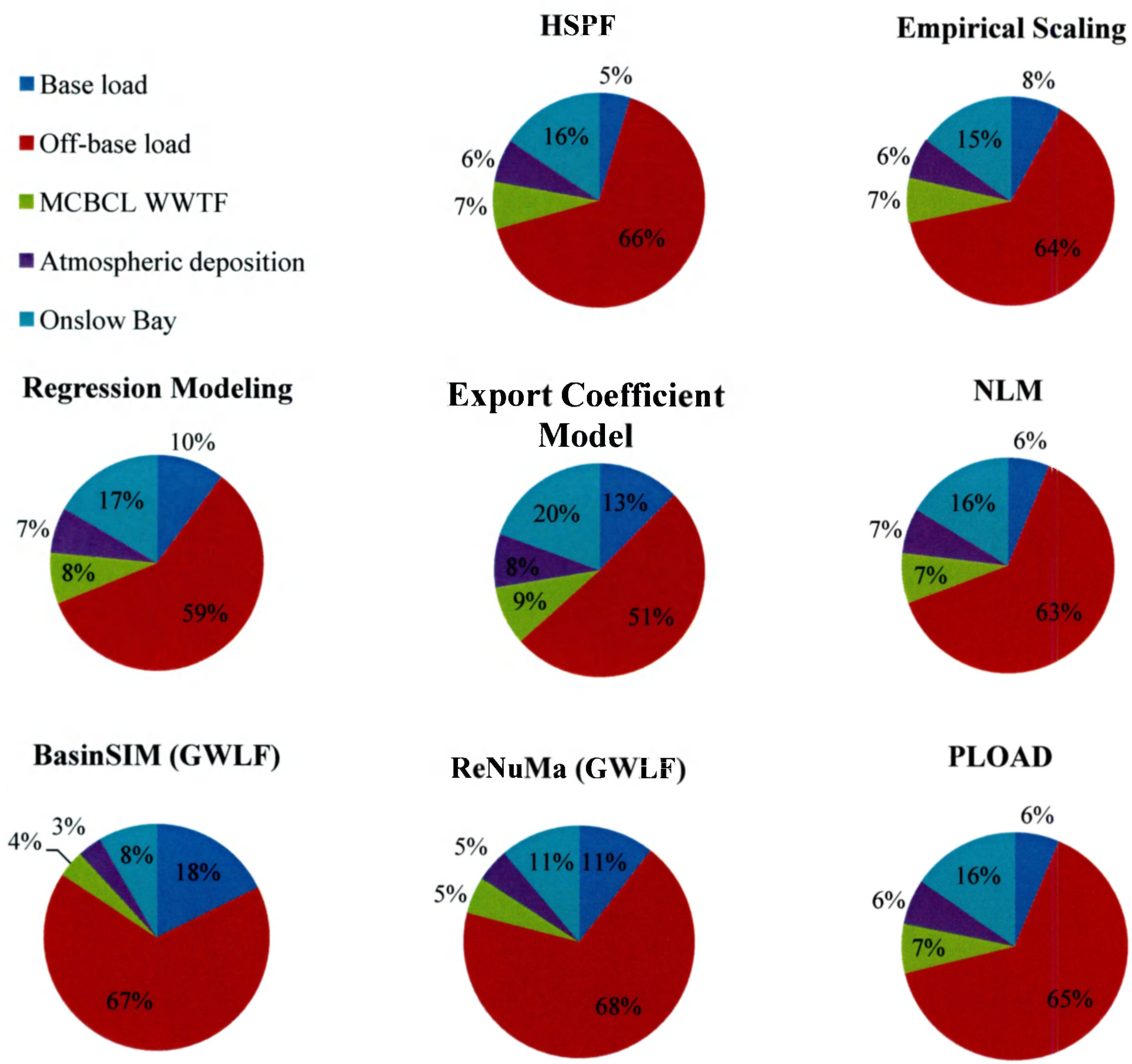
Base load
Off-base load
MCBCL WWTF
Atmospheric deposition
Onslow Bay
HSPF
5%
16%
6%
7%
66%
Empirical Scaling
8%
15%
6%
7%
64%
Regression Modeling
10%
17%
7%
8%
59%
Export Coefficient Model
20%
13%
8%
9%
51%
NLM
6%
16%
7%
7%
63%
BasinSIM (GWLF)
4%
3%
8%
18%
67%
ReNuMa (GWLF)
5%
5%
11%
11%
68%
PLOAD
6%
16%
6%
7%
65%

Land Use Scenarios

HSPF was used to simulate ongoing devlopment on the Base, by running scenarios with 5%, 10%, 15%, 20%, 25% and 30% of Base land designated as impervious surfaces with all meoterological conditions remaining the same. Current land use on the Base includes 13% impervious surfaces, so for the 5 and 10% scenarios impervious surfaces were converted to forested lands, while in the 15, 20, 25, and 30% scenarios forested lands were converted into impervious surfaces. HSPF predicted increasing loads with increasing impervious cover, with relatively large impacts on loads of freshwater, NH_4^+, and PO_4^{3-}, and much smaller effects on loads of sediments and NO_x^- (Fig 19).

Figure 19. Predicted loads entering the New River Estuary from MCBCL with 5%, 10%, 15%, 20%, 25%, and 30% of the Base covered by impervious surfaces. Measured loads under the current 13% impervious cover on the Base ("current") are shown for reference.

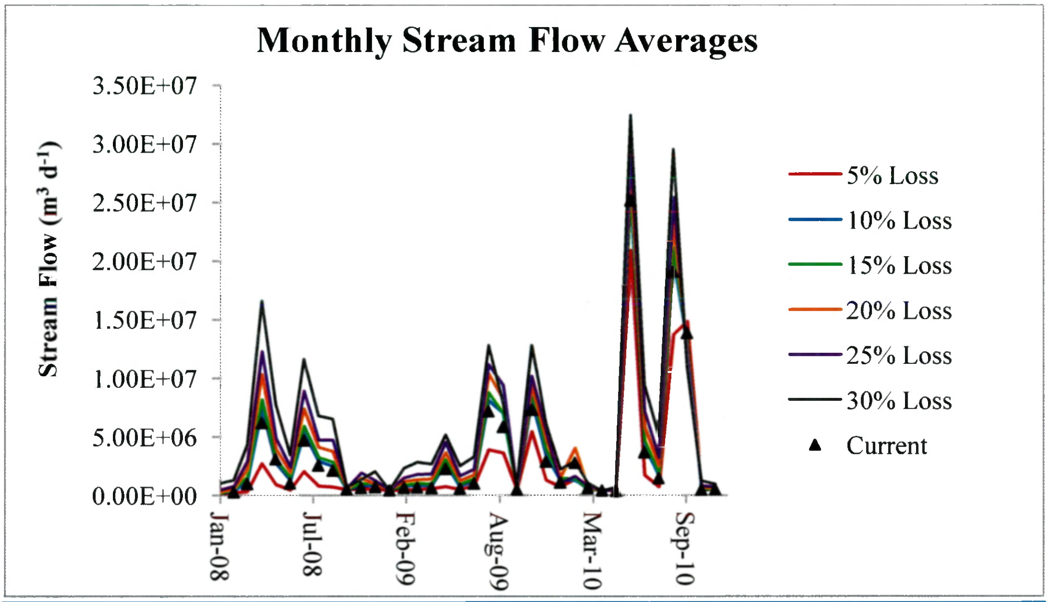

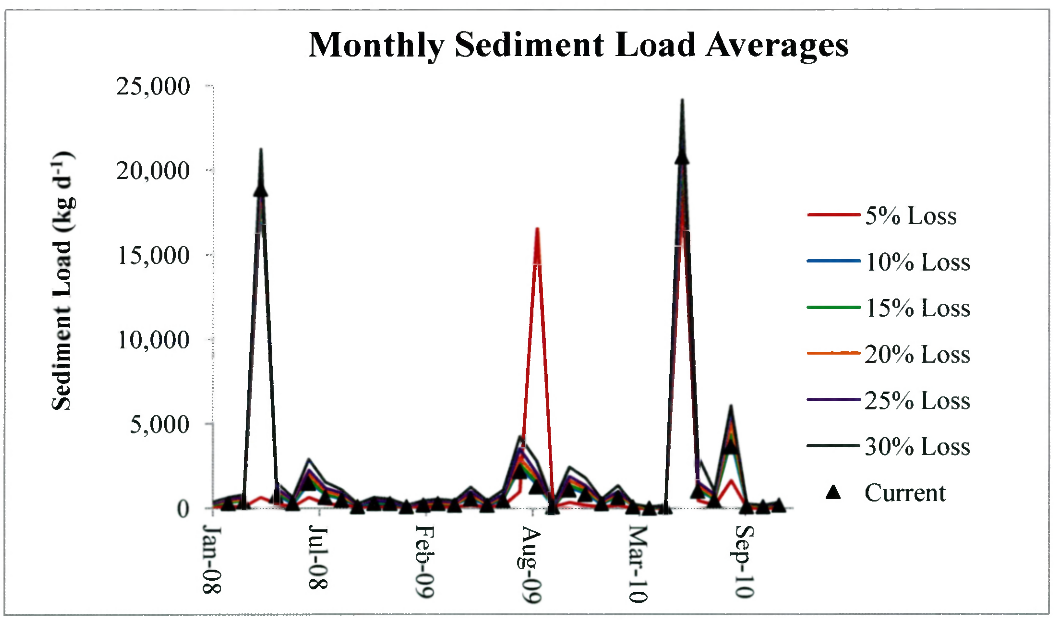

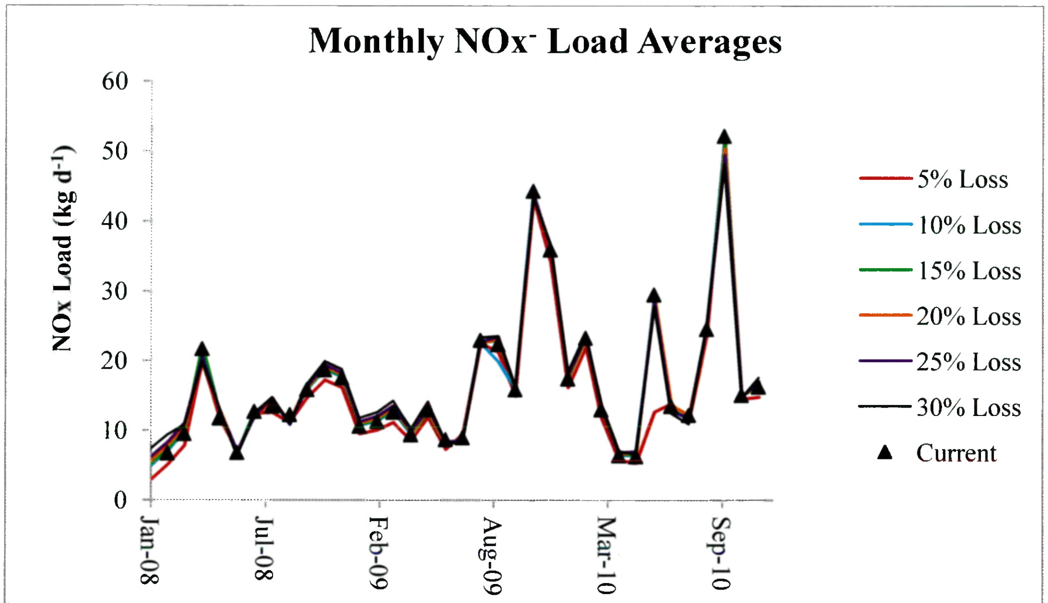

Monthly NOx⁻ Load Averages
NOx Load (kg d-1)
60
50
40
30
20
10
0
Jan-08
Jul-08
Feb-09
Aug-09
Mar-10
Sep-10
5% Loss
10% Loss
15% Loss
20% Loss
25% Loss
30% Loss
Current

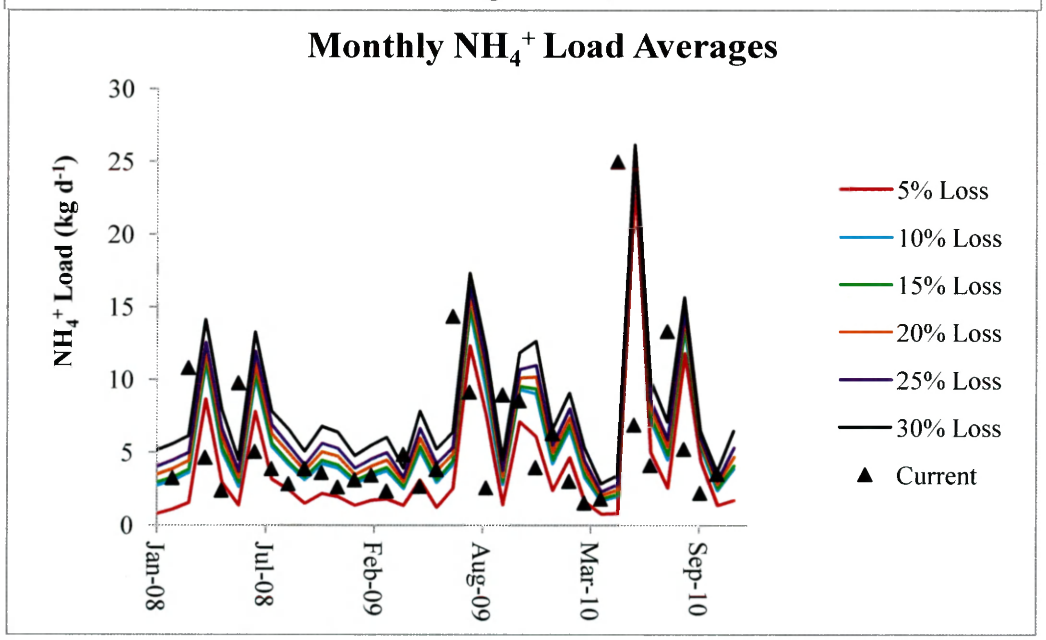

Monthly NH4+ Load Averages
NH4+ Load (kg d-1)
30
25
20
15
10
5
0
Jan-08
Jul-08
Feb-09
Aug-09
Mar-10
Sep-10
5% Loss
10% Loss
15% Loss
20% Loss
25% Loss
30% Loss
Current

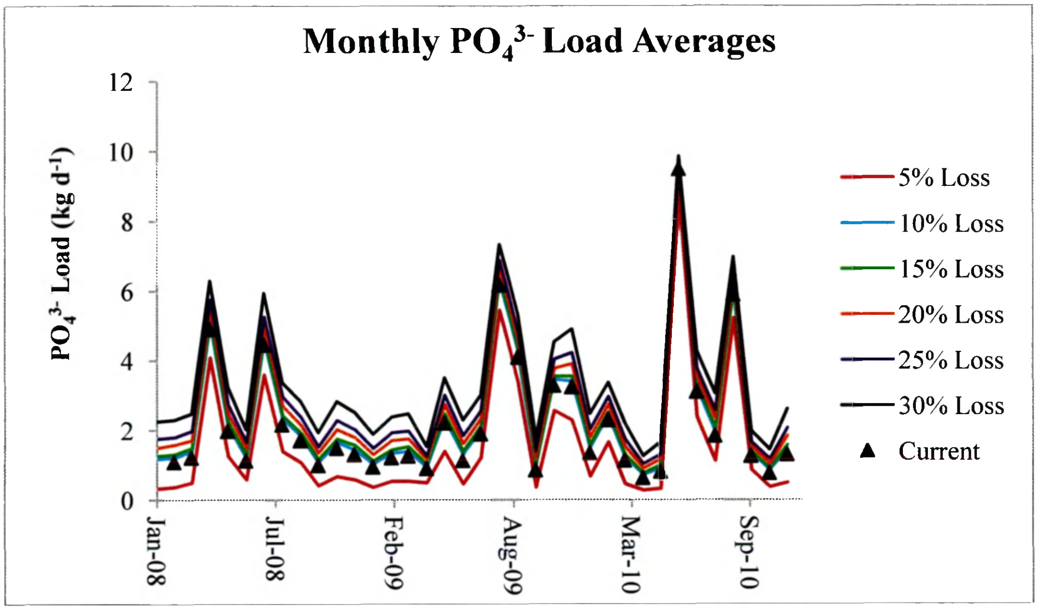

Monthly PO_4^{3-} Load Averages
PO_4^{3-} Load (kg d^{-1})
12
10
8
6
4
2
0
Jan-08
Jul-08
Feb-09
Aug-09
Mar-10
Sep-10
5% Loss
10% Loss
15% Loss
20% Loss
25% Loss
30% Loss
Current

Model Comparison

Model results from the current study (both HSPF and PLOAD) were compared to results from the other models applied to MCBCL as part of DCERP. These other models are summarized by Brush (2012) and range from application of empirical regressions to compute loads from land use distributions and physical watershed characteristics such as mean slope, an export coefficient spreadsheet model (Watershedss), a spreadsheet model with bulk attenuation coefficients (NLM – Nitrogen Loading Model), and two applications of the Generalized Watershed Loading Functions approach (BasinSim and ReNuMa). The latter two models predict loads on both monthly and annual scales, while all others predict loads at the annual scale.

The annual loads of total nitrogen (TN), phosphorus (TP or PO_4^{3-}), and total suspended solids (TSS) predicted by each model for 2008 and 2009 were compared graphically (Fig. 20) and by comparison of coefficients of determination from regressions of observed and modeled loads (Table 2). ReNuMa tended to most accurately predict observed TN loads considering 2008 and 2009 together. BasinSim, PLOAD, and Watershedss tended to over-predict TN loads while HSPF tended to under-predict loads. HSPF had the highest overall R^2 for phosphorus loads, and modeled values were within the same range as the observations. Again, BasinSim and PLOAD over-predicted phosphorus loads to the sub-watersheds. PLOAD had the highest overall R^2 for TSS loads, and the annual predicted loads were within the same range as the observations.

Figure 20. Comparison of predicted and observed annual loads of total nitrogen (TN) from all models applied to MCBCL sub-watersheds. Two models also predicted dissolved nitrogen (DN) loads; these plots are provided for comparison.

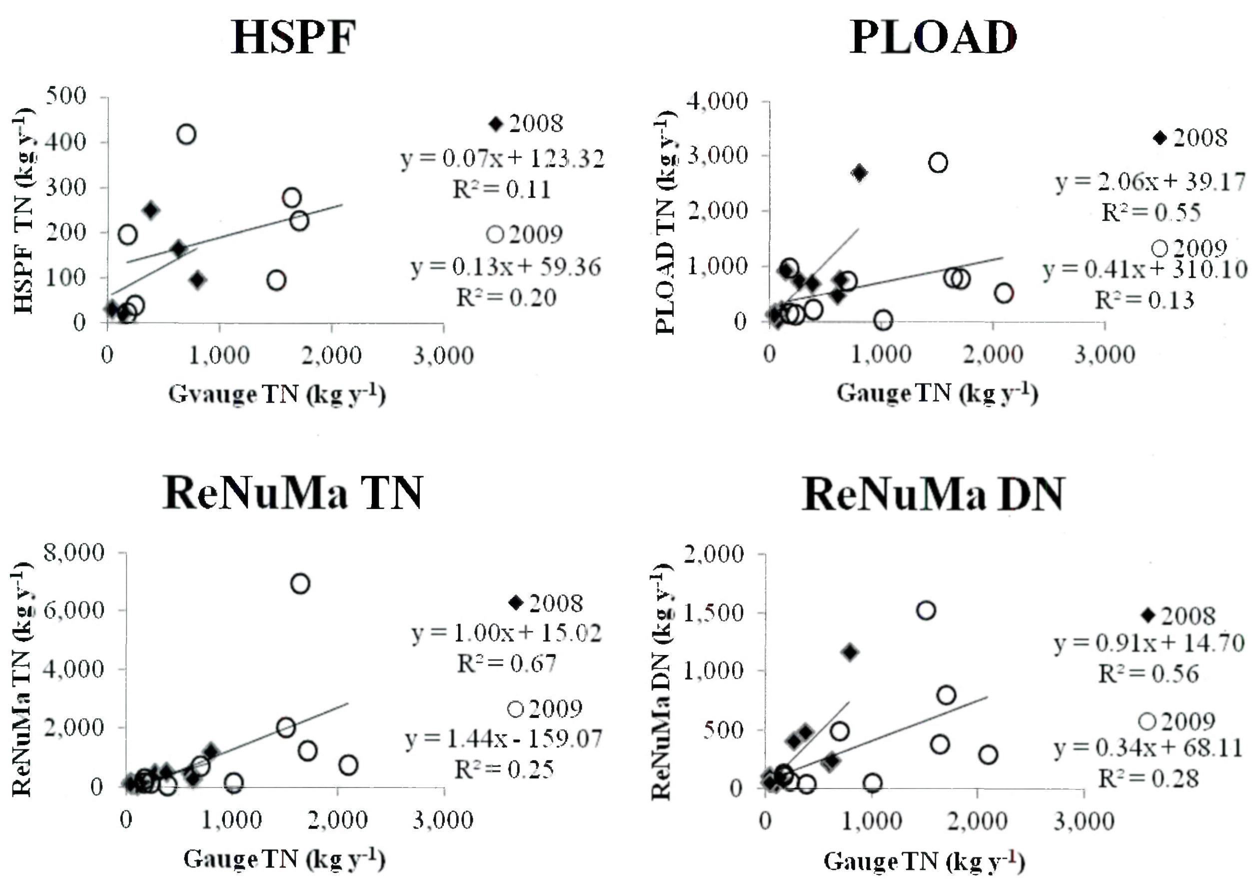

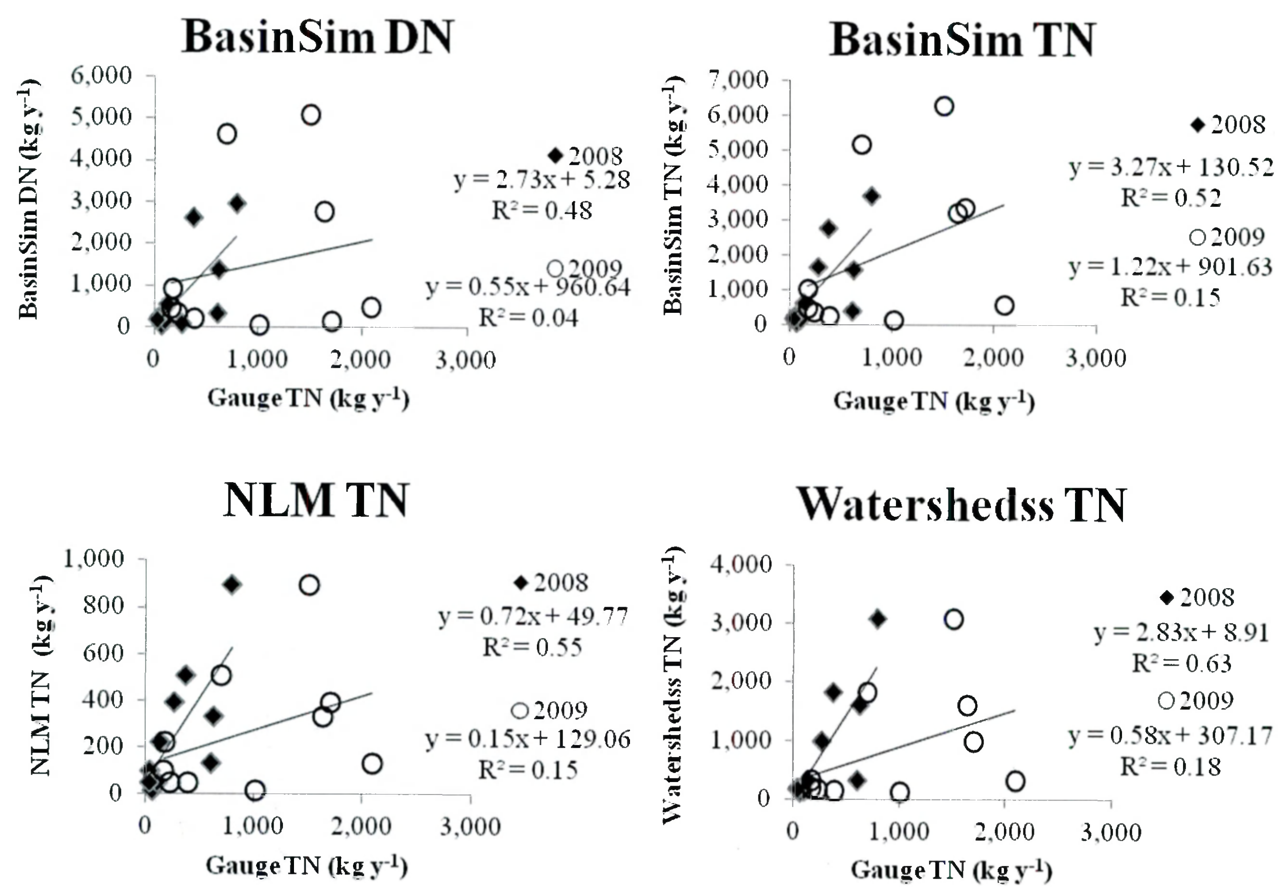
BasinSim DN
BasinSim DN (kg y-1)
Gauge TN (kg y-1)
◆2008
y = 2.73x + 5.28
R² = 0.48
○2009
y = 0.55x + 960.64
R² = 0.04
BasinSim TN
BasinSim TN (kg y-1)
Gauge TN (kg y-1)
◆2008
y = 3.27x + 130.52
R² = 0.52
○2009
y = 1.22x + 901.63
R² = 0.15
NLM TN
NLM TN (kg y-1)
Gauge TN (kg y-1)
◆2008
y = 0.72x + 49.77
R² = 0.55
○2009
y = 0.15x + 129.06
R² = 0.15
Watershedss TN
Watershedss TN (kg y-1)
Gauge TN (kg y-1)
◆2008
y = 2.83x + 8.91
R² = 0.63
○2009
y = 0.58x + 307.17
R² = 0.18

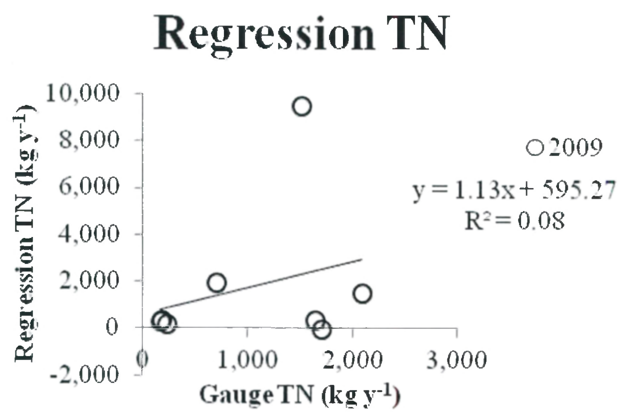
Regression TN
10,000
8,000
6,000
4,000
2,000
0
-2,000
Regression TN (kg y-1)
0
1,000
2,000
3,000
Gauge TN (kg y-1)
2009
y = 1.13x + 595.27
R² = 0.08

Table 8. R^2 values of modeled annual loads compared to gauge measurements from nine sub-watersheds on MCBCL.

Nitrogen									
	HSPF	NLM TN	BasinSim DN	BasinSim TN	ReNuMa TN	ReNuMa DN	Regression TN	Watershedss TN	PLOAD
Jul 2008-Jun2009	0.00	0.55	0.48	0.52	0.67	0.56		0.63	0.55
Jul 2009 - Jun 2010	0.01	0.15	0.04	0.15	0.25	0.28	0.08	0.18	0.13
Phosphorus									
	HSPF		BasinSim DP	BasinSim TP	ReNeMa TP	ReNuMa DP	Regression PO4	Watershedss TP	PLOAD
Jul 2008-Jun2009	0.576		0.286	0.306	0.106	0.153		0.278	0.295
Jul 2009 - Jun 2010	0.342		0.073	0.080	0.039	0.064	0.666	0.072	0.082
Total Suspended Solids									
	HSPF		BasinSim		ReNuMa	Regression			PLOAD
Jul 2008-Jun2009	0.415		0.513		0.017				0.602
Jul 2009 - Jun 2010	6.216E-08		0.016		0.034	0.871			0.048

Finally, results of the land use conversion scenarios in HSPF were compared to those conducted by Brush (2012) using NLM and ReNuma (Fig. 21). All models predicted watershed yields of TN (loads per hectare) in the correct range, but the ReNuMa model followed the observations most closely.

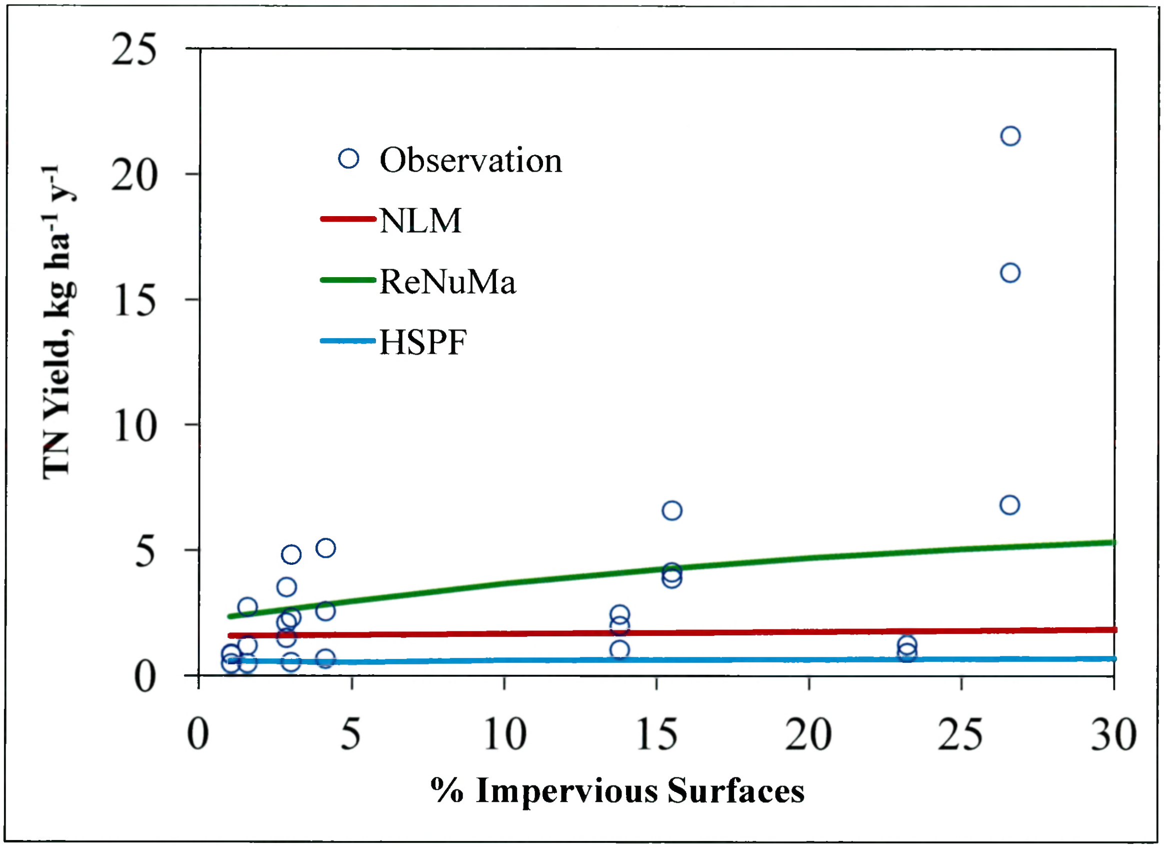

Figure 21. Comparison of NLM, ReNuMa, and HSPF loads of TN per hectare from MCBCL across a range of watershed imperviousness. Model predictions are plotted with measured DCERP gauge data from the nine sub-watersheds on MCBCL.

DISCUSSION

Model Calibration

The large number of parameters and ability to vary them on a monthly basis in the HSPF model gives the user the ability to fine-tune model predictions, but often there were no local data available to constrain parameter values during calibration. The HSPF model determines watershed runoff based on land use type and elevation, but the model does not create flow paths through the land. There was greater precipitation on MCBCL in 2009 than in 2008, but HSPF generally overestimated loads in 2008 and underestimated loads in 2009. The difference in annual precipitation between the two years may have resulted in the switch from positive to negative slopes between observed and modeled loads in 2008-09 and 2009-10, respectively, for all parameters except NOx^- (Figs. 8, 10, 12, and 14). Similarly, slopes between observed and modeled loads using PLOAD displayed lower slopes in the second year (Figs. 15-17). Our focus, however, was on estimating long term average loads (multiple years) rather than short term loads (from year to year). Therefore, while changes in the annual regression slopes from year to year are important in this instance, if the models are used to estimate loads over longer periods of time, then these changes are less important. Cogdels was the first sub-watershed calibrated in HSPF, and coincidentally its land use distribution most closely reflected that of the entire MCBCL. Forested land and urban surfaces combined make up 67% of Cogdels (Fig. 4) and 55% of MCBCL (Fig. 3) land area, and these two land uses have significant effects on HSPF output. Therefore, starting calibration with Cogdels was also advantageous given the availability of a full two years of gauge data.

Since the model was calibrated to Cogdels, it was expected that model output would best match the measured loads in this sub-watershed. Predicted loads in Cogdels were generally on the same scale as the observed values and R^2 values were generally the highest across the sub-watersheds. Although modeled freshwater stream flows were higher than the measured gauge data, the model generally followed the trends (e.g., peaks in loads) in the data. When the freshwater stream flow was initially calibrated, the model more closely matched flows. However, when the sediment and nutrient simulations were initiated, predicted loads were far lower than observed loads. Therefore, the amount freshwater stream flow was intentionally increased in order to more accurately simulate the sediment and nutrient output. HSPF output followed the same general trend as the gauge data for sediments and nutrients in Cogdels, but in all cases missed the peaks in late fall 2009 and early spring 2010. The precipitation peaks during this time were only slightly higher than those recorded prior to that time frame, and it is unknown what caused the higher than normal gauge measurements. Spatial variability in rainfall across MCBCL was noted during the data collection phase of DCERP, which could explain variations in freshwater output across sub-watersheds.

HSPF least accurately reproduced freshwater flow, sediment loads, and nutrient loads to Airport and French sub-watersheds. The model underestimated all output from Airport, even though the freshwater stream flow and sediment loads were correlated and had R^2 values above 0.5. The large area of impervious surfaces and the intricate ditches running through this sub-watershed likely limit the ability of the model in this system because the model is a lumped parameter model that does not specify flow paths from the land when estimating stream flows. Models previously applied to Airport were also unable to reproduce the magnitude of and trends in freshwater flow, sediment loads, and nutrient loads (Brush, 2012). In contrast, the land use distribution in the Courthouse sub-watershed is most similar to that of Airport, but HSPF-predicted loads in this system generally followed the same trends as the gauge data and were within the same range as the measurements. The French sub-watershed is comprised mostly of grassland and wetlands, with very little forest or urban surfaces, unlike Cogdels. Since parameter values were used from the original Cogdels calibration, this could explain why HSPF overestimated loads in this sub-watershed.

The limited accuracy of HSPF in reproducing variations in loads between years and across sub-watersheds may be due to a number of factors. As noted above, HSPF is a lumped parameter model that does not specify flow paths from the land when estimating stream flows. This project focused on the low flow, non-tidal fresh water streams on MCBCL which often go dry, and HSPF is not able to model these conditions. Unlike traditional applications of HSPF, the landscape at MCBCL has little relief, contains several wetlands, and contains streams that often have little flow and act more like wetlands (M. Piehler, pers. comm.). HSPF has been noted to not perform well where the landscape is flat and wetland-dominated (J. Shen, pers. comm.), which is a problem on MCBCL since wetlands are sites of increased nutrient cycling and retention/removal prior to release to the estuary. These factors might partially explain why HSPF overestimated loads in the French Creek sub-watershed, since parameter values were used from the original Cogdels calibration where urban and forest are the primary land uses. If a sub-watershed that had a higher percentage of wetlands was calibrated first and those values were used to estimate loads in the other sub-watersheds the modeled loads could potentially align with measured loads more closely.

Past applications of watershed models to the Tarawa sub-watershed have been problematic due to removal and construction of new MCBCL housing units (Brush, 2012). During construction, storm water Best Management Practices (BMPs) were also implemented. The BMP construction required the release of water between January and February 2010 that caused higher than normal freshwater stream flow, sediment loads, and nutrient loads. When these elevated flows were excluded from the gauge record, HSPF estimates of freshwater stream flow, sediment loads, and nutrient loads followed the measured loads more closely, but still not well enough to be considered reliable. After February 2010, HSPF over-predicted freshwater stream flow, but the R^2 improved from 0.035 to 0.23. HSPF-predicted sediment loads continued to underestimate gauge measurements, but the R^2 improved from 0.087 to 0.10. Since construction within Tarawa is now complete, current freshwater flows and sediment and nutrient loads are now the norm and should make future model implementation easier and predictions more reliable.

Scale-up and Scenario Analysis

Model scale up to estimate loads from MCBCL was relatively easy, and the scale up reinforced previous findings (Brush, 2012) that MCBCL is a relatively small source of TN to the estuary. Since land use is the driving factor used by HSPF to estimate watershed loads, the use of Codgels for initial calibration provides confidence in the scale up to MCBCL given the similar land use distributions in the two watersheds. Even though MCBCL is a relatively small source of nitrogen to the NRE, the entry points of this nitrogen in the mid to lower portion of the estuary which is nitrogen-limited may cause these inputs to be more important than expected based on the small overall load.

Model Comparison and Recommendations

To date, there has not been a spectrum of models, from simple to complex, applied to a coastal plain setting and compared. This project provided an opportunity to make this comparison in a relatively small watershed with multiple gauged sub-watersheds with contrasting land use distributions. The various models that were applied produced a range of estimates, and no one model did the best at estimating loads of nitrogen, phosphorus, and total suspended solids. Both HSPF and PLOAD produced reasonable results that were within the same magnitude or at least followed the same general trends as the gauged loads. With the widespread use of the HSPF model, it was hypothesized that the model would have performed better relative to simpler models like PLOAD or those applied by Brush (2012). The PLOAD model was simple and straightforward to use, and predicted intermediate loads to the sub-basins. PLOAD is calibrated by adjusting the event mean concentrations (EMC) and the export coefficients, and each are based on run-off from different land use types. Due to the simplicity of the PLOAD model, it was expected that it would be able to reproduce general trends but not have the same fine tuning capabilities as an intermediate or more advanced model.

The EPA developed the BASINS modeling suite as a user-friendly, yet highly technical program that is widely accepted for management decision making. Yet, the results of this study show that the highly technical models are not able to predict fresh water, sediment, and nutrient loads to the estuary better than simpler models. While there is ample literature available through the BASINS website on how to do the most basic model set up and runs, there is little information available on how to adapt the model in order to use non-standard input data. The HSPF manual is helpful, but does not inform the user about the underlying governing equations and the main controlling parameters. The technical notes were helpful in calibrating the freshwater stream flow and sediments, but the guidance was based on previous applications of the model rather than on direct measurements of parameter values. HSPF provides users the ability to control aspects of a watershed model that are not available in more simplified models. While this can be helpful to fine-tune a model and determine how various meteorological and land use changes affect watershed loads, it can also make it difficult to base parameter values on scientific measurements. The multitude of parameters can also require more model spin-up time. For example, the high initial estimates of sediment and NOx^- in Southwest are most likely attributed to model spin up rather than inaccuracies in estimated parameter values. Parameters can also be difficult to calibrate because some can vary monthly and across land use types, and these specific measurements are usually unavailable, as was the case in the current project. The inability to review the governing equations was another difficulty with using and learning the HSPF model, which might partially explain why a formal peer-reviewed, published sensitivity analysis has not been conducted. HSPF is a comprehensive model, but it is difficult to learn and implement without formal training and may not be suitable for management personnel not highly familiar with the program.

PLOAD was straight forward and worked as the EPA described, as a simplified model to determine general trends due to anthropogenic and climatic changes. PLOAD was easy to implement and provided estimates that fit general annual trends across the sub-watersheds. It is also capable of modeling implementation of BMPs, although this feature was not required for this project. Between the two models applied to MCBCL in the study, PLOAD is recommended for use by MCBCL management personnel for investigation of potential changes in watershed loads that could result from implementation of BMPs and other changes in the landscape. The management personnel on MCBCL need a simple model that is well calibrated and annually-focused; PLOAD meets these requirements. However, since no one model in the entire spectrum of models applied to MCBCL performed best (Brush, 2012), more than one model may be needed to capture the annual trends of the constituents studied. Based on statistical performance (Fig. 20, Table 7) and ease of use, ReNuMa is also recommended for modeling total nitrogen loads. Together PLOAD and ReNuMa can easily be used in conjunction by management personnel to estimate and model nitrogen loads to the New River Estuary.

APPENDIX

Appendix Figure 1. Average daily observed and HSPF-modeled stream flow in each sub-watershed.

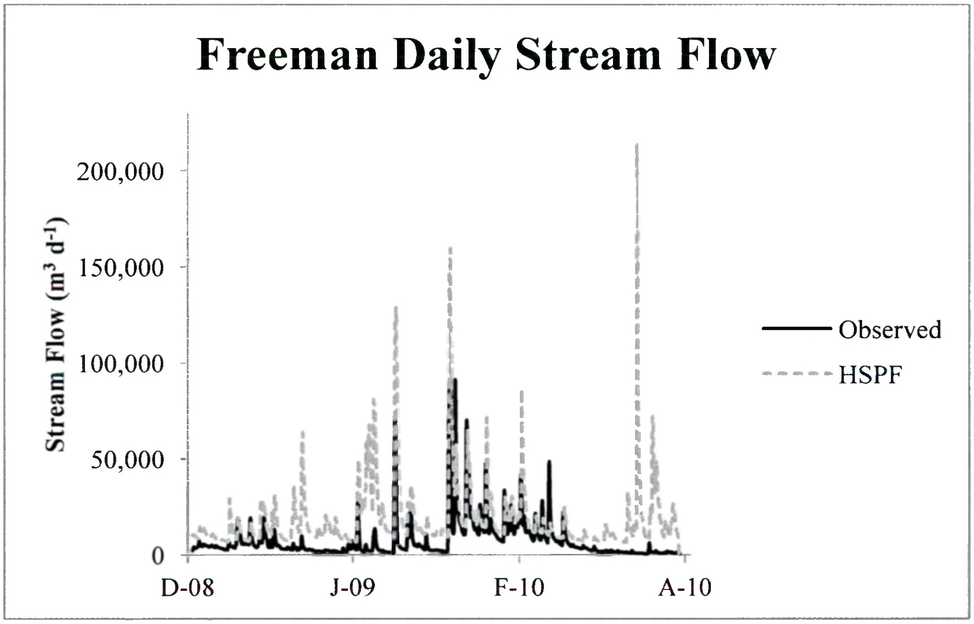

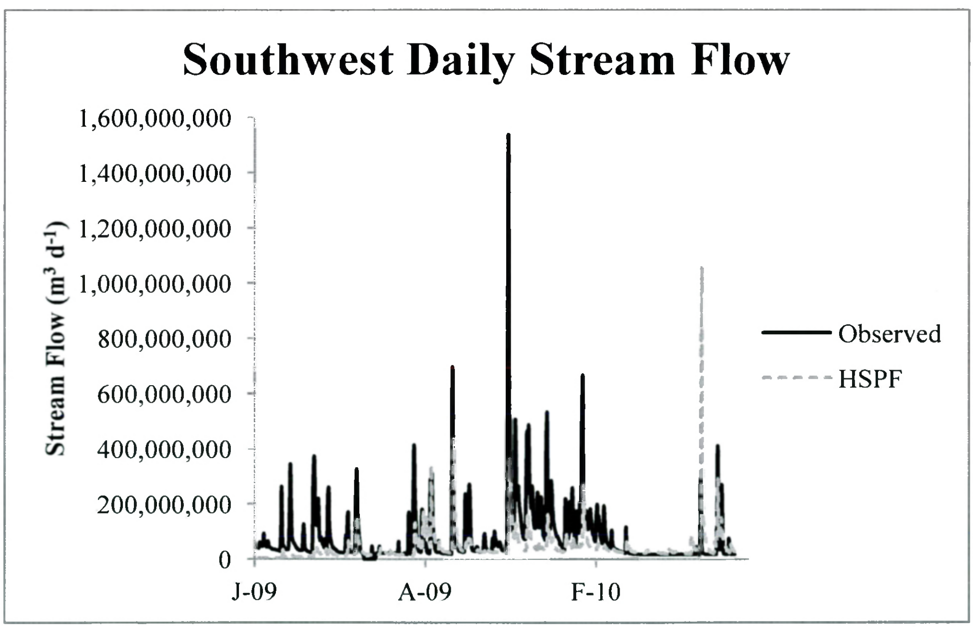

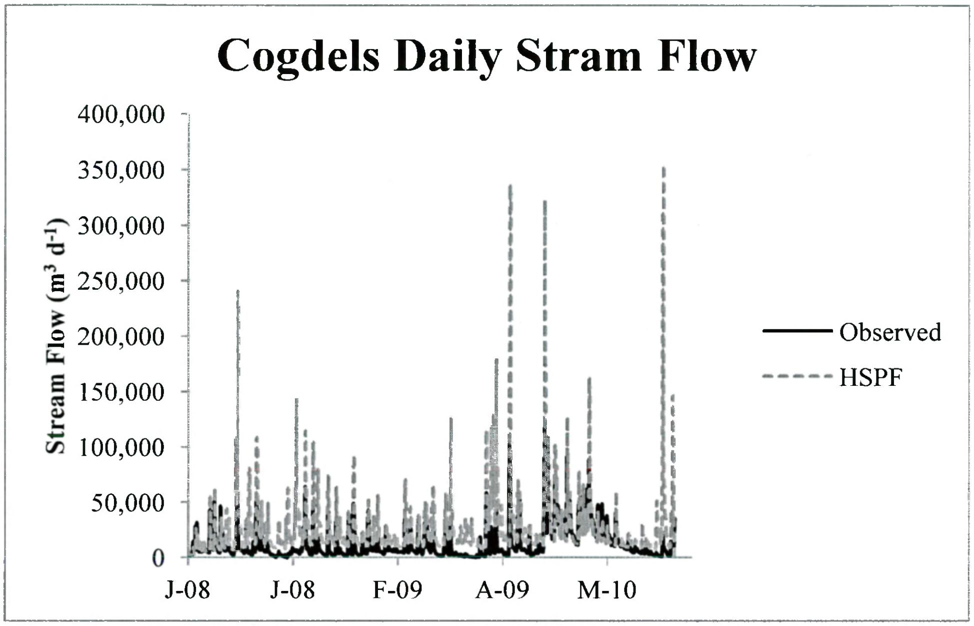
Cogdels Daily Stram Flow
400,000
350,000
300,000
250,000
200,000
150,000
100,000
50,000
0
Stream Flow (m3 d-1)
J-08
J-08
F-09
A-09
M-10
Observed
HSPF

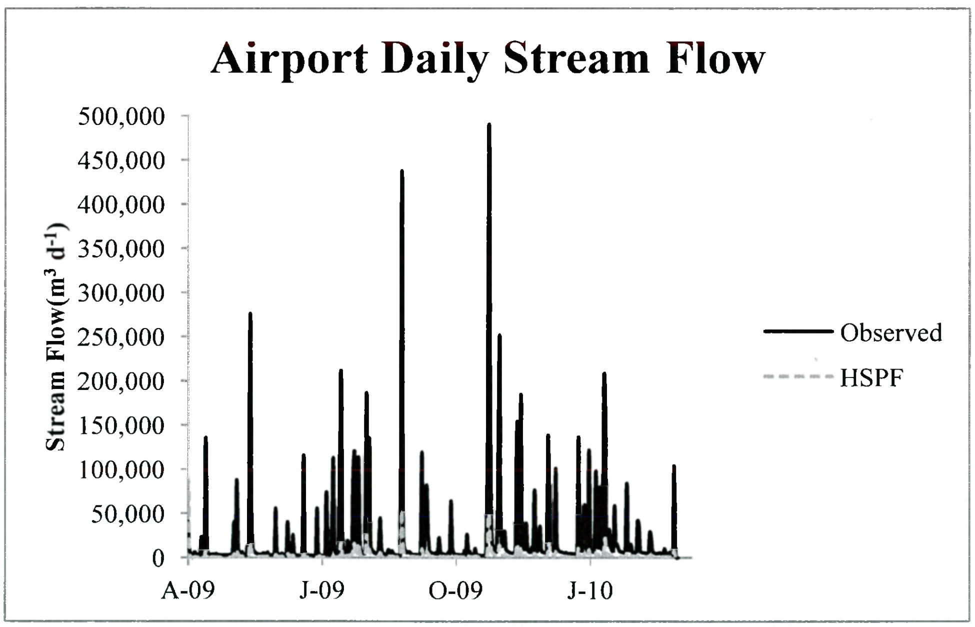
Airport Daily Stream Flow
500,000
450,000
400,000
350,000
300,000
250,000
200,000
150,000
100,000
50,000
0
Stream Flow(m3 d-1)
A-09
J-09
O-09
J-10
Observed
HSPF

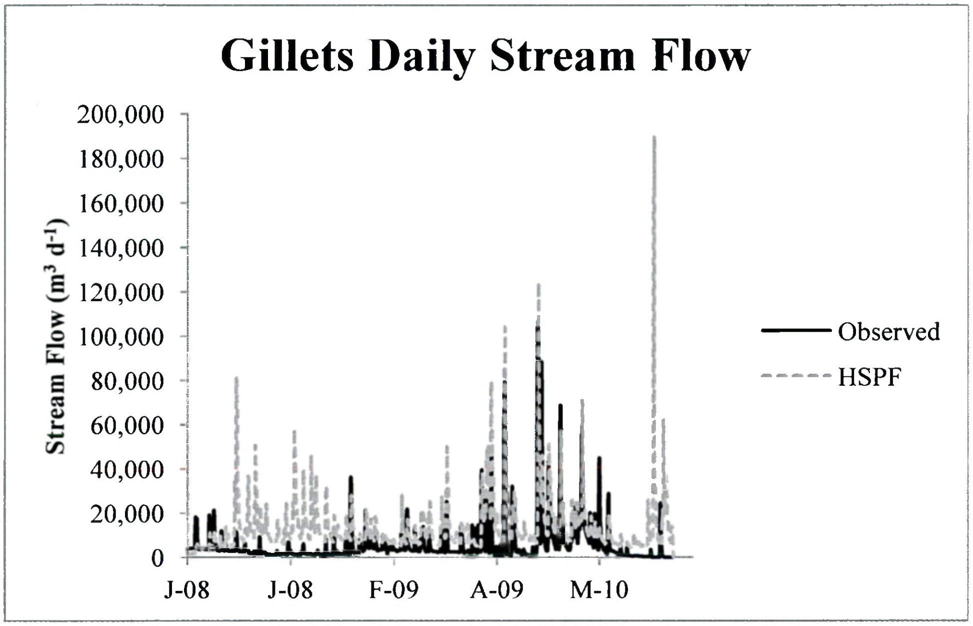
Gillets Daily Stream Flow
200,000
180,000
160,000
140,000
120,000
100,000
80,000
60,000
40,000
20,000
0
Stream Flow (m³ d⁻¹)
J-08
J-08
F-09
A-09
M-10
Observed
HSPF

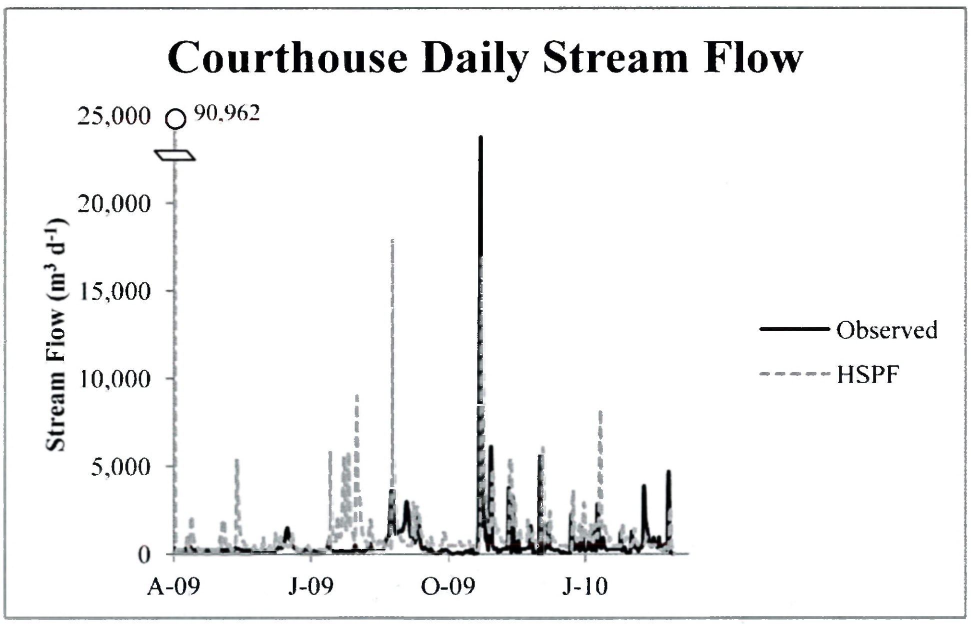
Courthouse Daily Stream Flow
25,000
90,962
20,000
15,000
10,000
5,000
0
Stream Flow (m³ d⁻¹)
A-09
J-09
O-09
J-10
Observed
HSPF

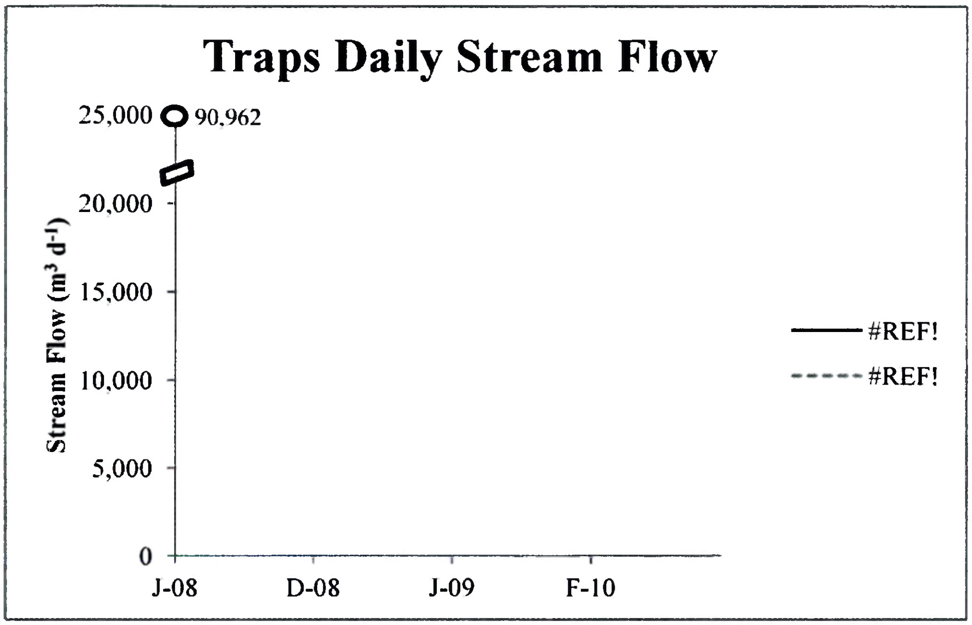
Traps Daily Stream Flow
25,000
90,962
20,000
15,000
10,000
5,000
0
Stream Flow (m3 d-1)
J-08
D-08
J-09
F-10
#REF!
#REF!

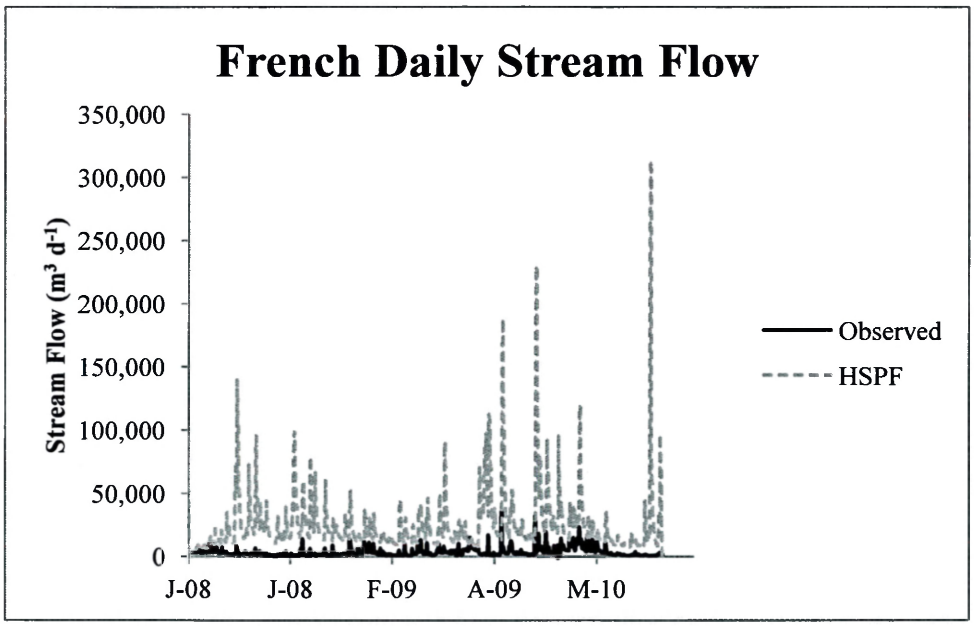
French Daily Stream Flow
350,000
300,000
250,000
200,000
150,000
100,000
50,000
0
Stream Flow (m3 d-1)
J-08
J-08
F-09
A-09
M-10
Observed
HSPF

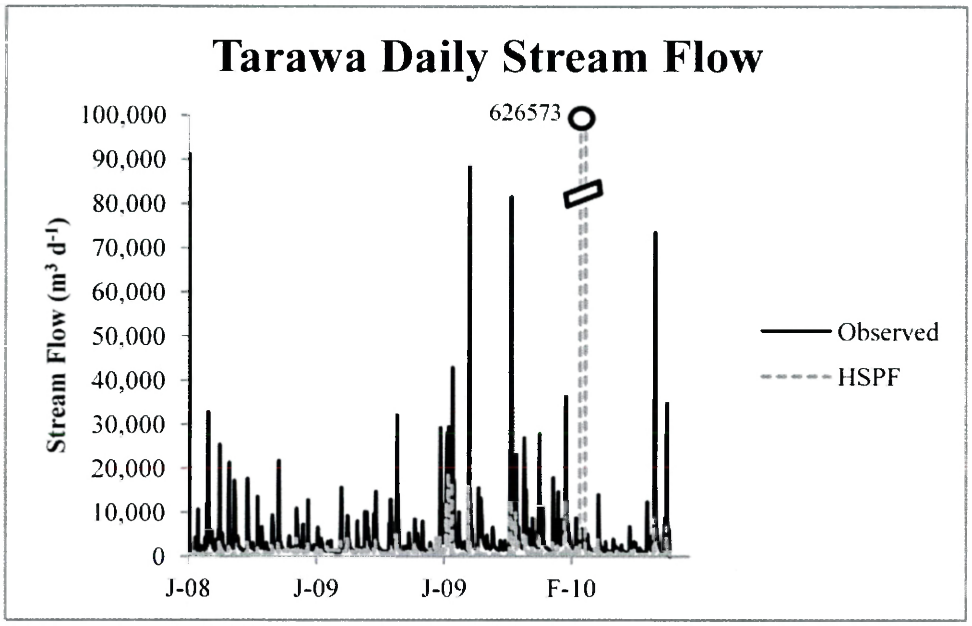

Tarawa Daily Stream Flow
626573
Stream Flow (m³ d⁻¹)
100,000
90,000
80,000
70,000
60,000
50,000
40,000
30,000
20,000
10,000
0
J-08
J-09
J-09
F-10
Observed
HSPF

Appendix Figure 2. Average daily observed and HSPF-modeled sediment loads from each sub-watershed.

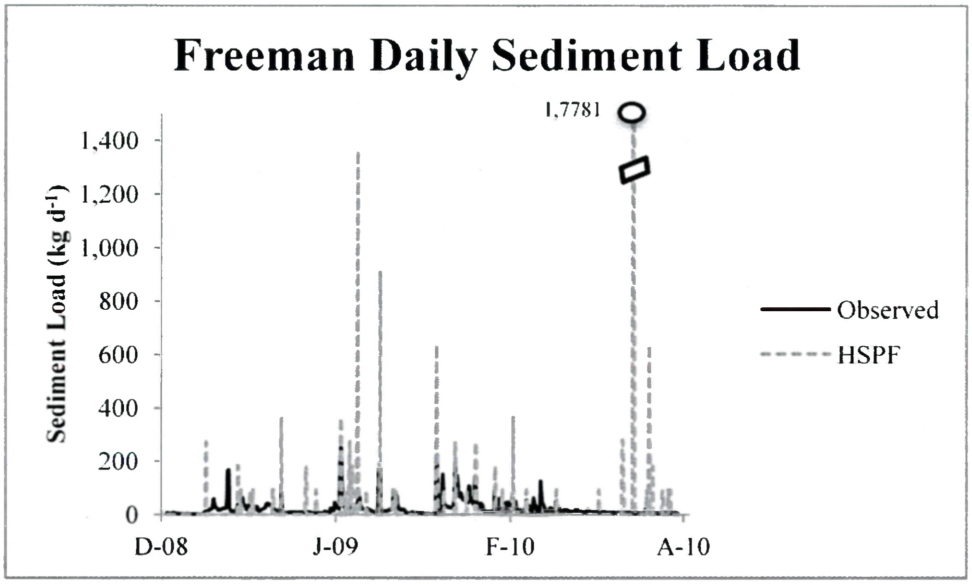

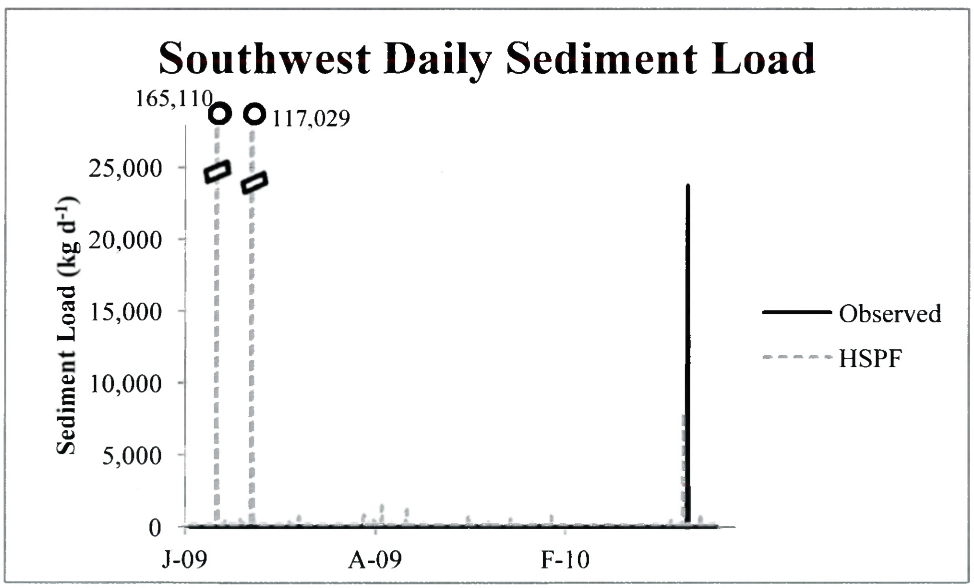

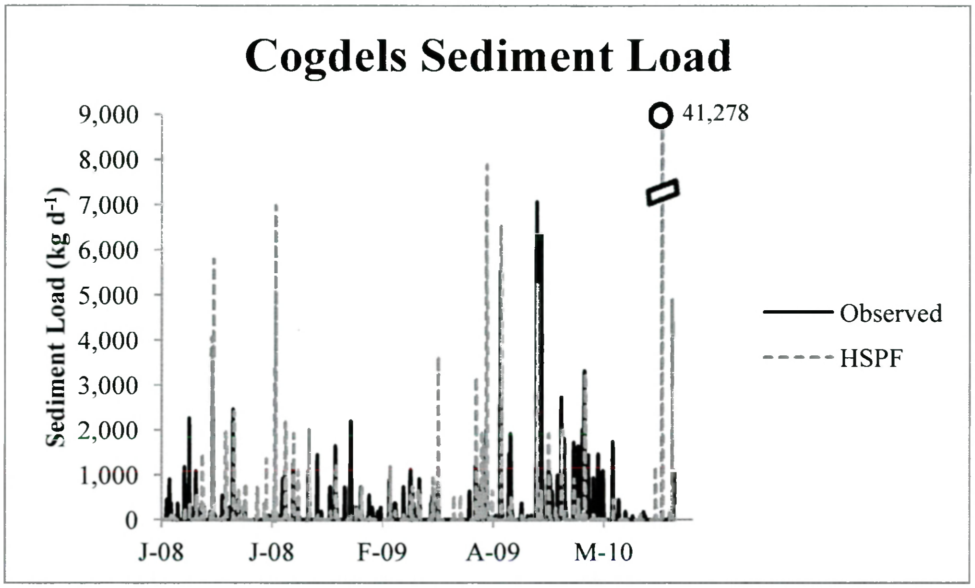
Cogdels Sediment Load
Sediment Load (kg d-1)
9,000
8,000
7,000
6,000
5,000
4,000
3,000
2,000
1,000
0
41,278
J-08
J-08
F-09
A-09
M-10
Observed
HSPF

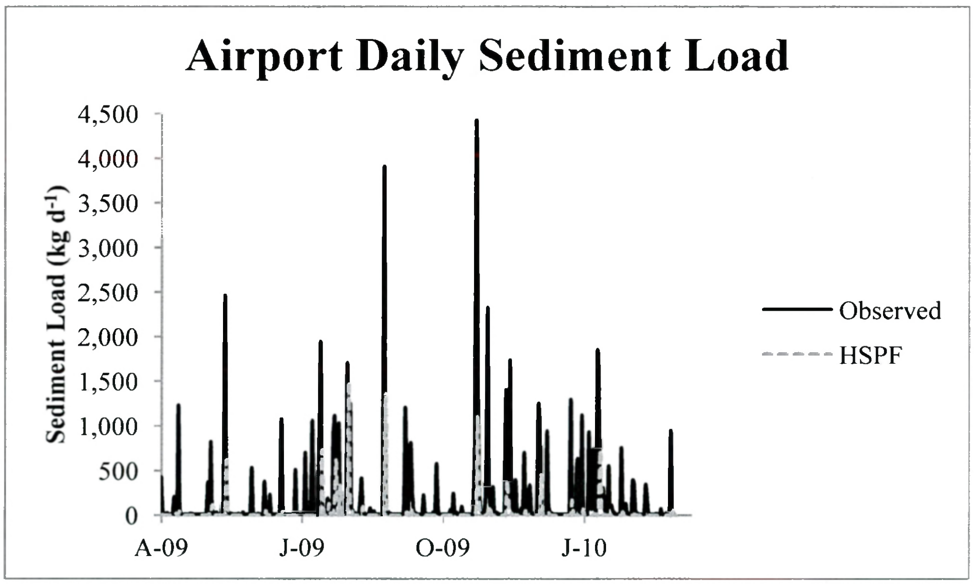
Airport Daily Sediment Load
Sediment Load (kg d-1)
4,500
4,000
3,500
3,000
2,500
2,000
1,500
1,000
500
0
A-09
J-09
O-09
J-10
Observed
HSPF

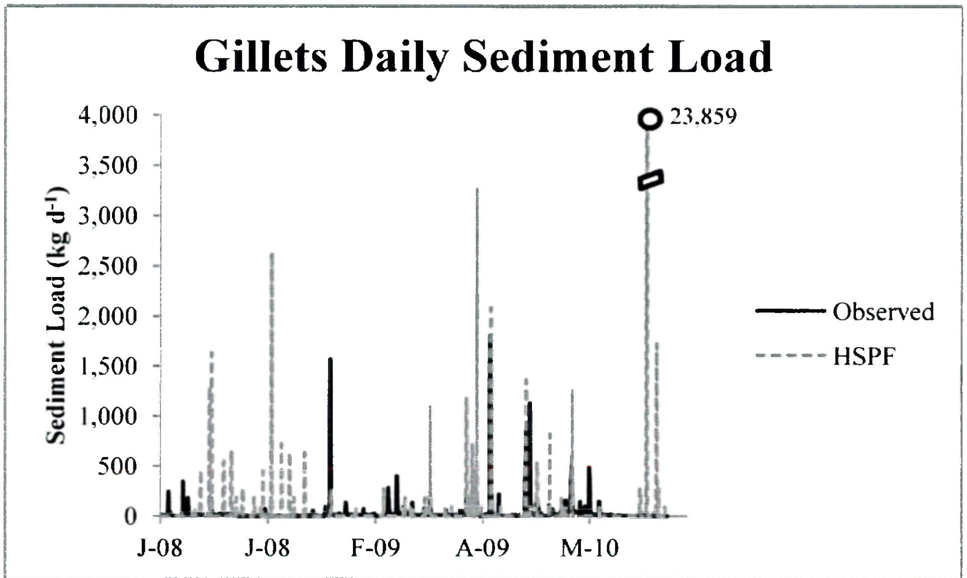
Gillets Daily Sediment Load
4,000
3,500
3,000
2,500
2,000
1,500
1,000
500
0
Sediment Load (kg d-1)
23,859
J-08
J-08
F-09
A-09
M-10
Observed
HSPF

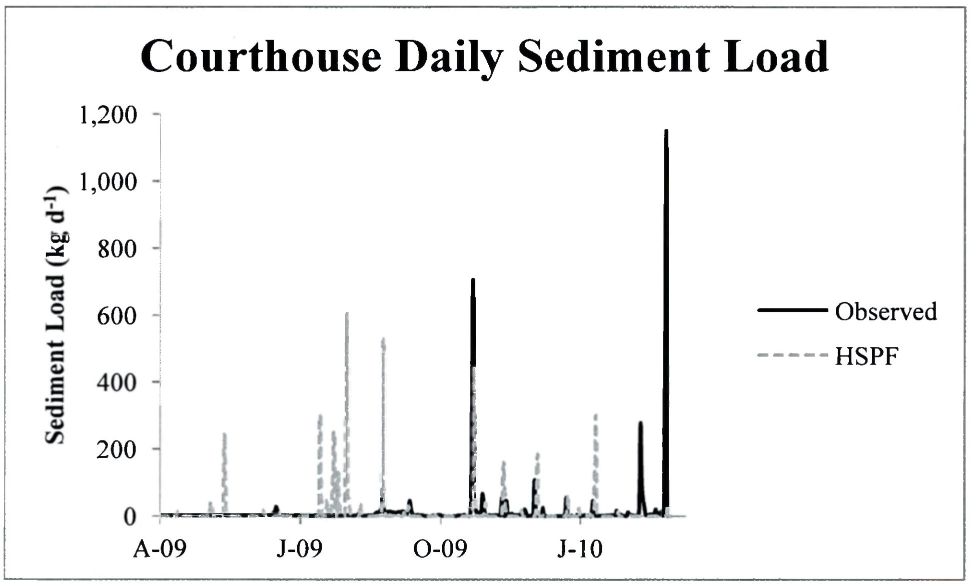
Courthouse Daily Sediment Load
1,200
1,000
800
600
400
200
0
Sediment Load (kg d-1)
A-09
J-09
O-09
J-10
Observed
HSPF

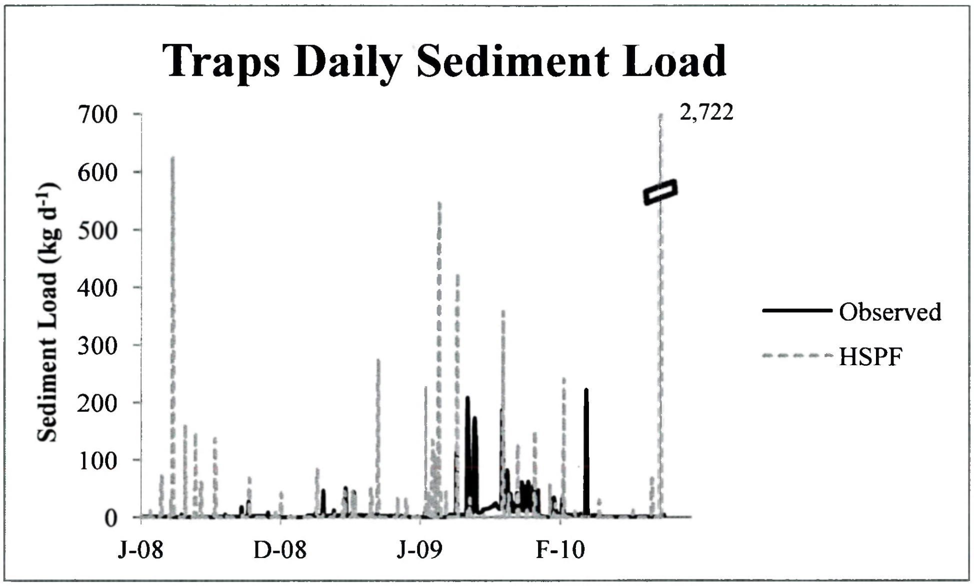
Traps Daily Sediment Load
700
600
500
400
300
200
100
0
2,722
Sediment Load (kg d-1)
J-08
D-08
J-09
F-10
Observed
HSPF

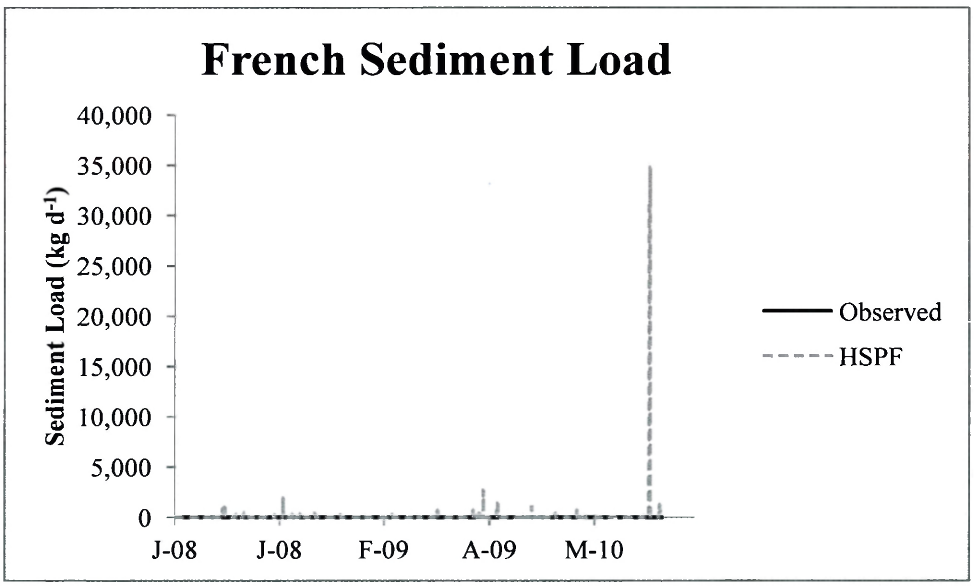
French Sediment Load
40,000
35,000
30,000
25,000
20,000
15,000
10,000
5,000
0
Sediment Load (kg d-1)
J-08
J-08
F-09
A-09
M-10
Observed
HSPF

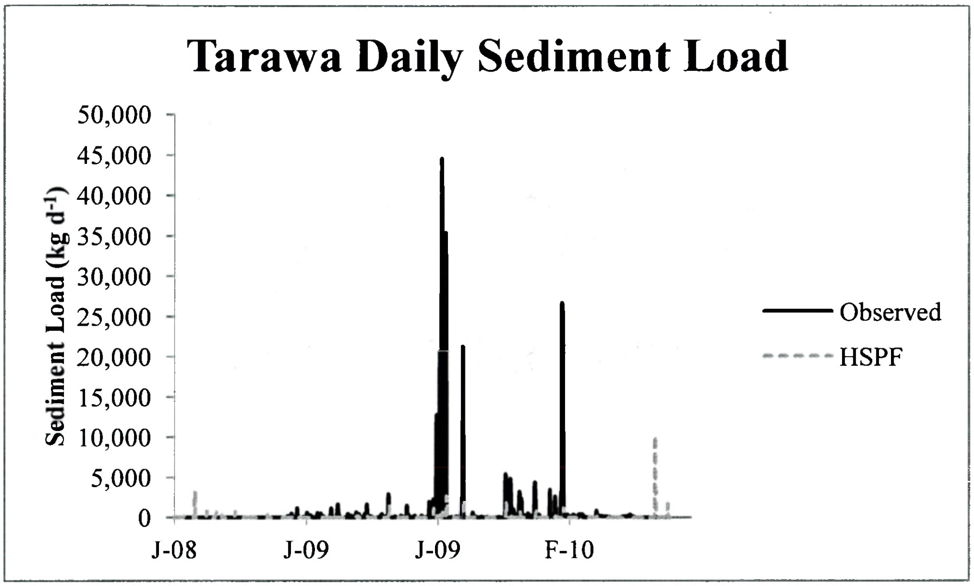
Tarawa Daily Sediment Load
Sediment Load (kg d-1)
50,000
45,000
40,000
35,000
30,000
25,000
20,000
15,000
10,000
5,000
0
J-08
J-09
J-09
F-10
Observed
HSPF

Appendix Figure 3. Average daily observed and HSPF-modeled NOx⁻ loads from each sub-watershed.

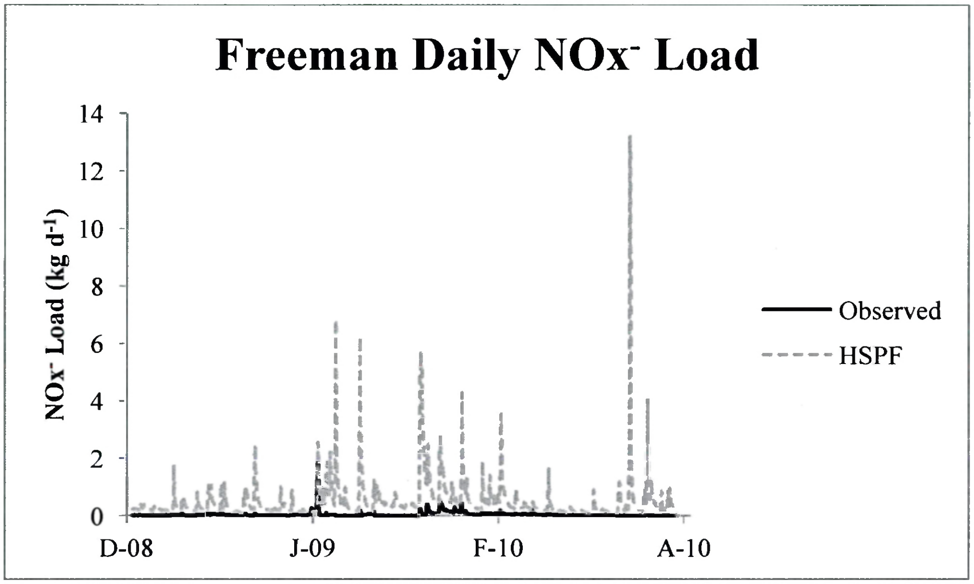

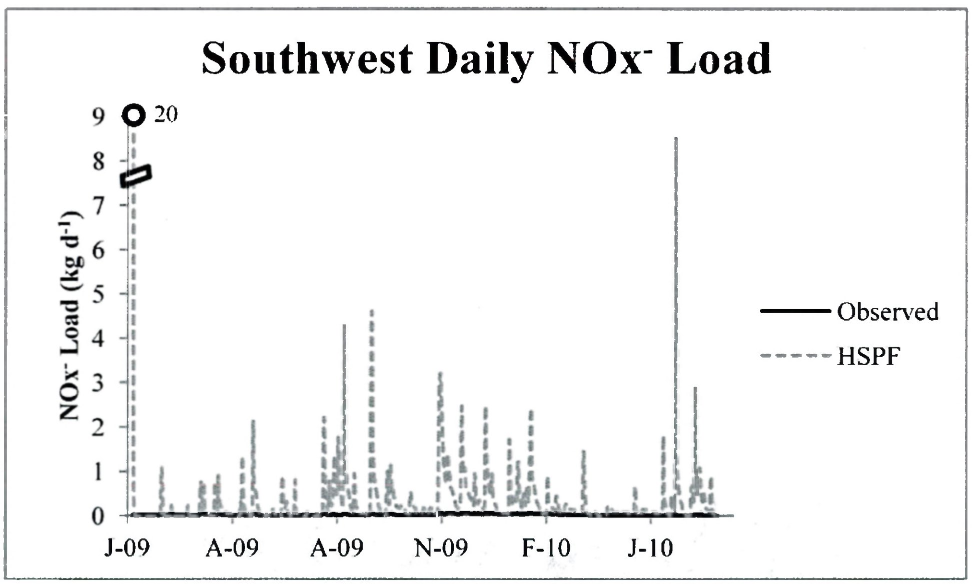

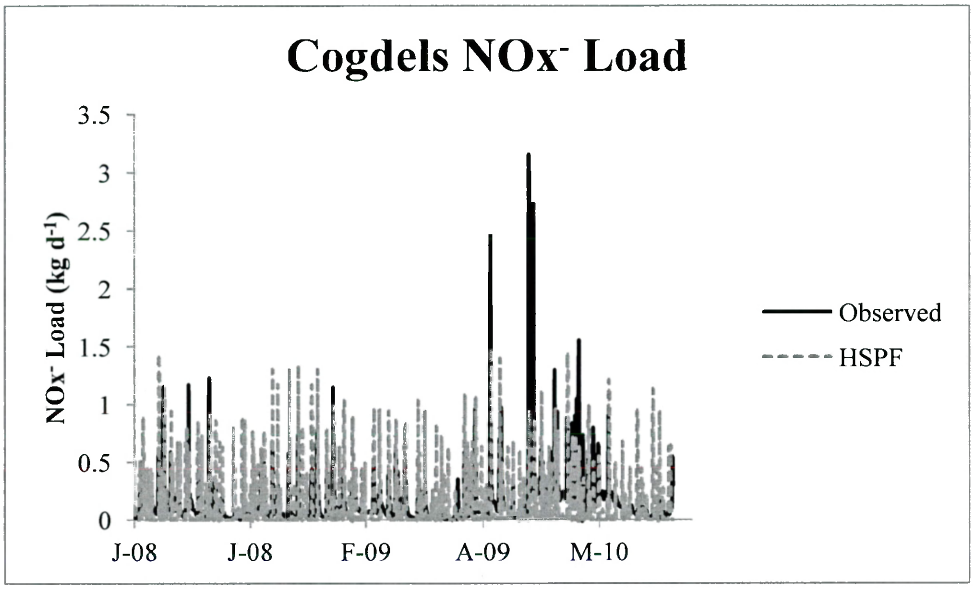

Cogdels NOx⁻ Load
3.5
3
2.5
2
1.5
1
0.5
0
NOx⁻ Load (kg d⁻¹)
J-08
J-08
F-09
A-09
M-10
Observed
HSPF

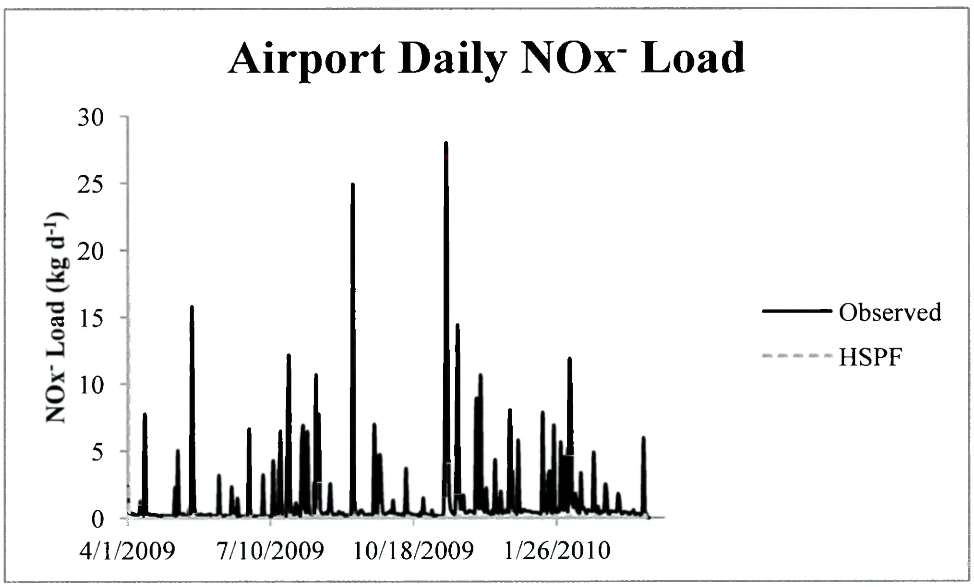

Airport Daily NOx⁻ Load
30
25
20
15
10
5
0
NOx⁻ Load (kg d⁻¹)
4/1/2009
7/10/2009
10/18/2009
1/26/2010
Observed
HSPF

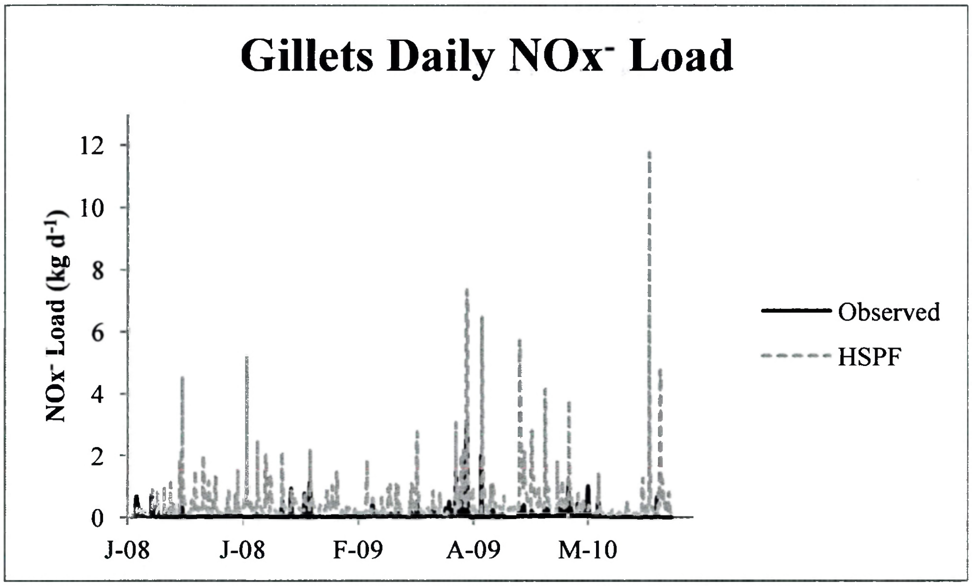
Gillets Daily NOx- Load
NOx- Load (kg d-1)
12
10
8
6
4
2
0
J-08
J-08
F-09
A-09
M-10
Observed
HSPF

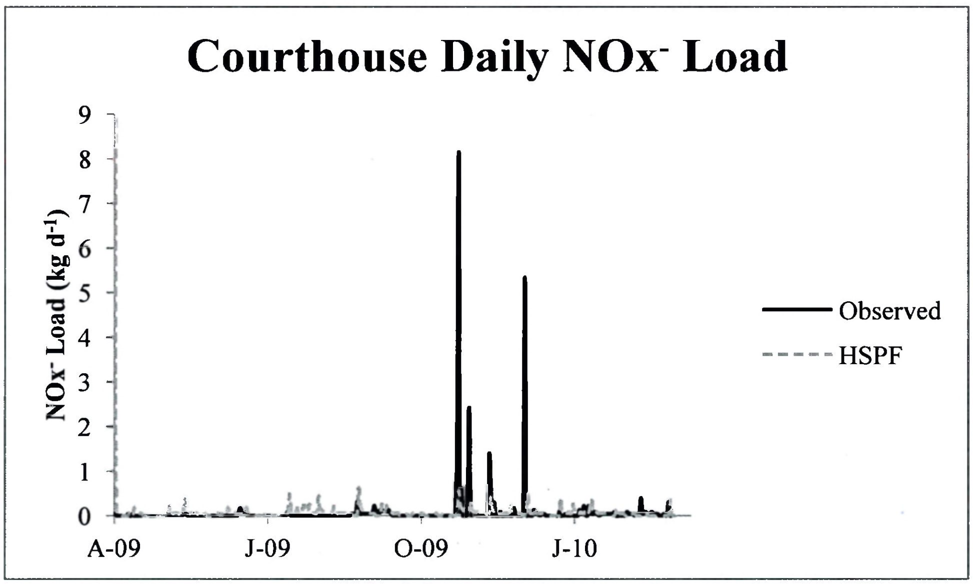
Courthouse Daily NOx- Load
NOx- Load (kg d-1)
9
8
7
6
5
4
3
2
1
0
A-09
J-09
O-09
J-10
Observed
HSPF

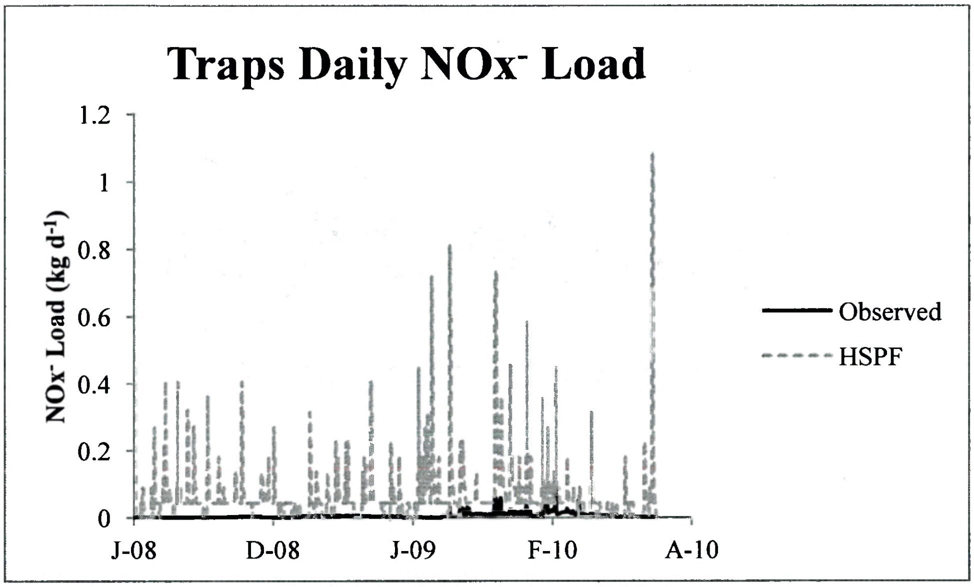
Traps Daily NOx- Load
1.2
1
0.8
0.6
0.4
0.2
0
NOx- Load (kg d-1)
J-08
D-08
J-09
F-10
A-10
Observed
HSPF

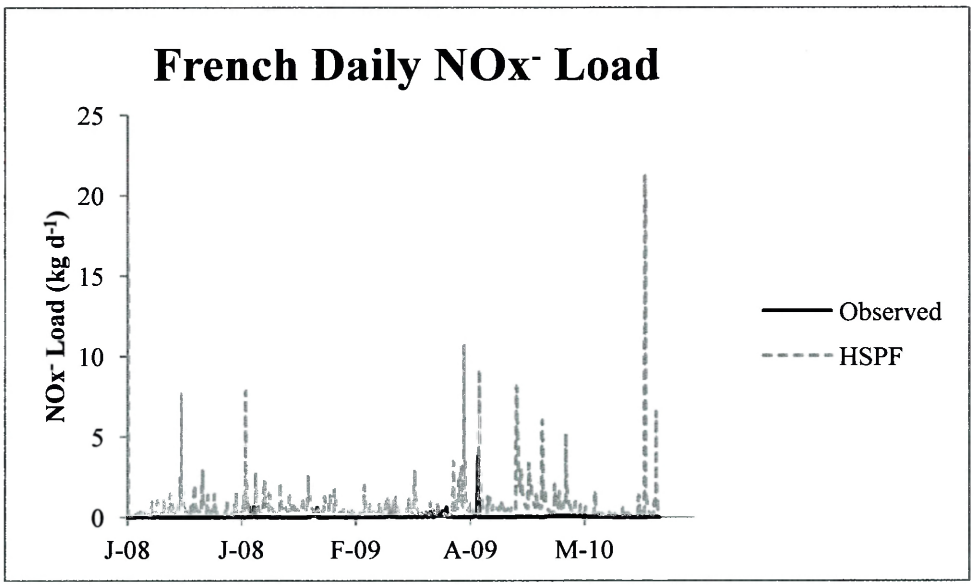
French Daily NOx- Load
25
20
15
10
5
0
NOx- Load (kg d-1)
J-08
J-08
F-09
A-09
M-10
Observed
HSPF

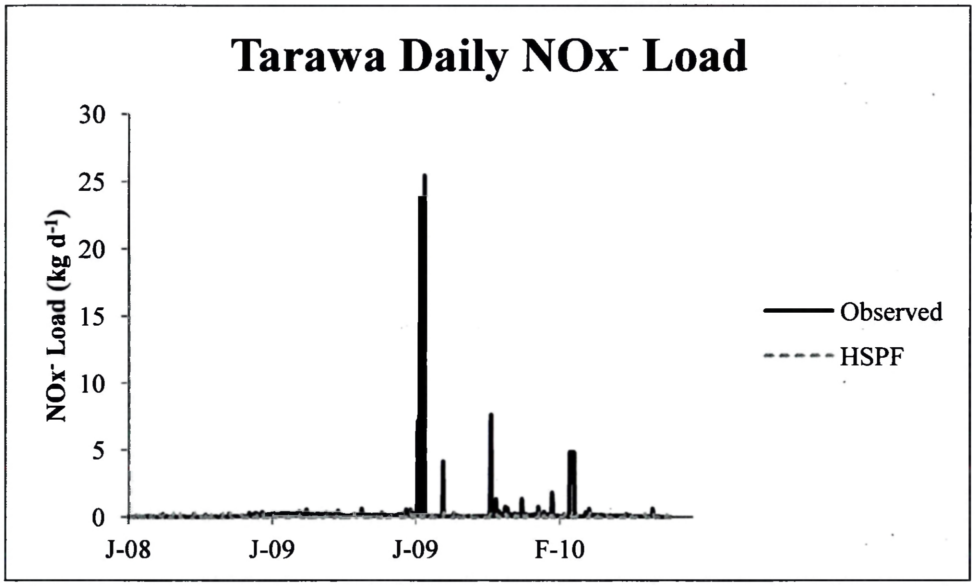
Tarawa Daily NOx- Load
30
25
20
15
10
5
0
NOx- Load (kg d-1)
J-08
J-09
J-09
F-10
Observed
HSPF

Appendix Figure 4. Average daily observed and HSPF-modeled NH_4^+ loads from each sub-watershed.

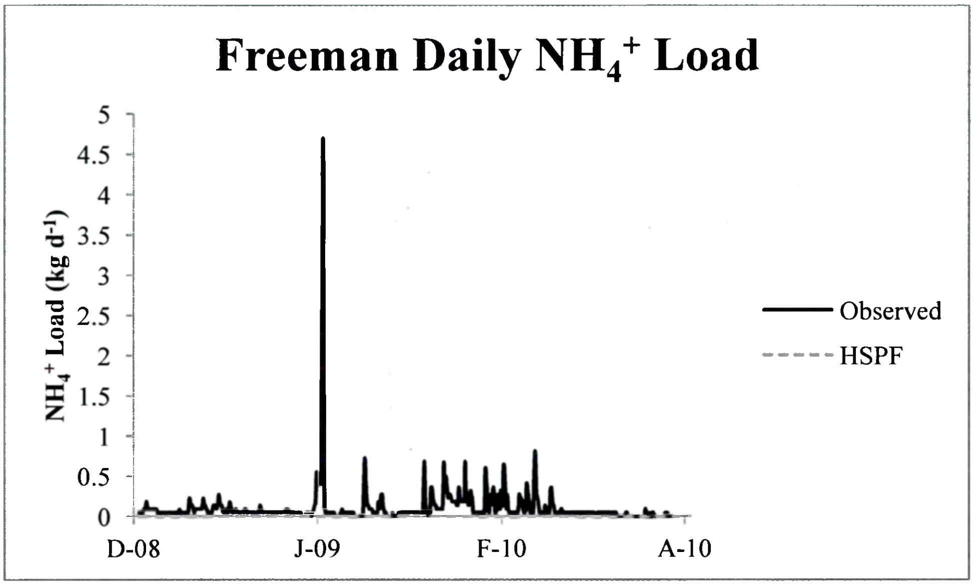

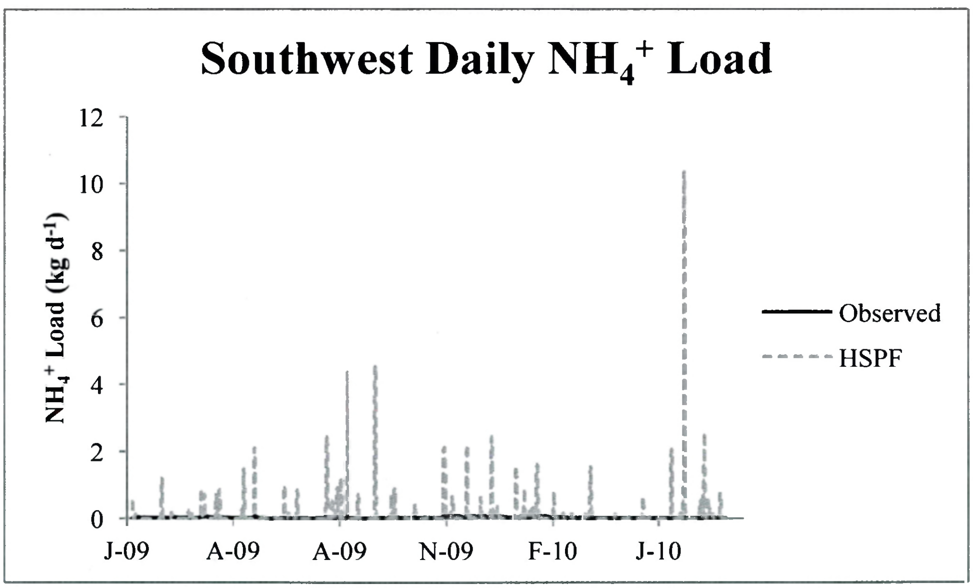

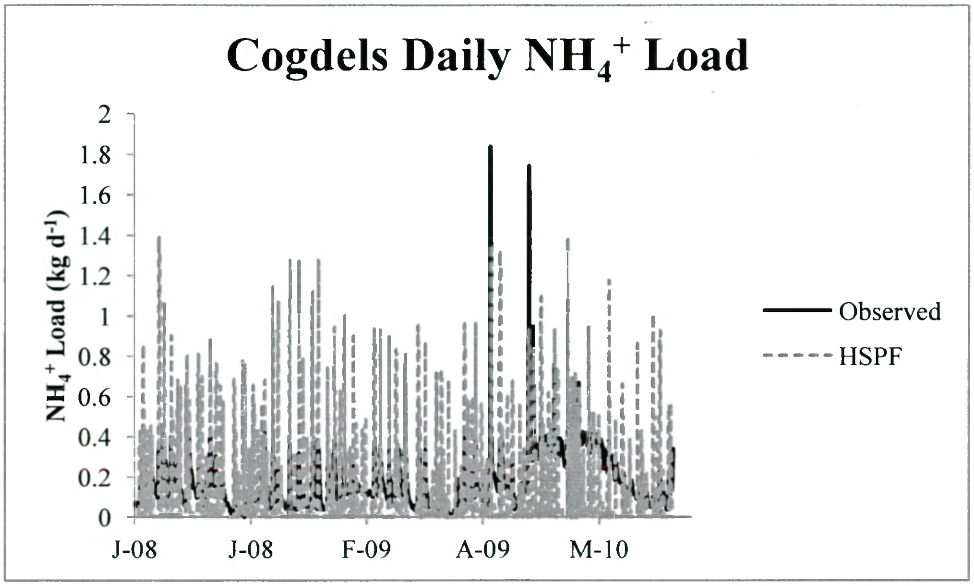
Cogdels Daily NH_4^+ Load
2
1.8
1.6
1.4
1.2
1
0.8
0.6
0.4
0.2
0
NH_4^+ Load (kg d^{-1})
J-08
J-08
F-09
A-09
M-10
Observed
HSPF

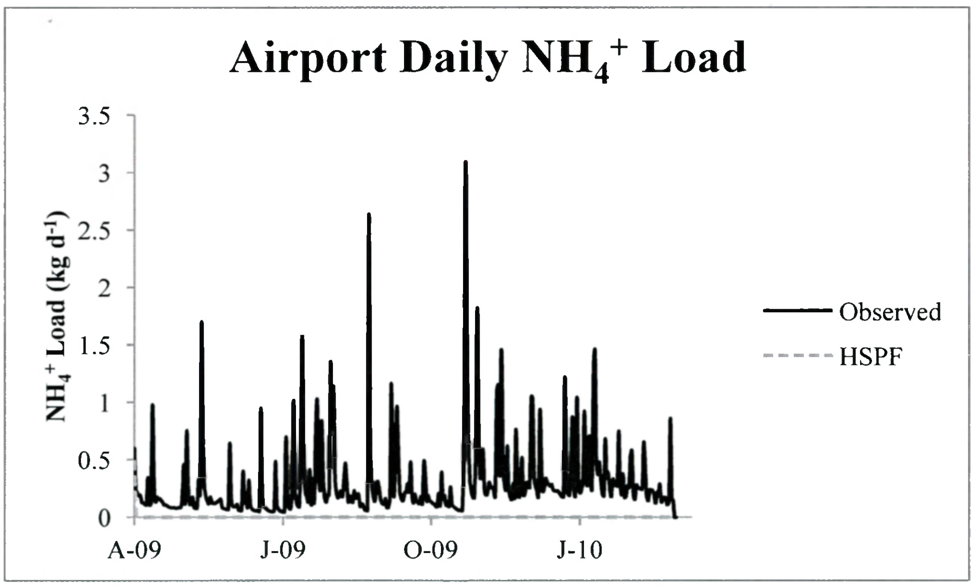
Airport Daily NH_4^+ Load
3.5
3
2.5
2
1.5
1
0.5
0
NH_4^+ Load (kg d^{-1})
A-09
J-09
O-09
J-10
Observed
HSPF

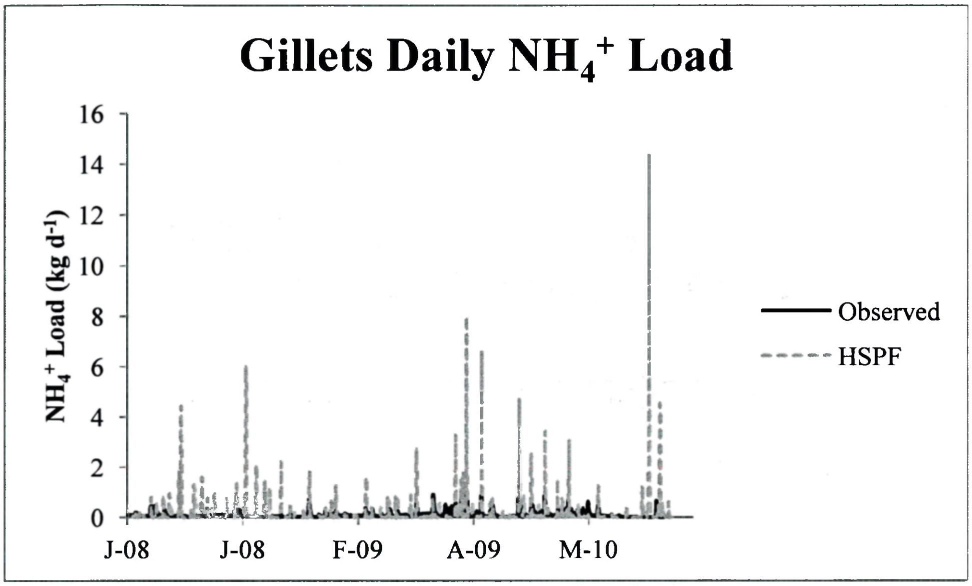

Gillets Daily NH4+ Load
NH4+ Load (kg d-1)
16
14
12
10
8
6
4
2
0
J-08
J-08
F-09
A-09
M-10
Observed
HSPF

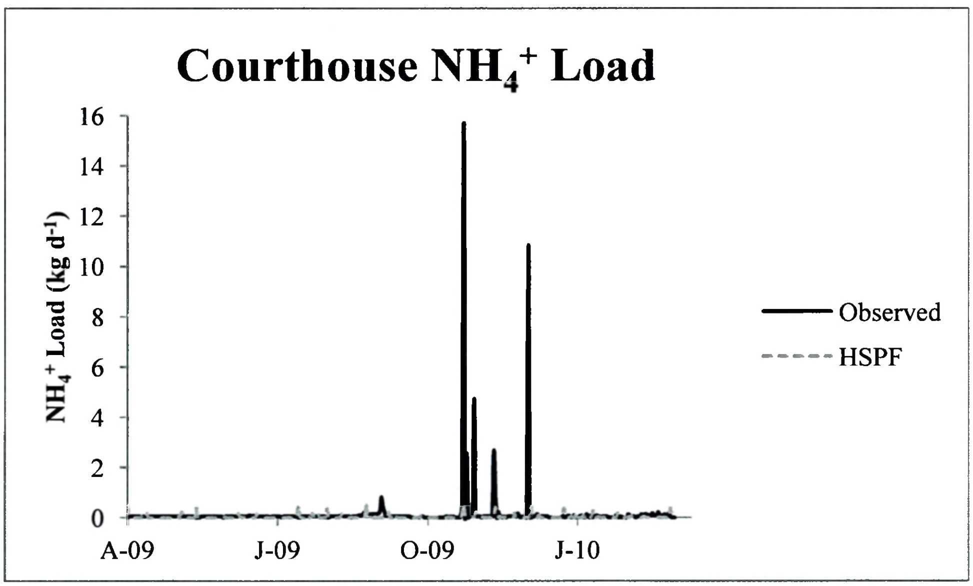

Courthouse NH4+ Load
NH4+ Load (kg d-1)
16
14
12
10
8
6
4
2
0
A-09
J-09
O-09
J-10
Observed
HSPF

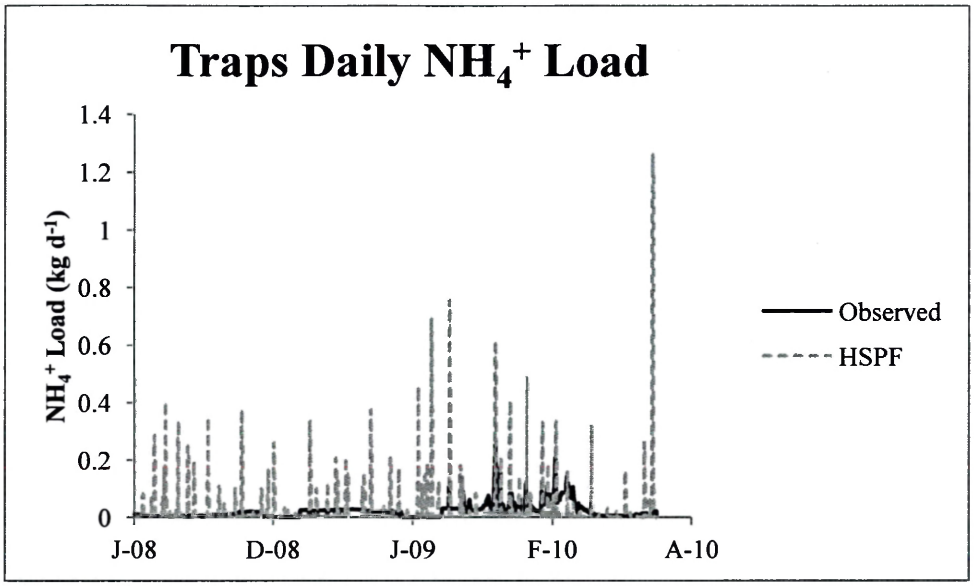
Traps Daily NH4+ Load
NH4+ Load (kg d-1)
1.4
1.2
1
0.8
0.6
0.4
0.2
0
J-08
D-08
J-09
F-10
A-10
Observed
HSPF

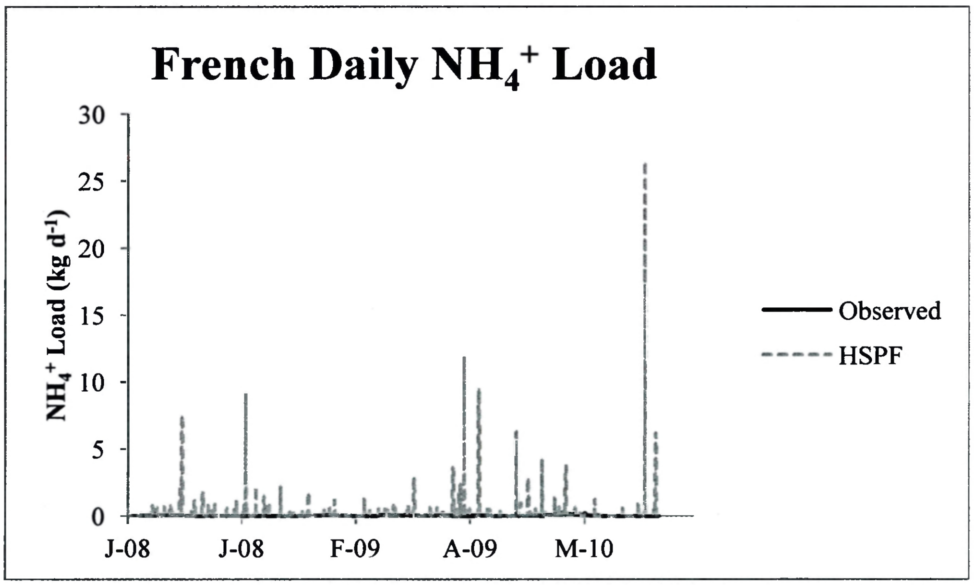
French Daily NH4+ Load
NH4+ Load (kg d-1)
30
25
20
15
10
5
0
J-08
J-08
F-09
A-09
M-10
Observed
HSPF

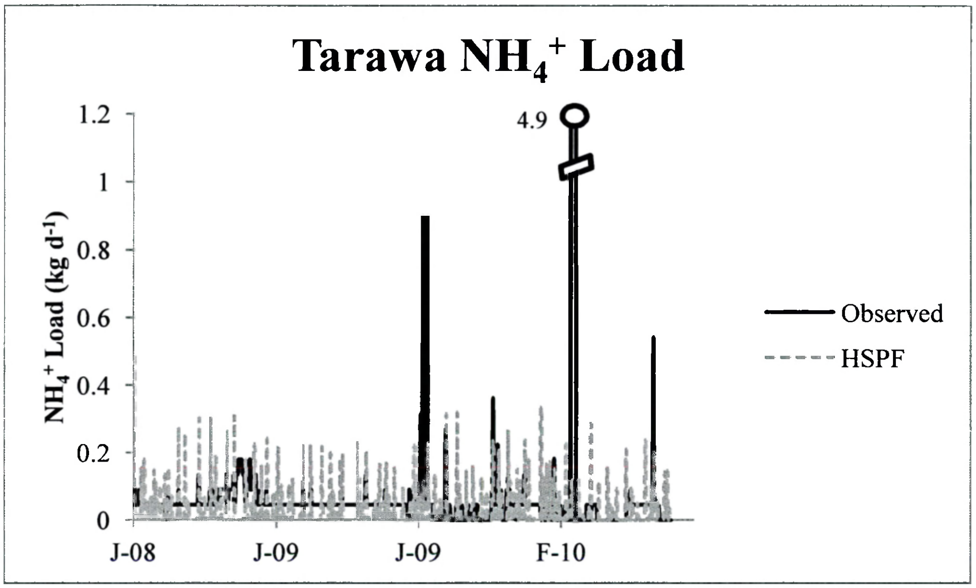

Tarawa NH_4^+ Load
NH_4^+ Load (kg d^{-1})
1.2
1
0.8
0.6
0.4
0.2
0
4.9
J-08
J-09
J-09
F-10
Observed
HSPF

Appendix Figure 5. Average daily observed and HSPF-modeled PO_4^{3-} loads from each sub-watershed.

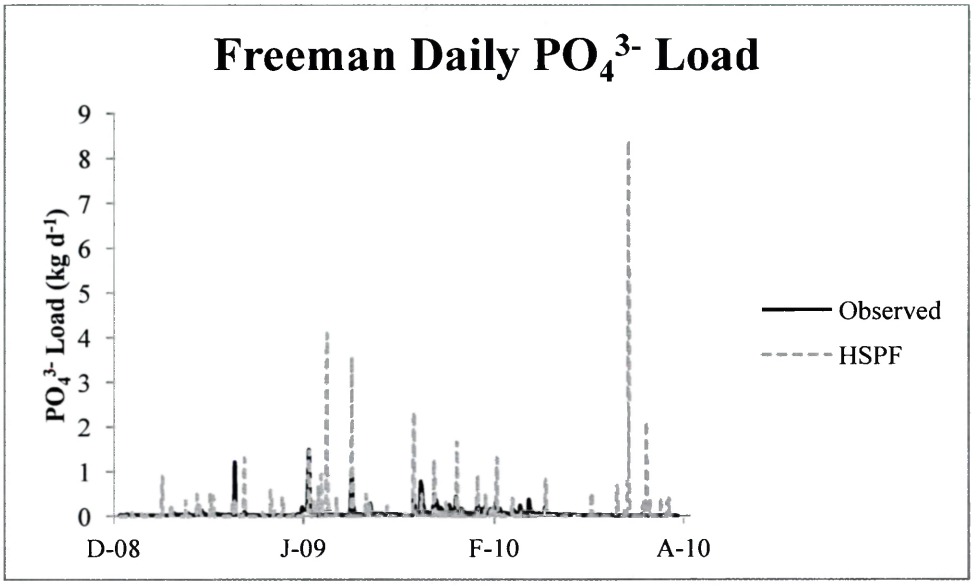

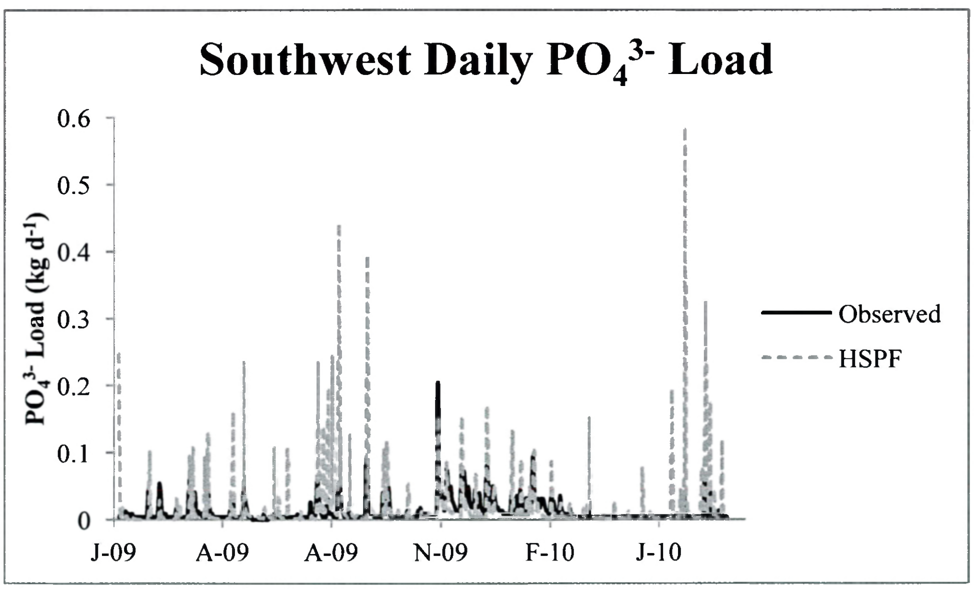

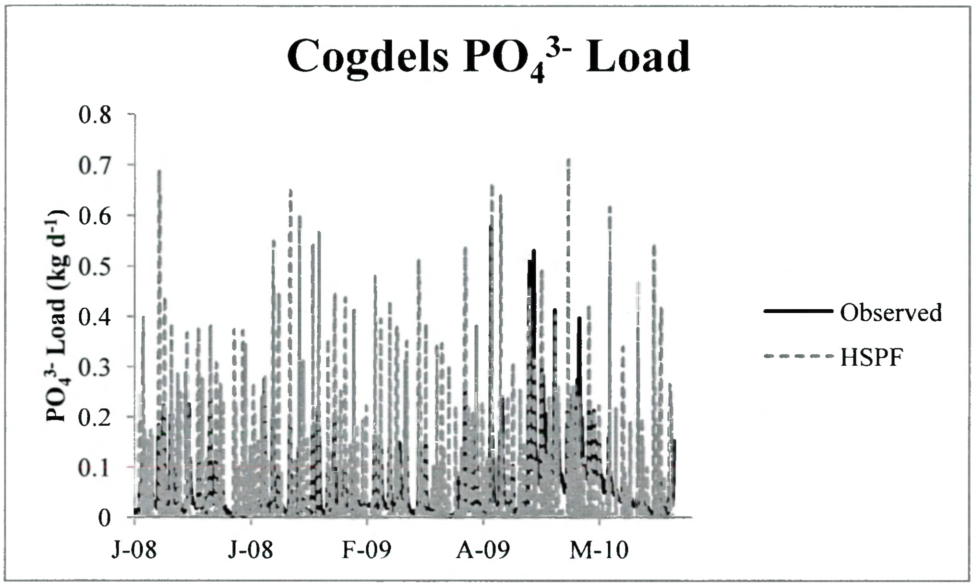
Cogdels PO_4^{3-} Load
PO_4^{3-} Load (kg d^{-1})
0.8
0.7
0.6
0.5
0.4
0.3
0.2
0.1
0
J-08
J-08
F-09
A-09
M-10
Observed
HSPF

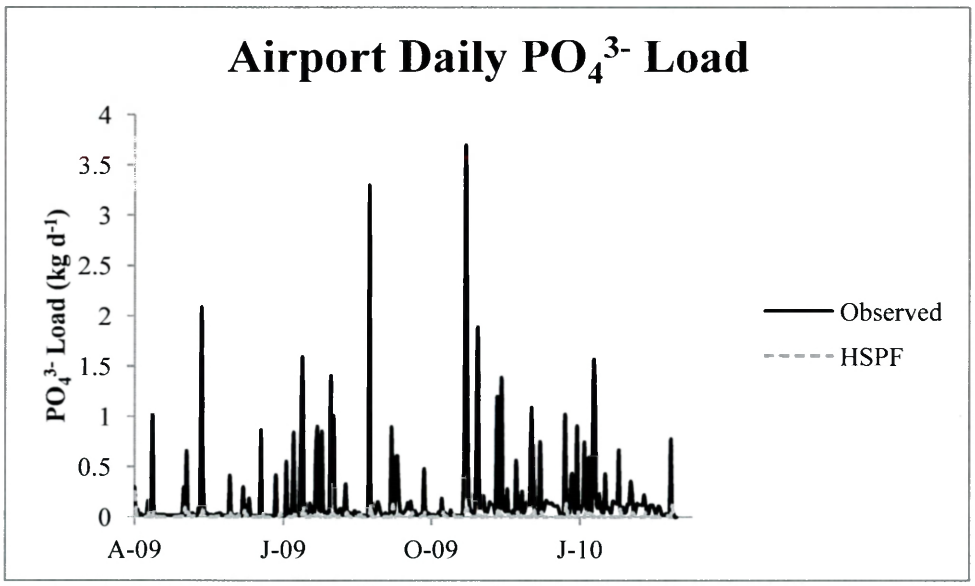
Airport Daily PO_4^{3-} Load
PO_4^{3-} Load (kg d^{-1})
4
3.5
3
2.5
2
1.5
1
0.5
0
A-09
J-09
O-09
J-10
Observed
HSPF

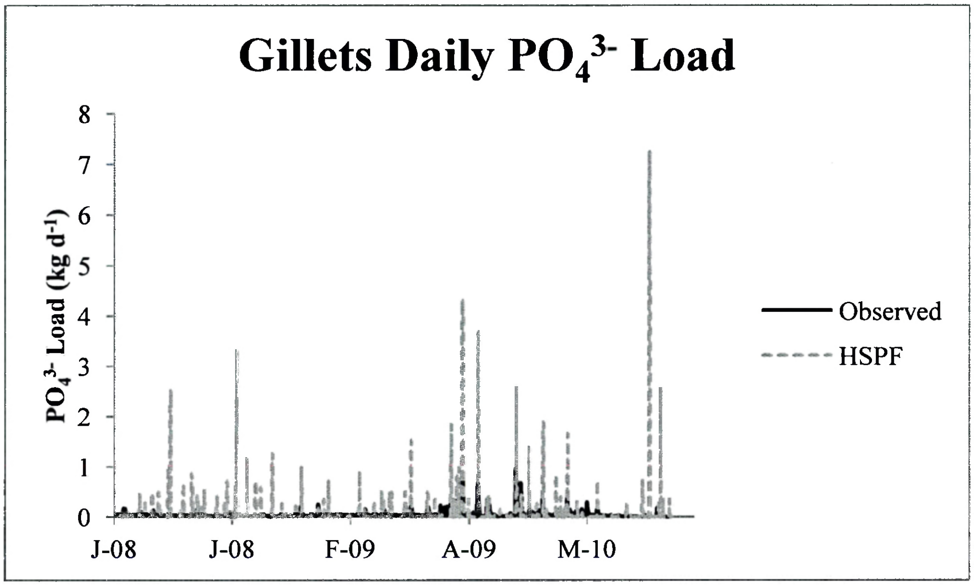
Gillets Daily PO_4^{3-} Load
PO_4^{3-} Load (kg d^{-1})
8
7
6
5
4
3
2
1
0
J-08
J-08
F-09
A-09
M-10
Observed
HSPF

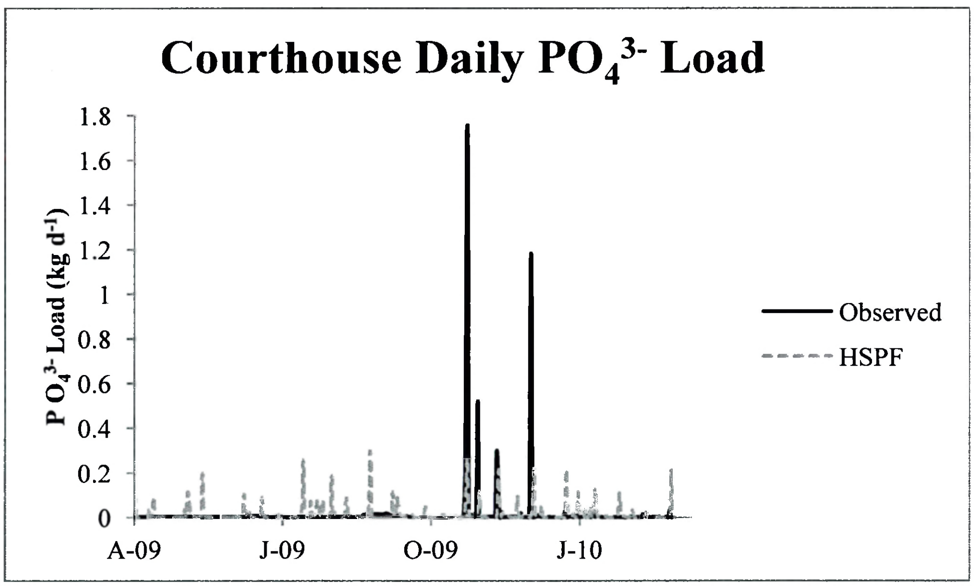
Courthouse Daily PO_4^{3-} Load
P O_4^{3-} Load (kg d^{-1})
1.8
1.6
1.4
1.2
1
0.8
0.6
0.4
0.2
0
A-09
J-09
O-09
J-10
Observed
HSPF

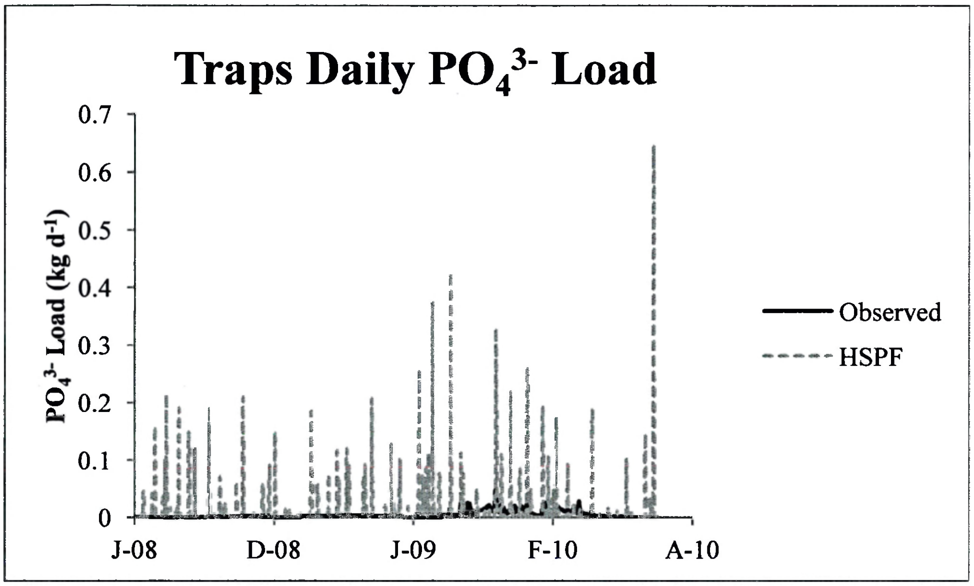
Traps Daily PO_4^{3-} Load
PO_4^{3-} Load (kg d^{-1})
0.7
0.6
0.5
0.4
0.3
0.2
0.1
0
J-08
D-08
J-09
F-10
A-10
Observed
HSPF

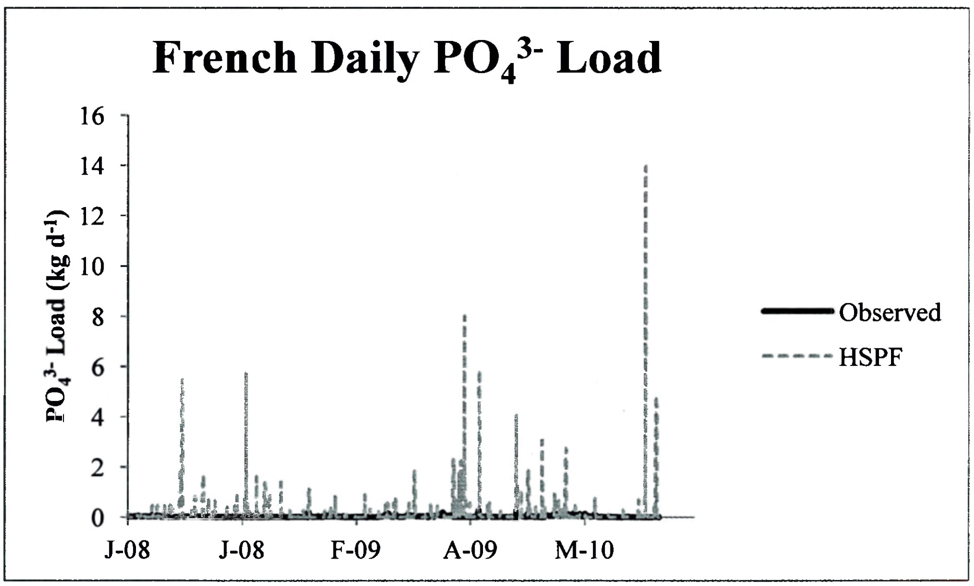
French Daily PO_4^{3-} Load
PO_4^{3-} Load (kg d^{-1})
16
14
12
10
8
6
4
2
0
J-08
J-08
F-09
A-09
M-10
Observed
HSPF

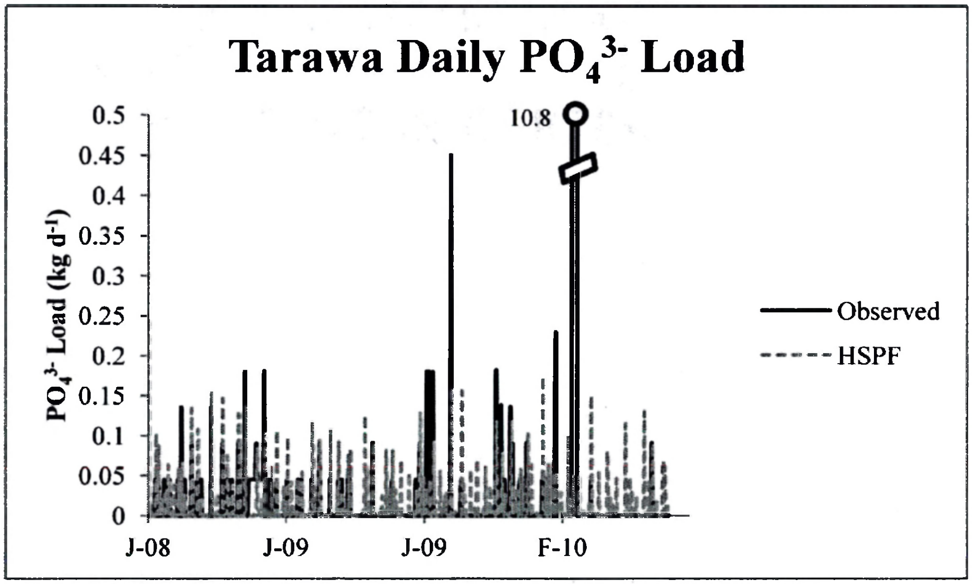

Tarawa Daily PO_4^{3-} Load
PO_4^{3-} Load (kg d^{-1})
0.5
0.45
0.4
0.35
0.3
0.25
0.2
0.15
0.1
0.05
0
10.8
J-08
J-09
J-09
F-10
Observed
HSPF

Appendix Table 1. Measured (gauge) and modeled (HSPF) annual average freshwater stream flow, sediment load, and nutrient loads from the nine MCBCL sub-watersheds. Computation of modeled annual averages covered the time span over which computed gauge data was available from each sub-watershed.

Freeman			Southwest			Cogdels			Airport			Gillets		
Stream Flow		$m^3 d^{-1}$	Stream Flow		$m^3 d^{-1}$	Stream Flow		$m^3 d^{-1}$	Stream Flow		$m^3 d^{-1}$	Stream Flow		$m^3 d^{-1}$
	Gauge	HSPF		Gauge	HSPF		Gauge	HSPF		Gauge	HSPF		Gauge	HSPF
						2008	9314	22740				2008	3774	12241
2009	7887	20152	2009	91929600	41126400	2009	12822	28788	2009	23757	2927	2009	7500	15555
Sediments		$kg d^{-1}$	Sediments		$kg d^{-1}$	Sediments		$kg d^{-1}$	Sediments		$kg d^{-1}$	Sediments		$kg d^{-1}$
	Gauge	HSPF		Gauge	HSPF		Gauge	HSPF		Gauge	HSPF		Gauge	HSPF
						2008	115	146				2008	17	42
2009	26	21	2009	15	1016	2009	208	147	2009	198	31	2009	41	43
NOx		$kg d^{-1}$	NOx		$kg d^{-1}$	NOx		$kg d^{-1}$	NOx		$kg d^{-1}$	NOx		$kg d^{-1}$
	Gauge	HSPF		Gauge	HSPF		Gauge	HSPF		Gauge	HSPF		Gauge	HSPF
						2008	0.12	0.16				2008	0.06	0.45
2009	0.05	0.57	2009	0.03	0.36	2009	0.17	0.14	2009	1.35	0.08	2009	0.09	0.50
NH_4^+		$kg d^{-1}$	NH_4^+		$kg d^{-1}$	NH_4^+		$kg d^{-1}$	NH_4^+		$kg d^{-1}$	NH_4^+		$kg d^{-1}$
	Gauge	HSPF		Gauge	HSPF		Gauge	HSPF		Gauge	HSPF		Gauge	HSPF
						2008	0.13	0.14				2008	0.09	0.15
2009	0.11	0.00	2009	0.03	0.13	2009	0.18	0.13	2009	0.31	0.00	2009	0.15	0.18
PO_4^{3-}		$kg d^{-1}$	PO_4^{3-}		$kg d^{-1}$	PO_4^{3-}		$kg d^{-1}$	PO_4^{3-}		$kg d^{-1}$	PO_4^{3-}		$kg d^{-1}$
	Gauge	HSPF		Gauge	HSPF		Gauge	HSPF		Gauge	HSPF		Gauge	HSPF
						2008	0.04	0.06				2008	0.04	0.08
2009	0.08	0.09	2009	0.01	0.02	2009	0.06	0.06	2009	0.18	0.01	2009	0.07	0.09

Courthouse			Traps			French			Tarawa		
Stream Flow		$m^3\ d^{-1}$	Stream Flow		$m^3\ d^{-1}$	Stream Flow		$m^3\ d^{-1}$	Stream Flow		$m^3\ d^{-1}$
	Gauge	HSPF		Gauge	HSPF		Gauge	HSPF		Gauge	HSPF
			2008	239	1442	2008	2830	22982	2008	1045	1057
2009	593	600	2009	1679	1773	2009	3895	28063	2009	13185	13339
Sediment		$kg\ d^{-1}$	Sediment		$kg\ d^{-1}$	Sediment		$kg\ d^{-1}$	Sediment		$kg\ d^{-1}$
Annual				Gauge	HSPF		Gauge	HSPF		Gauge	HSPF
	Gauge	HSPF	2008	2	7	2008	0.15	32	2008	81	35
2009	12.3	12.2	2009	12	9	2009	0.37	34	2009	721	77
NOx		$kg\ d^{-1}$	NOx		$kg\ d^{-1}$	NOx		$kg\ d^{-1}$	NOx		$kg\ d^{-1}$
	Gauge	HSPF		Gauge	HSPF		Gauge	HSPF		Gauge	HSPF
			2008	0.00	0.11	2008	0.03	0.63	2008	0.12	0.09
2009	0.08	0.12	2009	0.01	0.07	2009	0.06	0.76	2009	0.41	0.03
NH_4^+		$kg\ d^{-1}$	NH_4^+		$kg\ d^{-1}$	NH_4^+		$kg\ d^{-1}$	NH_4^+		$kg\ d^{-1}$
	Gauge	HSPF		Gauge	HSPF		Gauge	HSPF		Gauge	HPSF
			2008	0.01	0.02	2008	0.04	0.18	2008	0.06	0.03
2009	0.15	0.03	2009	0.03	0.03	2009	0.05	0.22	2009	0.13	0.03
PO_4^{3-}		$kg\ d^{-1}$	PO_4^{3-}		$kg\ d^{-1}$	PO_4^{3-}		$kg\ d^{-1}$	PO_4^{3-}		$kg\ d^{-1}$
	Gauge	HSPF		Gauge	HSPF		Gauge	HSPF		Gauge	HSPF
			2008	0.002	0.01	2008	0.03	0.12	2008	0.02	0.01
2009	0.02	0.02	2009	0.01	0.01	2009	0.04	0.15	2009	0.22	0.01

Appendix Table 2. Computation of modeled (PLOAD) annual loads of phosphate (PO_4^{3-}), total nitrogen (TN), and total suspended solids (TSS) covered the time span over which computed gauge data was available in each MCBCL sub-watershed. PLOAD predictions use the annual rainfall totals as noted (see text for details).

Jul2008-Jun2009	Gauge Load (kg/yr)	PLOAD PO4 Load (kg/yr)	Jul2008-Jun2009	Gauge Load (kg/yr)	PLOAD TN Load (kg/yr)	Jul2008-Jun2009	Gauge Load (kg/yr)	PLOAD TSS Load (kg/yr)
Precipitation (in)		46	Precipitation (in)		46	Precipitation (in)		46
Airport	20.6	47	Airport	604	473	Airport	16,957	13034
Camp Johnson	2.5	1	Camp Johnson	66	16	Camp Johnson	6,309	855
Cogdel	15.3	269	Cogdel	793	2690	Cogdel	50,310	91352
Courthouse	1.6	19	Courthouse	103	187	Courthouse	1,736	6396
Freemans	7.4	71	Freemans	266	713	Freemans	3,016	32298
French	12.1	67	French	372	670	French	3,924	37582
Giletts	15.3	75	Giletts	623	749	Giletts	8,161	34340
Southwest	1.6	14	Southwest	42	136	Southwest	1,323	4853
Tarawa	7.1	90	Tarawa	131	901	Tarawa	29,785	24969
Trapps	0.7	11	Trapps	32	109	Trapps	898	3773
R^2		0.295	R^2		0.552	R^2		0.602
Jul2009-Jun2010	**Gauge Load (kg/yr)**	**PLOAD PO4 Load (kg/yr)**	**Jul2009-Jun2010**	**Gauge Load (kg/yr)**	**PLOAD TN Load (kg/yr)**	**Jul2009-Jun2010**	**Gauge Load (kg/yr)**	**PLOAD TSS (kg/yr)**
Precipitation (in)		49	Precipitation (in)		49	Precipitation (in)		49
Airport	63	50	Airport	2094	504	Airport	67,340	12236
Camp Johnson	5	1	Camp Johnson	1013	17	Camp Johnson	131,801	802
Cogdel	27	286	Cogdel	1505	2866	Cogdel	128,528	85759
Courthouse	5	20	Courthouse	389	200	Courthouse	4,448	6005
Freemans	32	76	Freemans	1705	760	Freemans	9,760	30320
French	16	71	French	697	714	French	6,400	35281
Giletts	28	80	Giletts	1637	798	Giletts	16,212	32238
Southwest	5	14	Southwest	168	145	Southwest	5,285	4556
Tarawa	5	96	Tarawa	173	960	Tarawa	261,107	23440
Trapps	3	11	Trapps	231	116	Trapps	4,482	3542
R^2		0.082	R^2		0.132	R^2		0.048

REFERENCES

Alexander, R.B., Johnes, P.J., Boyer, E.W. and Smith, R.A., 2002. A comparison of models for estimating the riverine export of nitrogen from large watersheds. Biogeochemistry 57-58, 295-339.

Anderson, I.C., M.J. Brush, M.F. Piehler, and C.A. Currin. 2012. Developing indicators of ecosystem function for shallow estuaries: benthic functional responses in the New River Estuary. Final report to the Strategic Environmental Research and Development Program, Department of Defense, Washington, DC.

Anderson, I.C., K.J. McGlathery and A.C. Tyler. 2003. Microbial Mediation of 'Reactive' Nitrogen Transformations in a Temperate Lagoon. Marine Ecology Progress Series, 246: 73-84.

BASINS Technical Note #6: Estimating Hydrology and Hydraulic parameters for HSPF. 2000. United States Environmental Protection Agency.

BASINS Technical Note #8: Sediment Parameter and Calibration Guidance for HSPF. 2006. United States Environmental Protection Agency.

Bicknell, B.R., J.C. Imhoff, J.L. Kittle, Jr., T.H. Jobes and A.S Donigian, Jr. 2005. HSPF Version 12.2 User's Manual. Office of Surface Water: Water Resources Discipline.

Borah, D.K., G. Yagow, P.L. Barnes, W. Rosenthal, E.C. Krug and L.M. Hauck. 2006. Sediment and Nutrient Modeling for TMDL Development and Implementation. American Society of Agricultural and Biological Engineers, 49: 967-986.

Boynton, W.R., J.H. Garber, R. Summers and W.M. Kemp. 1995. Inputs, Transformation, and Transport of Nitrogen and Phosphorus in Chesapeake Bay and Selected Tributaries. Estuaries, 18: 285-314.

Boynton, W.R., J.D. Hagy, J.C. Cornwell, W.M. Kemp, S.M. Greene, M.S. Owens, J.E. Baker and R.K. Larsen. 2008. Nutrient Budgets and management Actions in the Patuxent River Estuary, Maryland. Estuaries and Coasts, 31: 623-651.

Boynton, W.R., J.D. Hagy, L. Murray, C. Stokes and W.M. Kemp. 1996. A Comparative Analysis of Eutrophication Patterns in Temperate Coastal Lagoons. Estuaries, 19: 406-421.

Boynton, W.R. and W.M. Kemp. 2000. Influences of River Flow and Nutrient Loads on Selected Ecosystem Processes: A Synthesis of Chesapeake Bay Data. Estuarine Science: A Synthetic Approach to Research and Practice, chapter 11:269-298.

Boynton, W.R., W.M. Kemp, and C.W. Keefe. 1982. A Comparative Analysis of Nutrients and Other Factors Influencing Estuarine Phytoplankton Production. Pp. 69-90 *in:* Kennedy, V.S. (ed.), Estuarine Comparisons. Academic Press, New York.

Breitburg, D.L., J.K. Craig, R.S. Fulford, K.A. Rose, W.R. Boynton, D.C. Brady, B.J. Ciotti, R.J. Diaz, K.D. Friedland, J.D. Hagy, P.J.B. Hart, A.H. Hines, E.D. Houde, S.E. Kolesar, S.W. Nixon, J.A. Rice, D.H. Secor, and T.E. Targett. 2009. Nutrient Enrichment and Fisheries Exploitation: Interactive Effects on Estuarine Living Resources and Their Management. Hydrobiologia 629(1):31-47.

Bricker, S.B., C.G. Clement, D.E. Pirhalla, S.P. Orlando and D.R.G. Farrow. 1999. National Estuarine Eutrophication Assessment: Effects of nutrient Enrichment in the Nation's Estuaries. U.S. Department of Commerce: National Oceanic and Atmospheric Administration, National Ocean Service.

Brush, G.S. 2001. Natural and anthropogenic changes in Chesapeake Bay during the last 1000 years. Human and Ecological Risk Assessment 7(5):1283-1296.

Brush, M.J. 2012. Development and application of watershed and estuarine simulation models for the New River Estuary. Chapter 6in: Final Technical Report to the Defense Coastal/Estuarine Research Program (DCERP), RTI International, Research Triangle Park, NC.

Clean Estuaries Act of 2010. March 17, 2010. 2nd Session House of Representatives. 111th Congress Report.

Cloern, J.E. 2001. Our evolving conceptual model of the coast eutrophication problem. Marine Ecology Progress Series 210, 223-253.

Donigian, A.S. and J.C. Imhoff. 2006. From the Stanford Model to BASINS: 40 Years of Watershed Modeling. AQUA TERRA Consultants.

Duarte, C.M., Conley, D.J., Carstensen, J. and Sanchez-Camacho, M., 2009. Return to Neverland: Shifting Baselines Affect Eutrophication Restoration Targets. Estuaries and Coasts 32, 29-36.

Ensign, S.H., Halls, J.N, and Mallin, M.A., 2004. Application of digital bathymetry data in an analysis of flushing times of two large estuaries. Computers & Geosciences 30(5):501-511.

EPA (Environmental Protection Agency), 1999. Protocol for Developing Nutrient TMDLs. Report 841-B-99-007, Office of Water, U.S. Environmental Protection Agency, Washington, DC, 137 pp.

EPA-PCS (Environmental Protection Agency - Permit Compliance System). 2009. Water Discharge Permit Query using EnviroFacts database. <http://www.epa.gov/enviro/html/pcs/pcs_query.html>.

Gillson, J. 2011. Freshwater Flow and Fisheries Production in Estuarine and Coastal Systems: Where a Drop of Rain is Not Lost. Reviews in Fisheries Science 19(3):168-186.

Greening, H. and A. Janicki. 2006. Toward Reversal of Eutrophic Conditions in a Subtropical Estuary: Water Quality and Seagrass Response to Nitrogen Loading Reduction in Tampa Bay, Florida, USA. Environmental Management, 38: 163-178.

Gutiérrez-Magness, A.L., 2005. A Strategy for Calibrating the HSPF Model. PhD Dissertation. University of Maryland at College Park.

Hagy, J.D. III and M.C. Murrell. 2007. Susceptibility of a northern Gulf of Mexico Estuary to Hypoxia: An Analysis Using Box Models. Estuarine Coastal and Shelf Science, 74: 239-253.

Hagy, J.D., W.R. Boynton, C.W. Keefe and K.V. Wood. 2004. Hypoxia in Chesapeake Bay, 1950-2001: Long-term Change in Relation to Nutrient Loading and River Flow. Estuaries, 27: 634-659.

Houde, E.D. and E.S. Rutherford. 1993. Recent Trends in Estuarine Fisheries: Predictions of Fish Production and Yield. Estuaries 16(2):161-176.

Howarth, R.W., J.R. Fruci, and D. Sherman. 1991. Inputs of Sediment and Carbon to an Estuarine Ecosystem: Influence of Land Use. Ecological Applications 1(1):27-39.

Im, S., Brannan, K.M., Mostaghimi, S. and Kim, S.M., 2007. Comparison of HSPF and SWAT models performance for runoff and sediment yield prediction. Journal of Environmental Science and Health, Part A: Toxic/Hazardous Substances & Environmental Engineering 42, 1561-1570.

Kemp, W.M., W. R. Boynton, J. E. Adolf, D. F. Boesch, W. C. Boicourt, G. Brush, J. C. Cornwell, T. R. Fisher, P. M. Glibert, J. D. Hagy, L.W. Harding, E. D. Houde, D. G. Kimmel, W. D. Miller, R. I. E. Newell, M. R. Roman, E. M. Smith and J.C. Stevenson. 2005. Eutrophication of Chesapeake Bay: Historical Trends and Ecological Interactions. Marien Ecology Progress Series, 303: 1-29.

Kim, H-C. and P.A. Montagna. 2009. Implications of Colorado River (Texas, USA) Freshwater Inflow to Benthic Ecosystem Dynamics: A Modeling Study. Estuarine, Coastal, and Shelf Science 83:491-504.

Lucas, L.V., J.K. Thompson, and L.R. Brown. 2009. Why Are Diverse Relationships Observed Between Phytoplankton Biomass and Transport Time? Limnology and Oceanography 54(1):381–390.

Lumb, A.M., R.B. McCammon and J.L Kittle, Jr. 1994. Users Manual for an Expert System (HSPEXP) for Calibration for the Hydrologic Simulation Program-Fortran. U.S. Geological Survey: Water-Resources Investigations Report 94-4168.

Mallin, M.A., McIver, M.R., Wells, H.A., Parsons, D.C. and Johnson, V.L., 2005. Reversal of Eutrophication Following Sewage Treatment Upgrades in the New River Estuary, North Carolina. Estuaries 28, 750-760.

McGlathery, K.J., K. Sundbäck and I.C. Anderson. 2007. Eutrophication in Shallow Coastal bays and Lagoons: The Role of Plants in the Coastal Filter. Marine Ecology Progress Series, 348: 1-18.

Monbet, Y. 1992. Control of Phytoplankton Biomass in Estuaries: A Comparative Analysis of Microtidal and Macrotidal Estuaries. Estuaries 15(4):563-571.

Mudd, S.M., S.M. Howell, and J.T. Morris. 2009. Impact of Dynamic Feedbacks between Sedimentation, Sea-level Rise, and Biomass Production on Near-surface Marsh Stratigraphy and Carbon Accumulation. Estuarine, Coastal and Shelf Science 82(3):377-389.

National Atlas. North Carolina Annual Average Precipitation. Accessed May 15, 2012. <www.nationalatlas.gov/printable/images/pdf/.../pageprecip_nc3.pdf>.

National Research Council. 2000. Clean Coastal Waters: Understanding and Reducing the Effects of Nutrient Pollution. National Academy Press.

Nixon, S., 1995. Coastal marine eutrophication: A definition, social causes, and future concerns. Ophelia 41, 199-219.

Nixon, S.W., 2009. Eutrophication and the Macroscope. Hydrobiologia 629, 5-19.

Nixon, S.W. and B.A. Buckley. 2002. "A strikingly rich zone" – nutrient enrichment and secondary production in coastal marine ecosystems. Estuaries 25(4B):782-796.

Nixon, S.W., J.W. Ammerman, L.P. Atkinson, V.M. Berounsky, G. Billen, W.C. Boicourt, W.R. Boynton, T.M. Church, D.M. Ditoro, R. Elmgren, J.H. Garber, A.E. Giblin, R.A. Jahnke, N.J.P. Owens, M.E.Q. Pilson and S.P. Seitzinger. 1996. The Fate of Nitrogen and Phosphorus at the Land-Sea Margin of the North Atlantic Ocean. Biogeochemistry, 35: 141-180.

Paerl, H. 1998. Structure and Function of Anthropogenically Altered Microbial Communities in Coastal Waters. Current Opinion in Microbiology, 1: 296-302.

Paerl, H.W. 2009. Controlling Eutrophication Along the Freshwater-marine Continuum: Dual Nutrient (N and P) Reductions are Essential. Estuaries and Coasts, 32: 593-601.

Paerl, H.W. and J. Huisman. 2008. Blooms Like it Hot. Science 320:57-58.

Paerl, H.W., J.L. Pinckney, J.M. Fear, and B.L. Peierls. 1998. Ecosystem Responses to Internal and Watershed Organic Matter Loading: Consequences for Hypoxia in the Eutrophying Neuse River Estuary, North Carolina, USA. Marine Ecology Progress Series 166:17-25.

Paerl, H.W. and K.H. Reckhow. 2012. Develop and Deploy Microalgal Indicators as Measures of Water Quality, Harmful Algal Bloom Dynamics, and Ecosystem Condition. Final report to the Strategic Environmental Research and Development Program, Department of Defense, Washington, DC.

Paerl, H.W. and J.T. Scott. 2004. Throwing Fuel on the Fire: Synergistic Effects of Excessive Nitrogen Inputs and Global Warming on Harmful Algal Blooms. Environmental Science and Technology, 44: 7756-7758.

Pinckney, J.L., H.W. Pearl, P. Tester and T.L. Richardson. 2001. The Role of Nutrient Loading and Eutrophication on Estuarine Ecology. Environmental Health Perspectives, 109: 699-706.

PLOAD version 3.0 User's Manual. 2001. An ArcView GIS Tool to Calculate Nonpoint Sources of Pollution in Watershed and Stormwater Projects. United States Environmental Protection Agency.

Roberts, A., Prince, S., Jantz, C. and Goetz, S., 2009. Effects of projected future urban land cover on nitrogen and phosphorus runoff to Chesapeake Bay. Ecological Engineering 35, 1758-1772.

Schwartz, R. 2010. Land Use Affects and the Timing and magnitude of Material Delivery to Headwater Streams in Coastal North Carolina (Masters Thesis). University of North Carolina at Chapel Hill.

Thrush, S.F., J.E. Hewitt, V.J. Cummings, J.I. Ellis, C. Hatton, A. Lohrer and A. Norkko. 2004. Muddy Waters: Elevating Sediment Input to Coastal and Estuarine Habitats. The Ecological Society of America, 2: 299-306.

United States Environmental Protection Agency. 2009. BASINS 4.0 Climate Assessment Tool (CAT): Supporting Documentation and User's Manual. Office of Research and Development, 191 pp.

Valette-Silver, N.J. 1993. The use of sediment cores to reconstruct historical trends in contamination of estuarine and coastal sediments. Estuaries 16(3B):577-588.

Valiela, I., J.McClelland, J. Hauxwell, P.J. Behr, D. Hersh, and K. Foreman. 1997. Macroalgal blooms in shallow estuaries: Controls and ecophysiological and ecosystem consequences. Limnology and Oceanography, 45(5 part 2):1105-1118.

VITA

BRITTANI JEAN KOROKNAY

Born April 11, 1984 in Toledo, Ohio. In 2002, graduated from Central Catholic High School in Toledo, Ohio. Upon graduation, attended the Naval Academy Preparatory School and immediately followed by attendance to the Coast Guard Academy. A B.S. in Marine and Environmental Science was earned at the Coast Guard Academy. After graduation, was stationed at Coast Guard Sector Hampton Roads in Portsmouth, VA. Selected for the United States Coast Guard post graduate program to study Environmental Management. Entered the M.S. program at the Virginia Institute of Marine Science, College of William and Mary under graduate advisor Dr. Mark J. Brush in 2010.